An International Journal

ISSN:1545 – 0740
Volume 3, Number 1, 2005

Nature and Science

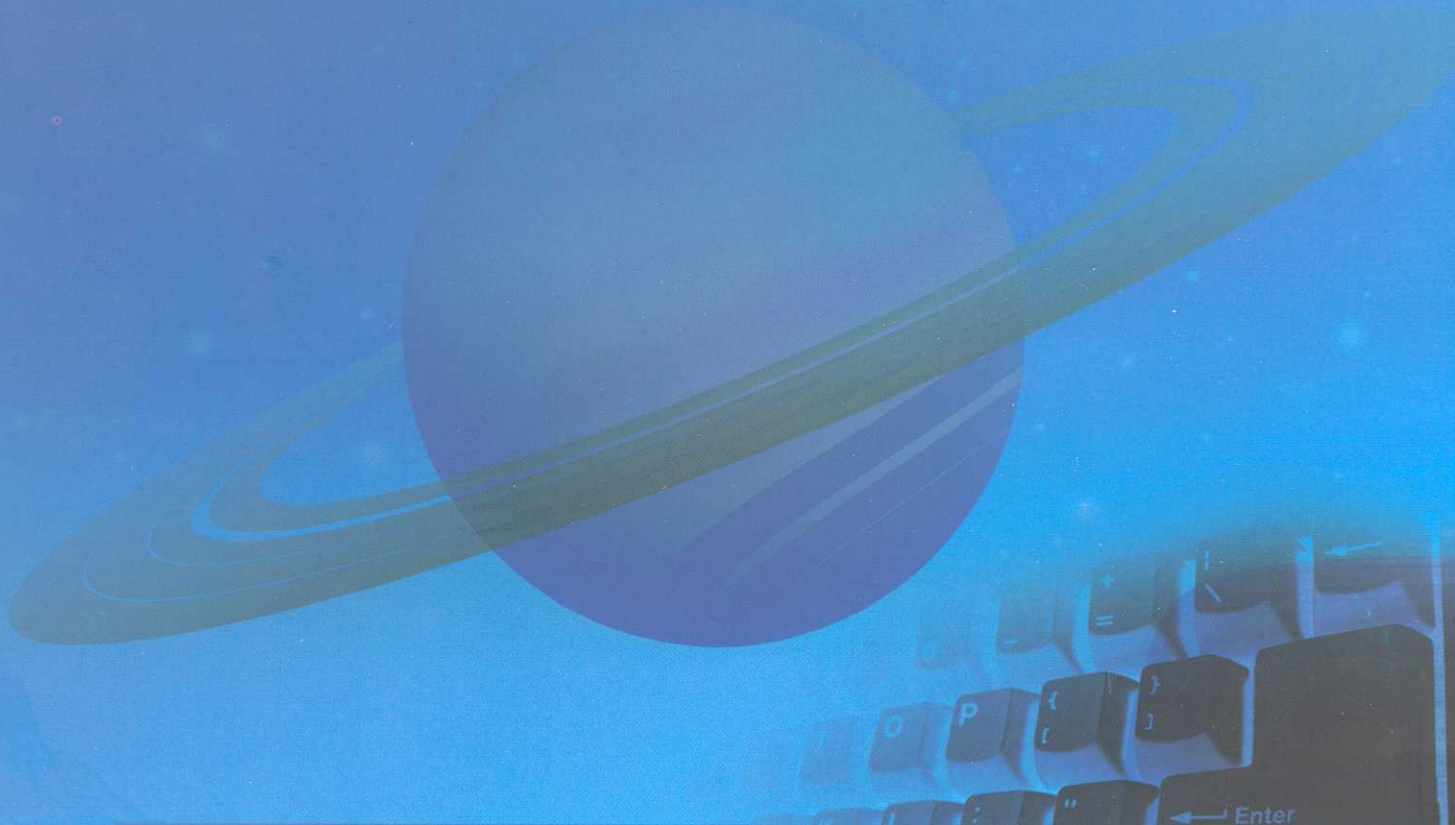

Nature and Science

The **Nature and Science** is an international journal with a purpose to enhance our natural and scientific knowledge dissemination in the world under the free publication principle. Any valuable papers that describe natural phenomena and existence or any reports that convey scientific research and pursuit are welcome, including both natural and social sciences. Papers submitted could be reviews, objective descriptions, research reports, opinions/debates, news, letters, and other types of writings that are nature and science related. The journal is calling for papers and seeking co-operators and editors as well.

Introductions to Authors

1. General Information

(1) Goals: As an international journal published both in print and on internet, Nature and Science is dedicated to the dissemination of fundamental knowledge in all areas of nature and science. The main purpose of Nature and Science is to enhance our knowledge spreading in the world under the free publication principle. It publishes full-length papers (original contributions), reviews, rapid communications, and any debates and opinions in all the fields of nature and science.

(2) What to Do: The Nature and Science provides a place for discussion of scientific news, research, theory, philosophy, profession and technology - that will drive scientific progress. Research reports and regular manuscripts that contain new and significant information of general interest are welcome.

(3) Who: All people are welcome to submit manuscripts in any fields of nature and science.

(4) Publication Costs: US$30 per printed page of an article to defray costs of the publication will be paid by the authors when the submission or after the acceptance. Extra expense for color reproduction of figures will be paid by authors (estimate of cost will be provided by the publisher for the author's approval).

(5) Journal Copies to Authors: One hard copy of the journal will be provided free of charge for each author.

(6) Additional Copies Bought by Authors: Additional hard copies could be purchased with the price of US$4/issue.

(7) Distributions: Web version of the journal is freely opened to the world without any payment or registration. The journal will be distributed to the selected libraries and institutions for free. US$5/issue hard copy is charged for the subscription of other readers.

(8) Advertisements: The price will be calculated as US$400/page, i.e. US$200/a half page, US$100/a quarter page, etc. Any size of the advertisement is welcome.

2. Manuscripts Submission

(1) Submission Methods: Electronic submission through email is encouraged and hard copies plus an IBM formatted computer diskette would also be accepted.

(2) Software: The Microsoft Word file will be preferred.

(3) Font: Normal, Times New Roman, 10 pt, single space.

(4) Indent: Type 4 spaces in the beginning of each new paragraph.

(5) Manuscript: Don't use "Footnote" or "Header and Footer".

(6) Cover Page: Put detail information of authors and a short title in the cover page.

(7) Title: Use Title Case in the title and subtitles, e.g. "**Debt and Agency Costs".**

(8) Figures and Tables: Use full word of figure and table, e.g. **"Figure 1.** Annul Income of Different Groups**", Table 1. Annual Increase of Investment".**

(9) References: Cite references by "last name, year", e.g. "(Smith, 2003)". References should include all the authors' last names and initials, title, journal, year, volume, issue, and pages etc.

Reference Examples:

Journal Article: Hacker J, Hentschel U, Dobrindt U. Prokaryotic chromosomes and disease. Science 2003;301(34):790-3.

Book: Berkowitz BA, Katzung BG. Basic and clinical evaluation of new drugs. In: Katzung BG, ed. Basic and clinical pharmacology. Appleton & Lange Publisher. Norwalk, Connecticut, USA. 1995:60-9.

(10) Submission Address: editor@sciencepub.net, Marsland Company, P.O. Box 753, East Lansing, Michigan 48826, The United States, 517-505-7688.

(11) Reviewers: Authors are encouraged to suggest 2-8 competent reviewers with their name and email.

2. Manuscript Preparation

Each manuscript is suggested to include the following components but authors can do their own ways:

(1) Title page: including the complete article title; each author's full name; institution(s) with which each author is affiliated, with city, state/province, zip code, and country; and the name, complete mailing address, telephone number, facsimile number (if available), and e-mail address for all correspondence.

(2) Abstract: including Background, Materials and Methods, Results, and Discussions.

(3) Key Words.

(4) Introduction.

(**5) Materials and Methods**.

(**6) Results**.

(**7) Discussions**.

(**8) References**.

(**9) Acknowledgments**.

Journal Address:

Marsland Company
P.O. Box 21126
East Lansing, Michigan 48909,
The United States
Telephone: (517) 980-4106
E-mail: editor@sciencepub.net
Homepage: http://www.sciencepub.org

Nature and Science

(Quarterly, Started in 2003)

Volume 3 - Number 1 (Cumulated No. 6), March 1, 2005

CONTENTS

Cosmology Based on Absolute Motion

Ken H. Seto

KHS Publishing, 260 Yorkshire Lane, Xenia, OH 45385, USA
kenseto@erinet.com; http://www.erinet.com/kenseto/book.html
Telephone: 937-3725298

Abstract: A new model of the universe called Model Mechanics was formulated. Model Mechanics explains all the forces of nature with the same mechanism and thus it is able to unite all the forces of nature naturally. In cosmology, Model Mechanics provides solutions to the following problematic cosmological observations: the observed accelerated expansion of the far reached regions of the universe disagrees with the prediction of GRT; the observed rotational curves of galaxies disagree with the predictions of GRT; the observed paths of travel of the space crafts Pioneer 10 and 11 disagree with the predictions of GRT; the observable universe appear to have a much larger horizon than it is allowed by its observed age and the GRT description of gravity gives rise to the observed flatness problem of the universe. Model Mechanics leads to a new theory of gravity called Doppler Theory of Gravity (DTG) and unites gravity with the electromagnetic and nuclear forces naturally [1,2,3]. It also leads to a complete theory of motion called Improved Relativity Theory (IRT). IRT includes Special Relativity Theory (SRT) as a subset. However, unlike SRT, the equations of IRT are valid in all environments…including gravity. Model Mechanics is based on the existence of absolute motions of objects in a stationary and structured light-conducting medium called the E-Matrix. Proposed experiments to detect absolute motions in the E-Matrix were also formulated. [Nature and Science. 2005;3(1):1-12].

Key Words: cosmology; absolute motion;model

1 Model Mechanics Description of the Current Universe

Model Mechanics supposes that a stationary substance, called the 'E-Matrix', occupies all of pure-space (void) in our Universe. Subsequently, we perceive the E-Matrix as space. The E-Matrix, in turn, is composed of 'E-Strings', which are very thin three-dimensional elastic objects, of diameter estimated at 10^{-33} cm. The length of an E-String is not defined. Away from matter, the E-Strings are oriented randomly in all directions. This means that a slice of the E-Matrix in any direction will look the same. Near matter, the E-Strings are more organized: some emanate from the matter, and the number of these passing through a unit area followed the well-known inverse square law of physics. The E-Strings repel each other. This means that there is an unknown outside force that is compacting them together. The repulsive force and the compacting force are in equilibrium. This state of the E-Matrix allows massive matter particles to move freely within it. The motion of a matter particle or particle system in the E-Matrix is called 'absolute motion'. The absolute motion of matter in the E-Matrix will distort the local E-Strings. The E-Strings will recover to the non-distorted state after the passage of the matter particles. Light consists of wave-packets in neighboring E-Strings. On its way toward its target, a wave-packet will follow the geometry of these neighboring E-Strings. This description of light embodies 'duality', *i.e.* light possessing properties of a mass-bearing particle as well as a wave packet.

With this description of the E-Matrix (space), the next relevant question is: What is matter? All stable and visible matter is made from three basic particles: the electrons, the up quarks, and the down quarks. The protons and neutrons in the nuclei of all the atoms are made from the up quarks and the down quarks. The electrons orbit around the nuclei to complete the picture

of all the atoms. The three basic particles are, in turn, made from one truly fundamental mass-bearing particle, called the 'S-Particle'. An S-Particle is a three-dimensional spherical object. It is repulsive to the E-Strings surrounding it and therefore its motion in the E-Matrix is maintained. An S-Particle orbiting around an E-String in the helical counterclockwise direction is an electron. This motion of the S-Particle is the fastest in the E-Matrix, and it gives rise to one unit of negative electric charge. A down quark is also an S-Particle orbiting around an E-String in the helical counterclockwise direction. The speed of its orbiting motion is only 1/3 that of the electron, giving the down quark a negative 1/3 electric charge. An up quark is an S-Particle orbiting around an E-String in the helical clockwise direction at 2/3 the speed of the electron, resulting a 2/3 positive electric charge.

There is one more stable basic particle: the electron neutrino. An electron neutrino has no detectable electric charge, and therefore it does not interact with the other three charged basic particles. It is composed of an S-Particle orbiting around an E-String in the counterclockwise direction like the electron. However, it is moving in a corkscrew like motion away from the charged basic particles. This means that the distortion in the E-Matrix created by the absolute motion of the electron neutrino will have already dissipated by the time the charged basic particles are ready to interact with it. This is the reason why the electron neutrino does not interact electromagnetically with the charged basic particles.

This simple description of all stable visible matter can answer the thorny question: What *is* the mass of a basic particle? The answer is: mass is the evidence of the orbiting diameter of its S-Particle. Those S-Particles that are not in a state of orbiting motion do not possess any electric charge and therefore they will not interact with the basic charged particles electrically. They will, however, interact with them gravitationally. They are the dark matters predicted by the astronomers.

The next relevant question is: what are the processes that give rise to all the forces between matter particles? The proposed answers to this question are as follows:

1. All the processes of Nature are the result of matter particles reacting to the geometries of the E-Strings (*i.e*. distortions or waves) to which they are confined because of their orbiting motions around these E-Strings.
2. Absolute motions of two objects in the same direction in the E-Matrix will cause the objects to converge to each other--an attractive force. Absolute motions of two objects in the opposite directions in the E-Matrix will cause the objects to diverge from each other--a repulsive force.

This completes the Model Mechanical description of our current universe. All the particles, all the forces and all the processes of nature can be derived from this one description. Model Mechanics replaces the math constructs of space-time and field/virtual particle with the E-Matrix and the distortions or waves in the E-Matrix. It gives rise to the following postulates:

1. The E-Matrix is a stationary and structured light-conducting medium. It occupies all of pure space (pure void). It is comprised of very thin and elastic E-Strings and these E-Strings are repulsive to each other. There is an unknown compacting force that compresses these E-Strings together to form the E-Matrix.
2. The S-Particle is the only truly fundamental particle exists in our universe. The different orbiting motions of the S-Particles around the E-String(s) give rise to all the visible and stable particles in our universe.
3. All the processes of nature are the results of absolute motions of S-Particles or S-Particle systems in the E-Matrix.
4. All the forces of nature are the results of the S-Particle or S-Particle systems reacting to the distortions or waves in the E-Strings to which they are confined. The distortions or waves in the E-Strings, in turn, are the results of the absolute motions of the interacting S-Particles or S-Particle systems in the E-Matrix.
5. All the stable and visible matters are the results of orbiting motions of the S-Particles around specific E-Strings.

These postulates eliminate all the infinity problems that plagued both GRT and QM. It has the same mechanism for all the forces of nature and thus it unites all the forces of nature naturally. It gives an explanation why the force of gravity is capable of acting at a distance. It explains the provisions of the Uncertainty Principle. It explains the weird results of all quantum experiments [3]. It eliminates the need for the undetectable force messengers in Quantum Field Theories. It eliminates the need for the hypothetical and undetected Higgs particle. It explains the mass of a

particle and the charge of a particle. It leads to the discovery of the CRE force, which, in turn leads to a new theory of gravity. In short, Model Mechanics gives us a unique way to achieve the elusive goal of unifying all of physics.

2 Improved Relativity Theory (IRT)

Special Relativity Theory (SRT) posits that the speed of light is a universal constant in all inertial frames, but suppose the speed of light is not a universal physical constant as asserted by the SRT, but rather a constant mathematical ratio as follows:

$$\frac{\text{light path length of rod}\left(299,792,458\ \text{m}\right)}{\text{absolute time content of clock second co-moving with rod}}$$

This new interpretation for the speed of light revives the discarded notion of absolute time and physical space. It also makes the notion of absolute time and space compatible with SRT. Based on this interpretation for light speed, a new theory has been formulated for motion: Improved Relativity Theory (IRT). IRT includes SRT as a subset, but its equations are valid in all environments—including gravity. The following is a description of IRT:

The postulates:

1. The laws of physics based on a clock second and a light-second to measure length are the same for all observers in all inertial reference frames.
2. The speed of light in free space based on a clock second and a light-second to measure length has the same mathematical ratio c in all directions and all inertial frames.
3. The laws of physics based on a defined absolute second and the physical length of a rod is different in different frames of reference.
4. The one-way speed of light in free space based on a defined absolute second and the physical length of a measuring rod has a different mathematical ratio for light speed in different inertial frames. The speed of light based on a defined absolute second and the physical length of a measuring rod is a maximum in the rest frame of the E-Matrix.

The Consequences of these Postulates:

1. The speed of light is not a universal constant. It is a constant math ratio as follows:
   Light path length of rod (299,792,458 m)/the absolute time content for a clock second co-moving with the rod.
   The detailed explanation of this new definition:
   By definition the speed of light in the rest frame of the E-Matrix is as follows:
   Light path length of rod in the E-Matrix frame = 299,792,458 m.
   The absolute time content for a clock second in the E-Matrix frame = 1 E-Matrix frame clock second.
   Therefore the speed of light in the E-Matrix frame is: 299,792,458 m/1 E-Matrix clock second
   The speed of light in any frame moving in the stationary E-Matrix is determined as follows:
   The light path length of rod in the moving frame= γ (299,792,458 m)
   The absolute time content for a moving clock second= γ (E-Matrix clock seconds)
   Therefore the speed of light in any moving frame in the stationary E-Matrix is as follows:
   γ (299,792,458 m) / γ (E-Matrix clock seconds).
   This is reduced to a constant math ratio of: 299,792,458 m/1 E-Matrix clock second
2. The physical length of a rod remains the same in all frames of reference. The light path length of a rod changes with the state of absolute motion of the rod. The higher is the state of absolute motion the longer is its light path length.
3. The rate of a clock is dependent on the state of absolute motion of the clock. The higher is the state of absolute motion the slower is its clock rate.
4. Absolute time exists. The relationship between clock time and absolute time is as follows: A clock second will contain a different amount of absolute time in different states of absolute motion (different frames of reference). The higher is the state of absolute motion of the clock the higher is the absolute time content for a clock second.
5. Simultaneity is absolute. If two events are simultaneous in one frame, identical events will also be simultaneous in different frames. However the time interval for the simultaneity to occur will be different in different frames. This is due to that different frames are in different states of absolute motion.
6. Relative motion between two observers A and B is the vector difference of the vector component of A's absolute motion and the vector component of B's absolute motion along the line joining A and B.

3 The Math of IRT:

3.1 The time dilation (contraction) or expansion equations:

A and B are in relative motion from observer A's point of view:

$$T_{ab} = T_{aa}\left(\frac{F_{aa}}{F_{ab}}\right) \quad (1)$$

OR

$$T_{ab} = T_{aa}\left(\frac{F_{ab}}{F_{aa}}\right) \quad (2)$$

T_{aa} = A clock time interval in observer A's frame as measured by A

T_{ab} = A's prediction of B's clock time interval for an interval of T_{aa} in his frame.

F_{aa} = Frequency of a standard light source in A's frame as measured by A.

F_{ab} = Frequency of an identical light source in B's frame as measured by A. If F_{ab} is not constant the mean value is used.

Note: Even though T_{aa} and T_{ab} are two different clock time intervals but both of these clock time intervals contain the same amount of absolute time.

3.2 The light path length contraction or expansion equations:

$$L_{ab} = L_{aa}\left(\frac{F_{aa}}{F_{ab}}\right) \quad (3)$$

OR

$$L_{ab} = L_{aa}\left(\frac{F_{ab}}{F_{aa}}\right) \quad (4)$$

L_{aa} = The light path length of a rod in A's frame as measured by A.

L_{ab} = The light path length of an identical rod in B's frame as predicted by A.

Note: Even though L_{aa} and L_{ab} are two different light path lengths but these two light path lengths are derived from identical rods that have the same physical rod lengths. The different light path lengths are the results of different states absolute motion of the rods.

3.3 The Coordinate Transformation Equations:

$$x' = \frac{f_{aa}}{f_{ab}}\left[x + t\left(f_{aa} - f_{ab}\right)\lambda\right] \quad (5)$$

$$t' = \frac{f_{aa}}{f_{ab}}\left[t + x\left(\frac{\left(f_{aa} - fab\right)}{\lambda f_{aa}^2}\right)\right] \quad (6)$$

OR

$$x' = \frac{f_{ab}}{f_{aa}}\left[x - t\left(f_{aa} - f_{ab}\right)\lambda\right] \quad (7)$$

$$t' = \frac{f_{ab}}{f_{aa}}\left[t - x\left(\frac{\left(f_{aa} - f_{ab}\right)}{\lambda f_{aa}^2}\right)\right] \quad (8)$$

A is the observer's frame (unprimed) and B is the observed frame (primed).

f_{aa} = The instantaneous frequency measurement of a standard light source in A's frame as measured by A.

f_{ab} = The instantaneous frequency measurement of an identical light source in B's frame as measured by A.

λ = The wave length of the standard light source in A's frame as measured by A.

These coordinate transform equations are valid in all environments--including gravity. This means that IRT will give matching predictions as GRT and at the same time includes SRT as a subset.

3.4 Momentum of an object:

$$p = M_o\lambda\left(F_{aa} - F_{ab}\right) \quad (9)$$

3.5 Kinetic Energy of an object:

$$K = M_o\lambda^2 F_{aa}^2\left(\frac{F_{aa}}{F_{ab}} - 1\right) \quad (10)$$

3.6 Energy of a single particle:

$$E = M_o\lambda^2 F_{aa}^2 \quad (11)$$

3.7 Gravitational Red or Blue Shift:

$$\Delta F_{aa} = F_{aa}\left(1 - \left(\frac{F_{ab}}{F_{aa}}\right)\right) \quad (12)$$

3.8 A positive value represents a red shift from A's location. A negative value represents a blue shift from A's location.

3.9 Gravitational Time Contraction (Dilation) or Expansion:

$$\Delta T_{aa} = T_{aa}\left(1-\left(\frac{F_{ab}}{F_{aa}}\right)\right) \qquad (13)$$

A positive value represents gravitational time contraction (dilation) from A's location.

A negative value represents gravitational time expansion from A's location.

3.10 The IRT procedure for determining the Perihelion precession of Mercury without recourse to GRT is:

a) Set up a coordinate system for the Sun and Mercury.

b) Use the IRT coordinate transformation equations to predict the future positions of the Sun and Mercury.

c) The perihelion shift of Mercury will be revealed when these future positions are plotted against time. Also, the value of the shift can be determined from the plot.

4 Forces Based on Absolute Motions

The idea that absolute motion of interacting particles in the same direction gives rise to an attractive force, while absolute motion of interacting particles in the opposite directions gives rise to a repulsive force, is derived from the familiar electric current experiments in parallel wires. These experiments show that when electric currents are flowing in the wires in the same direction, the wires are attracted to each other, and when the currents are flowing in the opposite direction, the wires repel each other. Figs. 1 and 2 illustrate these experiments graphically. The absolute motions of the electrons in the same direction cause a distortion in the E-Matrix that pulls the wires together-an attractive force. Conversely, the directions of absolute motion of the electrons in the opposite directions will cause a distortion in the E-Matrix that pulls the wires apart–a repulsive force.

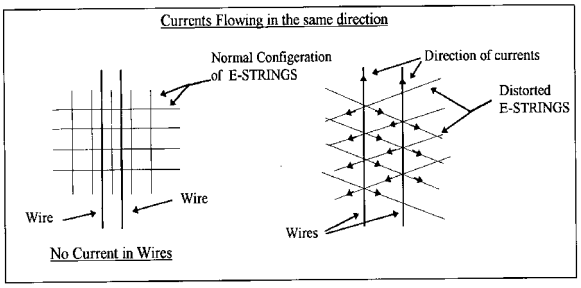

Figure 1. Currents (electrons) in the wires are flowing in the same direction, and therefore the force between the electrons is attractive. The right diagram that shows that the tension created in the E-Strings by the absolute motions of the electrons is pulling the wires together.

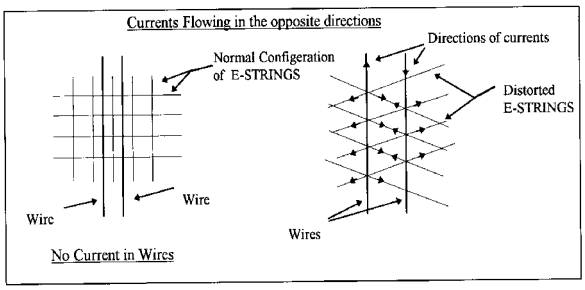

Figure 2. Currents (electrons) in the wires are flowing in the opposite direction, and therefore the force between the electrons is repulsive. The right diagram shows that the tension created in the E-Strings by the absolute motions of the electrons is pulling the wires apart.

Extending this interpretation of the electric-current experiments to include the orbiting motions of the S-Particles will enable us to explain all the nuclear forces between the interacting up quarks and down quarks [1,2]. This interpretation becomes the most important concept of Model Mechanics and it enables Model Mechanics to unite all the forces of nature naturally.

5 The CRE Force

Current physics posits that there are four forces of Nature: the electromagnetic force, the nuclear weak and strong forces, and gravity. Model Mechanics posits that there is a fifth force of Nature; the new force being the CRE force. As the name implies, the CRE force between any two objects is repulsive. While the CRE force is new to physical theory, it is not new to experience; it is what we commonly refer to as 'inertia'. In other words, the resistance between two objects to change their state of absolute motion is the CRE force

between them. The CRE force between any two objects is always repulsive, and it is derived from the diverging structure of the E-Matrix.

To understand the CRE force, recall the inverse square law of physics. This law states that the intensity of light, gravity and electromagnetic force decreases with increasing distance r from the source is inversely proportional to r^2. The geometry of neighboring E-Strings emanating from any two objects also obeys the inverse square law. This means that each object will follow the diverging geometry of these neighboring E-Strings. Therefore, their path of motions in the E-Matrix will have a tendency to diverge from each other. This repulsive effect is identified as the CRE force. The CRE force between any two objects is not constant; it increases with the square of the distance between the objects. The CRE force is not the cosmological constant that Einstein inserted into his original GRT field equations. Although the cosmological constant is repulsive, it is not the CRE force predicted by Model Mechanics for the simple reason that it is constant.

The CRE force played an important role in the formation of our Universe, and is continuing to do so today. The repulsive CRE force, along with the attractive electromagnetic force between gravitating objects shaped the primeval Universe into the Universe that we see today. The CRE force also played an important role in the manifestation of the nuclear weak force. Without the CRE force, there would be no nuclear weak force. It is the CRE force that initiates the radioactive decay of atoms. Perhaps, the most important function of the CRE force will be a role, in combination with the electromagnetic force, in the processes of life.

Model Mechanics predicted the repulsive CRE force in 1993. However, it was not discovered until 1998 when two independent groups of astronomers discovered that the Universe at the far reached regions is in a state of accelerated expansion. This observation is in direct conflict with the prediction of GRT. In order to explain this observation astronomers are now re-introducing the discarded repulsive Cosmological Constant to the GRT equation. The CRE force eliminates the need for this *ad hoc* approach.

6 Doppler Theory of Gravity (DTG)

Newton posited that gravity is a force, but he did not provide a mechanism for it. Newton's gravity model involved the unexplained phenomenon of action at a distance, which was troublesome for the physicists of his time. Also, Newton's equation for gravity was eventually found to be slightly inconsistent with observations. Recognizing the deficiencies in Newton's theory, Einstein formulated GRT, which is not a theory of force, but rather a theory of space-time, amounting to an extension of SRT to include gravity. IRT is a completed new theory of relativity. It includes SRT as a subset and its equations are valid in all environments including gravity. It gives the same correct predictions for gravity as does GRT, but it avoids the following problematic predictions of GRT:

1) The expansion rate of the Universe as predicted by GRT does not match what is currently observed. GRT predicts that the expansion of the Universe is slowing down, and yet observation confirms that the expansion is speeding up.

2) The galactic rotational curves as predicted by GRT do not match those that are currently observed.

3) The path of travel of Pioneer 10 as predicted by GRT does not match what is observed.

4) GRT predicts the existence of black holes and singularities. If these absurd objects exist, they should be as abundant as the stars, and yet none them have been positively detected.

5) GRT fails to predict the existence of dark matter and dark energy.

Model Mechanics also gives rise to a new theory of gravity called Doppler Theory of Gravity (DTG). Like Newton's theory, DTG also treats gravity as a force but with an identified mechanism. Based on the provisions of Model Mechanics, the mechanism of gravity between two objects A and B moving in the stationary E-Matrix is as follows:

1) If both A and B are moving absolutely in the same direction, this gives rise to an attractive force because A's absolute motion distorts the surrounding stationary E-Matrix and B's absolute motion is confined to follow the distortion created by A; conversely, B's absolute motion distorts the surrounding stationary E-Matrix and A's absolute motion is confined to follow the distortion created by B.

2) The global structure of the stationary E-Matrix is divergent. Both A and B are confined to this global divergent structure as they travel in the stationary E-Matrix. This gives rise to the repulsive CRE force between A and B globally.

The force of gravity between A and B is the combined result of items (1) and (2). It is noteworthy that gravity is the sum of an attractive and a repulsive force acting on both A and B. This explains why the force of gravity is so weak compared to the electromagnetic and nuclear forces.

The above description for gravity suggests that the Newtonian equation for gravity can be modified to make it consistent with observations. The following is a modified Newtonian equation based on the above description for the force of gravity:

$$F = \frac{G * M_a M_b (j_a) \bullet (\pm j_b)}{(r^2)(DF_a)} \qquad (14)$$

F = The force of gravity between A and B as determined by A

G = Universal gravitational constant m^3/s^2*kg

M_a = Mass of object A in kg

M_b = Mass of object B in kg

$(j_a)\bullet(j_b)$ = Dot product of the directional vectors j_a and j_b . [Note: This dot product can be positive or negative.]

r = Distance in meters between A and B

DF_a = Doppler Factor as determined by A

$DF_a = F_{aa} / F_{ab}$

F_{aa} = Frequency of a standard light source in A's own frame as measured by A.

F_{ab} = Frequency of an identical standard light source in B's frame as measured by A. If F_{ab} is not constant, a mean value is used.

The dot product $(j_a)\bullet(j_b)$ in this new equation expresses the concept that not all objects in the Universe attract each other gravitationally. A positive dot product represents an attractive force, but a negative dot product represents a repulsive force. Those objects that have the same direction of absolute motion are attracted to each other, but those objects that have absolute motions in the opposite direction exert a repulsive force on each other. Assuming the Big Bang model is correct then the dot product of the vectors for all local regions of the Universe is +1. This means that gravity in the local region is attractive. The dot product for a distant region, say beyond the radius of the observable Universe, is -1. Therefore, gravity for all those distant regions is repulsive.

7 Model Mechanics Explains the Problematic Cosmological Observations

One of the most pressing problems of the Standard Big Bang Model is the observed horizon problem. The age of our universe is determined to be 14 billion years old in all directions and yet we observe the horizon for the opposite regions of our universe to be 28 billion years apart. This means that these opposite regions of our universe cannot be in contact with each other at the Big Bang and this is known as the horizon problem. Cosmologists invented the ad hoc *Inflation* hypothesis to explain the horizon problem. Model Mechanics explains the horizon problem naturally without resorting to the ad hoc *Inflation* hypothesis. The earth is in a state of absolute motion in the E-Matrix. This motion curves the E-Strings surrounding the earth. What we perceive as normal and straight E-Strings are actually severely curved E-Strings. In other words, when we look up in the sky we are actually receiving light from these curved E-Strings. This means that no matter what direction we look we are looking into the same curved E-Strings and thus the same region of the universe. This means that the perceived opposite regions of the universe are really the same region and therefore the perceived horizon problem was never existed. As it turns out, there is a perfect physical example of this phenomenon. The medical device gastroscope made of fiber optics, allows a physician to examine the interior of a patient's stomach is such an example. No matter how the physician curves the eyepiece, he will still be seeing the same picture of the stomach.

In 1998 two independent groups of astronomers discovered that the far reached regions of the universe are in a state of accelerated expansion motion. This discovery is contrary to the predictions of GRT that predicts that the expansion of the universe should be slowing down. Astronomers revived the once discarded repulsive Cosmological Constant to explain the observed accelerated expansion. They posited that the universe is filled with a form of dark energy called Quintessence and this dark energy has the anti-gravity effect that gives rise to the Cosmological Constant. Model Mechanics predicted the accelerated expansion for those far reached regions of the universe in 1993. The basis for this Model Mechanical prediction is that

gravity at those regions is repulsive with respect to us as described in the DTG equation. The repulsive CRE force of DTG can be considered as the dark energy posited by the astronomers.

Another problem arise from the GRT description of gravity is called the flatness problem. The flatness problem is that the observable universe appears to exist between an open and a closed universe. In an open universe, the matter density is less than the critical value and thus the gravitational braking effect is not able to halt the Big Bang expansion. This means that the universe will keep on expanding forever. In a closed universe the matter density is greater than the critical value and thus the gravitational braking effect will be able to halt the Big Bang expansion. This means that the universe will re-collapse before any galaxy would have time to form. In order for our universe to exist between an open and a closed universe the matter density must be fine tuned to be within one part in 10^{50} f the critical density value when the universe was a fraction of a second old. The inability of the Big Bang theory to explain why this degree of fine-tuning existed is what is known as the flatness problem. In Model Mechanics (DTG), gravity is the result of two gravitating objects having the same direction of absolute motions in the E-Matrix less the repulsive CRE force that exists between them. This description of gravity avoids the flatness problem completely.

The observed rotational curves of galaxies disagree with the predictions of GRT. These observed anomalous rotational curves correspond to curves for galaxies that are much more massive than the observed visible matters for these galaxies. The observed path of travel of the Pioneer 10 spacecraft disagrees with the predicted path given by GRT. Pioneer 10 was observed to be in a state of accelerated motion toward the sun. Astronomers explain both of these anomalous observations by claiming the existence of a dark matter in space although such an existence of dark matters are not within the framework of GRT or the Standard Model. Model Mechanics explains both of these anomalous observations by positing the existence of a dark matter in the form of free non-orbiting S-Particles. In the case of Pioneer 10, the sun and all the planets contain a concentration of free non-orbiting S-Particles. When Pioneer 10 is outside the solar system the effect of these concentrations of free S-Particles contribute to an extra attractive force on the spacecraft and causes it to accelerate toward the sun.

8 Proposed Experiments To Detect Absolute Motions

Model Mechanics is based on the existence of the E-Matrix. Therefore absolute motions of objects in the E-Matrix should be detectable. However, numerous past attempts to detect absolute motion were failures. The most notable of these is the Michelson-Morley Experiment (MMX) [2]. In this experiment a light beam was split into two parts that were directed along the two arms of the instrument at right angles to each other, the two beams being reflected back to recombine and form interference fringes. Any shift in the interference fringes as the apparatus is rotated would mean the detection of absolute motion of the apparatus. To everyone's chagrin, the MMX produced a null result. However, the MMX null result does not mean that there is no absolute motion of the apparatus. In their interpretation of the MMX null result Michelson-Morley failed to ask the relevant question: What is the direction of absolute motion of the apparatus with respect to the defined horizontal plane of the light rays that will produce a null result for all the orientations of the horizontal arms? The answer to this question is: If the apparatus is moving vertically then a null result will be obtained for all the orientations of the horizontal arms. What this mean is that the MMX as designed is not capable of detecting the absolute motion of the apparatus. In order to detect absolute motion using the MMX, the plane of the arms must be oriented vertically. This conclusion is supported by the observed gravitational red shift (gravitational potential) in the vertical direction.

The new interpretation of the MMX null result gives rise to a new concept for the propagation of light as follows:

How does light get from point A to point B? The current assumption is that, locally, light travels in a straight line towards the target, and that, in a train of light pulses, the first pulse hits the target is the first one the source generated. These assumptions both make sense if the target is stationary relative to the light pulses, but if the target moves the second assumption could be erroneous. Fig 3 describes a thought experiment that is currently used by physicists to derive the time dilation equation. A light clock is constructed of two mirrors parallel to each other with light pulses bouncing between them. In one period of the clock, a light pulse travels up to the top mirror and

returns back to the bottom mirror. The diagram shows that the light pulse is presumed to travel a slant path when the light clock is in motion. This is not a realistic description of the actual event. It raises the question: How does light know when to follow a vertical path and when to follow one of the infinite numbers of slant paths? It is more realistic to say that light will always follow the perpendicular path on its way to the upper mirror. The reason is that the vertical path is the direction where all the light pulses are directed. Figure 4 shows this: the first pulse of a train of pulses follows the original path AB, but the pulse detected at "E" travels the path CE.

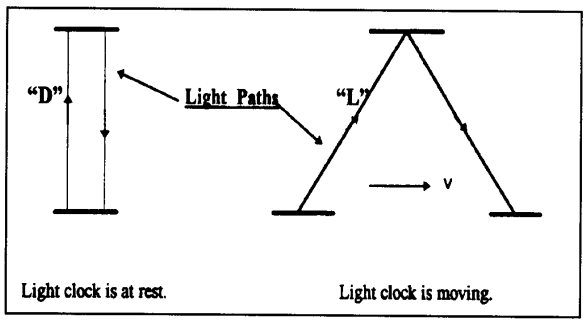

Figure 3. Light paths in a light clock at rest and in motion.

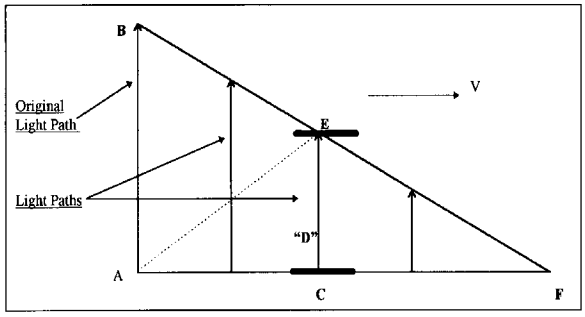

Figure 4. Current physics says that AE is the path that light follows to the upper mirror and the angle of this path is depended on the length AC that is depended on the speed of the light clock.

With this description of the light paths, the first pulse is never detected at "E." The light pulse detected at "E" is generated by the source at a later time. It turns out that this description of light paths is also capable of giving us the time dilation equation by using the Pythagorean theorem. The reason is that the original light path (AB) is equal to the assumed light path (AE) and both are the radii of a light sphere at the point of origin "A". It is noteworthy that as the speed of the mirrors approaches light speed a light pulse will take a longer time to reach the upper mirror. When the mirrors are moving at the speed of light, no light pulse is able to reach the upper mirror at all. Current physics interprets this situation as time standing still at the speed of light. The new interpretation is that time keeps on ticking at all speeds of the light clock. The amount of time (duration) passed depends on the length of the original light path AB divided by the speed of light 'c'. This new interpretation suggests that absolute time for a moving frame is not slowed or dilated as currently assumed. The specific amount of absolute time (duration) required for light to travel the original light path AB is equal in all frames. A light clock runs slow when it is in motion because it is not catching the first light pulses, but rather some later one. The lower elapsed time recorded by a moving clock because the passage of time is not fully detected when the clock is in a state of motion.

The new interpretation of the MMX null result and the new concept for the propagation of light enable us to design the following experiments to detect absolute motion:

Experimental Set Up:

1. Two sets of cesium clocks A1, A2 and B1, B2 are located at the middle of a 120 meters long straight rail track. Distances of 25 meters and 50 meters on both sides of the mid-point are marked off with a physical ruler.
2. Each set of clocks is equipped with a laser light sources and a beam splitter that splits the laser beam into two continuous beams. One beam goes to detector "A" and the other goes to detector "B".
3. Each set of clocks is equipped with a shutter that allows the two laser beams to pass through it for any desired time intervals.
4. Each set of clocks is equipped with a circular surface detector and the detecting surface can vary from 3 mm to 20 cm in diameter.
5. Each set of clock is equipped with a reflecting mirror.
6. A1 and B1 are not running. A2 and B2 are synchronized and running.

Experiment Group #1: To Detect The Absolute Motion of the Distant Clock at 50 Meters

1. Move both sets of clocks simultaneously in the opposite directions at a rate of 10 meters/day (1 day = 86,400 seconds) and stop them at the 25

meters marks (after 2.5 days). The clocks are now 50 meters apart.

2. Both detecting surfaces are set at 3mm in diameter.
3. Do the following experiments from A's location.
4. A trial of the experiment is consisted of an opening and closing of the shutter for a specific time interval. The following trials at the following time intervals are made: 1 second, 2 seconds, 3 seconds, 4 seconds, 5 seconds, 6 seconds, 7 seconds, 8 seconds, 9 seconds and 10 seconds. The trials are conducted from A's location.
5. Laser beam A will activate and de-activate clock A1 for each trial and the results are identified as T'a1, T'a2, T'a3, T'a4, T'a5, T'a6, T'a7, T'a8, T'a9 and T'a10.
6. Laser beam B will activate and de-activate clock B1 for each trial and the results are identified as T'b1, T'b2, T'b3, T'b4, T'b5, T'b6, T'b7, T'b8, T'b9 and T'b10.
7. The difference in activation time between clocks A1 and B1 for each trial is identified as follows: ΔT'1, ΔT'2, ΔT'3, ΔT'4, ΔT'5, ΔT'6, ΔT'7, ΔT'8, ΔT'9, and ΔT'10.
8. Increase the detecting surface to 20 cm in diameter then perform a trial using the 1-second time interval to establish that there is no difference in activation time between A1 and B1 for this large detecting surface. Now reduce the diameter of the detecting surface gradually to find the diameter where the activation time between A1 and B1 start to show a difference. Call this critical diameter D_{50}.
9. Cover the detecting surface completely with a 20 cm diameter dish. A slit of 2mm wide is cut from the center of the dish to the outer rim of the dish. Slowly rotate the dish to find the direction of absolute motion of the detector. That direction is evident when the slit is in line with the direction of absolute motion of the detector and activates the clock B1 for the same amount of time as the shutter opening and closing at A's location.
10. Repeat the above experiments from the "B" location.

The SRT Predictions For Group #1 Experiments:

- The activation time for the B1 clock is the same as that for the A1 clock for all trials.
- The difference in activation time between A1 and B1 is zero for each trial. ΔT'1=ΔT'2=ΔT'3=ΔT'4=ΔT'5=ΔT'6=ΔT'7=ΔT'8 =ΔT'9=ΔT'10=0.
- Increase the diameter of the detecting surface will have no effect on activation time on the B1 clock for each trial.
- There is no absolute motion of clock B1 and therefore there is no direction of absolute motion.
- Repeating the above experiments from the B location will get the same results as above.

The Model Mechanical Predictions For Group #1 Experiments:

- The activation time for the B1 clock is less than that for the A1 clock for each trial. This is due to the B1 clock is in a state of absolute motion in the vertical direction while the laser is in transit from A to B.
- The difference in activation time between A1 and B1 is the same for each trial and it is greater than zero.
- Increase the diameter of the detecting surface will bring the activation time for the B1 clock equal to that of the A1 clock.
- The absolute motion of the clock B1 (V_{50}) can be calculated using the following equation:
- $$V_{50} = \frac{D_{50}}{2\Delta T'1} \qquad (15)$$
- The direction of absolute motion of the B1 clock is vertical.
- Repeating the above experiments from the "B" location will get the same results as above.

Experiment Group #2: Measure the One-Way and Two-Way Speed of Light at 50 Meters

- The clocks A2 and B2 are 50 meters apart and are still synchronized according to SRT and Model Mechanics.
- Measure the one-way speed of light using clocks A2 and B2 from the "A" location.
- Measure the one-way speed of light using clocks B2 and A2 from the "B" location.
- Measure the two-way speed of light using clock A2.
- Measure the two-way speed of light using clock B2.

The SRT Predictions For Group #2 Experiments:

- The one-way speed of light is c as measured from the "A" location.
- The one-way speed of light is c as measured from the "B" location.
- The one-way speed of light is isotropic.
- The two-way speed of light is c using clock A2.
- The two-way speed of light is c using clock B2.
- The two-way speed of light is isotropic.

The Model Mechanical Predictions For Group #2 Experiments:

- The value for the one-way speed of light is less than c as measured from the "A" location.
- The value for the one-way speed of light is less than c as measured from the "B" location.
- The one-way speed of light is isotropic. In other words, the value for the one-way speed of light from A→B is equal to from B→A.
- The calculated value for the one-way speed of light can be make to equal to c by reducing the measured flight time by a factor of (ΔT'1).
- The two-way speed of light is c using clock A2.
- The two-way speed of light is c using clock B2.
- The two-way speed of light is isotropic.

Experiment Group #3: To Detect The Absolute Motion Of The Distant Clock At 100 Meters

1. Move both sets of clocks at the 25 meters marks simultaneously in the opposite directions at a rate of 10 meters/day and stop them at the 50 meters marks (after 2.5 days). The clocks are now 100 meters apart.
2. Both detecting surfaces are set at 3mm in diameter.
3. Do the following experiments from A's location.
4. A trial of the experiment is consisted of an opening and closing of the shutter for a specific time interval. The following trials at the following time intervals are made: 1 second, 2 seconds, 3 seconds, 4 seconds, 5 seconds, 6 seconds, 7 seconds, 8 seconds, 9 seconds and 10 seconds. The trials are conducted from A's location.
5. Laser beam A will activate and de-activate clock A1 for each trial and the results are identified as T"a1, T"a2, T"a3, T"a4, T"a5, T"a6, T"a7, T"a8, T"a9 and T"a10.
6. Laser beam B will activate and de-activate clock B1 for each trial and the results are identified as T"b1, T"b2, T"b3, T"b4, T"b5, T"b6, T"b7, T"b8, T"b9 and T"b10.
7. The difference in activation time between clocks A1 and B1 for each trial is identified as ΔT"1, ΔT"2, ΔT"3, ΔT"4, ΔT"5, ΔT"6, ΔT"7, ΔT"8, ΔT"9, and ΔT"10.
8. Increase the detecting surface to 20 cm in diameter then perform a trial using the 1-second time interval to establish that there is no difference in activation time between A1 and B1 for this large detecting surface. Now reduce the diameter of the detecting surface gradually to find the diameter where the activation time between A1 and B1 start to show a difference. Call this critical diameter D_{100}.
9. Cover the detecting surface completely with a 20 cm diameter dish. A slit of 3mm wide is cut from the center of the dish to the outer rim of the dish. Slowly rotate the dish to find the direction of absolute motion of the detector. That direction is evident when the slit is in line with the direction of absolute motion of the detector and activates the clock B1 for the same amount of time as the shutter opening and closing at A's location.
10. Repeat the above experiments from the "B" location.

The SRT Predictions For Group #3 Experiments:

- The difference in activation time between A1 and B1 is zero for each trial. ΔT"1=ΔT"2=ΔT"3=ΔT"4=ΔT"5=ΔT"6=ΔT"7=ΔT"8=ΔT"9=ΔT"10=0.
- Increase the diameter of the detecting surface will have no effect on activation time on the B1 clock for each trial.
- There is no absolute motion of clock B1 and therefore there is no direction of absolute motion.
- Repeating the above experiments from the B location will get the same results as above.

The Model Mechanical Predictions For Group #3 Experiments:

- The activation time for the A1 clock is greater than that for the B1 clock for each trial. This is due to the B1 clock is in a state of absolute motion in the vertical direction while the laser is in transit from A to B.

- The difference in activation time between A1 and B1 is the same for each trial.
- ΔT"1=ΔT"2=ΔT"3=ΔT"4=ΔT"5=ΔT"6=ΔT"7=ΔT"8=ΔT"9=ΔT"10
- Increase the diameter of the detecting surface will bring the activation time for the B1 clock equal to that of the A1 clock.
- The absolute motion of the clock B1 (V_{100}) can be calculated using the following equation:

$$V_{100} = \frac{D_{100}}{2\Delta T"1} \qquad (16)$$

- The direction of absolute motion of the B1 clock is vertical.
- Repeating the above experiments from the "B" location will get the same results as above.

Experiment Group #4: To Measure The One-Way And Two-Way Speed Of Light

1. The clocks A2 and B2 are 100 meters apart and are still synchronized according to SRT and Model Mechanics.
2. Measure the one-way speed of light using clocks A2 and B2 from the "A" location.
3. Measure the one-way speed of light using clocks B2 and A2 from the "B" location.
4. Measure the two-way speed of light using clock A2.
5. Measure the two-way speed of light using clock B2.

The SRT Predictions For Group #4 Experiments:

- The one-way speed of light is c as measured from the "A" location.
- The one-way speed of light is c as measured from the "B" location.
- The one-way speed of light is isotropic.
- The two-way speed of light is c using clock A2.
- The two-way speed of light is c using clock B2.
- The two-way speed of light is isotropic.

The Model Mechanical Predictions For Group #4 Experiments:

- The value for the one-way speed of light is less than c as measured from the "A" location.
- The value for the one-way speed of light is less than c as measured from the "B" location.
- The one-way speed of light is isotropic. In other words, the value for the one-way speed of light from A→B is equal to from B→A.
- The calculated value for the one-way speed of light can be make to equal to c by reducing the measured flight time by a factor of (ΔT"1).
- The two-way speed of light is c using clock A2.
- The two-way speed of light is c using clock B2.
- The two-way speed of light is isotropic.

9 Conclusions:

Model Mechanics leads to a new theory of relativity called IRT. IRT includes SRT as a subset. However, its equations are valid in all environments—including gravity. Model Mechanics also give rise to a new theory of gravity called DTG. Both IRT and DTG give matching predictions as GRT but they avoid the problematic predictions of GRT. A new interpretation of the MMX null results leads to a new concept for the propagation of light. This, in turn, enables us to design viable experiments to detect absolute motion. Performing these designed experiments will confirm the existence of absolute motion that, in turn, will provide a way to unify all of physic.

Correspondence to:
Ken H. Seto
KHS Publishing
260 Yorkshire Lane
Xenia, OH 45385, USA
Telephone: 937-372-5298
Email: kenseto@erinet.com
http://www.erinet.com/kenseto/book.html

References

[1] Seto KH. Unification of Physics. Journal of the Theoretics. pp 5-11, ttp://www.journaloftheoretics.com/Links/Papers/Seto.pdf
[2] Seto K.H. Unification of Physics. http://www.geocities.com/kn_seto/2005Unification.pdf
[3] Seto KH. The Physics of Absolute Motion. ISBN0-9647136-1-6, KHS Publishing, pp 57-70, http://www.erinet.com/kenseto/book.html

The New Concepts to Big Bang and to Black Holes: Both Had No Singularity at All (Part 2)

Dongsheng Zhang

Graduated in 1957 From Beijing University of Aeronautics and Astronautics. China.
Permanent address: 17 Pontiac Road, West Hartford, CT 06117-2129, U. S. A.
Email: ZhangDS12@hotmail.com; Telephone: 860-869-0741

Abstract: 1. Our Universe was born from Quantum Micro Black Holes (its mass ≈ 10^{-5} g), but not from Singularity or Big Bang of Singularity. 2. No Singularity existed in star-formed Schwarzchild's black holes, a steady mini black hole (its mass ≈ 10^{15} g) of long lifetime would certainly exist inside as a core to obstruct the collapse of energy-matters to become Singularity. The steady mini black hole (m_{om} ≈ 10^{15} g) in black holes instead of Singularity called by General Theory of Relativity (GTR) could resist the gravitational collapse. [Nature and Science. 2005;3(1):13-24].

Key Words: universe; singularity; big bang; black holes; Plank's era; cosmology

Part Two. No Singularity existed in star-formed Schwarzchild's black holes, a steady mini black hole (its mass ≈ 10^{15} g) of long lifetime would certainly exist inside as a core to obstruct the collapse of energy-matters to become Singularity.

Only Schwarzchild's star-formed BHs (no charges, no rotating and spherical symmetry) will be studied in this article below.

Introduction: Jean-pierre Luminet said: "Stephen W. Hawking and Roger Penrose, two scholars of Cambridge University in England, had proved in 1960s that Singularity is an indispensable component of General Theory of Relativity (GTR). It is unsure whether the finality of gravitational collapse for a real star would lead to the formation of a Black Hole (BH) with its Event Horizon. However, it is no doubt that the termination of gravitational collapse will inevitably cause Singularity in BH." <!>

According to GTR, any BH will be composed by three components. First, Event Horizon of BH is its boundary. Second, Singularity exists at the geometric center, R = 0, at which all energy-matters in BH would be contracted to infinity, and the space-time would be curved to infinity. Third, a real vacuum space is between Event Horizon and Singularity. It shows that Singularity is the existent premise of a BH. In addition, according to the explanations of GTR, time and space would exchange between each other in BH, the point at the center R = 0 would become the termination of time. After that, it would be "out of time". GTR could not explain the meaning of "out of time." <!> <3> <6> Thus, it can be seen, the description of GTR above would be inadequate inside BH. If concepts of GTR were correct, BH should disappear almost instantly with its establishment. Any Singularity that contains an infinite amount of energy and density at an infinitesimal point cannot exist too long. The mathematical equations of any theory should have their applied limits, just as the gas state equations cannot be applied to the boiling point of water. Since BHs can be found in universe and exist with long lifetime, the other suitable concepts gotten from many theories in this article should be accepted instead of sole GTR. (< >Reference Number.)

In part two of this article, it will be proved that, in any star-formed black hole (BH), a mini BH of mass (m_{om} ≈ 10^{15} g) would occupy the center as a solid core to prevent the energy-matters inside BH from collapse to become a Singularity. The mini BH of long lifetime would lead the whole BH to keep stability. The same numerical values of different physical parameters about mini BH are gotten from six formulas based on different current classical theories. It shows that the existence of mini BH (m_{om} ≈ 10^{15} g) is the true reality.

11. If mass (Mb) has collapsed to a Schwarzchild's BH, Rb is Schwarzchild's radius

According to the definition of GTR,

$R_b=2GM_b/C^2$ or $C^2=2GM_b/R_b$ (11a)

t_b is the passing time of light in BH from its Event Horizon to center, M_b is mass of BH,

$C \times t_b=R_b$, or $t_b=2GM_b/C^3$ (11b)

If $M_b = M_\theta$ (mass of sun), $t_b=2\times(6.67\times10^{-8})(2\times10^{33})/(3\times10^{10})^3=3\times10^{-5}$s, $R_b=C\times t_b=3$ km.

To understand the occurrence of a star-formed BH in universe, the contracting process of the original interstellar cloud (OIC) should be known at first. If OIC is in the state of thermodynamic equilibrium, the gas pressure intensity (P) should counterbalance its gravity (F). That is given according to Newton's mechanical equation and thermodynamics.

$dP/dR = -GM\rho/R^2$ <5> (11c)

$P = n\kappa T = \rho\kappa T/m_s$ (11d)

M--mass of OIC, R--radius of M, ρ--density of M, m_s--mass of a particle, T--temperature corresponding to R and M. G--gravitational constant, κ--Boltzmann's constant, n--number of particles in an unit volume.

In order to do the qualitative analysis, the precise solutions of formula (11c) need not to be gotten and are hardly solved. A qualitative solution should be given as below; α--coefficient

$\kappa T \neq GMm_s/R$, or $\alpha\kappa T = GMm_s/R$, (11e)

If $\kappa T < GMm_s/R$, $\alpha > 1$, OIC contracts.

If $\kappa T > GMm_s/R$, $\alpha < 1$, OIC expands.

If $\kappa T = GMm_s/R$, $\alpha = 1$, OIC keeps equilibrium.

Three ways can contract (R) in formula (11e); to decrease temperature (T), to increase mass (M) and to change the coefficient (α), (α) is related to structure, location and state in OIC.

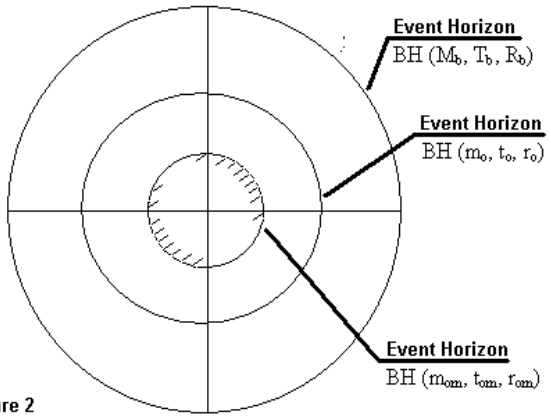

Figure 2

12. The mechanisms of objects to resist its gravitational collapse, Mθ --mass of sun

Universe itself is a gigantic BH (see part one before), if formulas (11c), (11d) and (11e) can be applied to the equilibrium of OIC in our universal BH, they may be used to research the equilibrium and the physical states in star-formed BHs too. No OIC in universe can directly contract to become a BH. In the processes of its contraction, there are many strong resistances. OIC contains about ¾ hydrogen (H_2). When an OIC of M_θ contracts to temperature over 10^7k in core with its gravity, the nuclear fusion will occur and keep a very long period. Any OIC of mass ($M \approx M_\theta$) can certainly attain to $T \approx 10^7$k of nuclear fusion with its gravitational contraction and form a more solid core of the higher temperature and density to resist the gravitational collapse of materials outside the core. <4>

After all (H_2) of mass (M_θ or more) in OIC had burned up, the burst of nova or supernova would take place. After that, the collapse of residues M_r of OIC would change into a compact object. M_r are just the dead bodies of a stars. In any compact object, a more solid core would become the antagonist to resist the gravitational collapse. Under the different conditions, the collapses of residues M_r of OIC would get the different outcomes: white dwarf ($M_r < 1.4M_\theta$--mass of sun), neutron star [$M_r \approx (3$ to $1.4M_\theta)$], BH ($M_r > 3M_\theta$) or a chunk of dust.<4> In nature, any object, body or particle has always a more solid core to resist the contraction of materials and simultaneously to attract the materials outside onto core to keep the stability of whole body, such as galaxy, star, cell, atom, etc. It will be without exception for BHs.

13. The stability and equilibrium of a star-formed BH (Suppose a BH had formed after nuclear fusion, 5Mθ>Mb≥1015g)

According to Hawking's theory of BH, the temperature (T_b) on the Event Horizon of BH is showed by formula (13a) below; M_b-mass of BH, M_θ-mass of sun, h-Plank's constant, κ-Boltzmann's constant, C-light speed,

$T_b = (C^3/4GM_b)\times(h/2\pi\kappa) \approx 0.4\times 10^{-6}M_\theta/M_b$ <2> (13a)

$R_b=2GM_b/C^2$, or $M_b/R_b=C^2/2G$ (11a)

$dP/dR = -GM\rho/R^2$ <5><7> (11c)

$P = n\kappa T = \rho\kappa T/m_s$ (11d)

$\alpha\ \kappa T = m_s\ GM/R$ (11e)

Five formulas above are all idealized. They will be applied in BHs effectively. They can jointly constitute the stability and equilibrium of a BH and reveal the macro physical states in a BH.

Formula (11a) is the necessary condition to construct a BH according to GTR. Formula (13a) is the necessary temperature on the Event Horizon of a BH derived from Hawking's theory of BH. Formula (11c) is an equilibrium equation between pressure intensity and gravity in any BH and can be simplified and idealized instead of Tolman-Oppenheimer-Volkoff's (TOV) equation.[7] Since TOV equation had been successfully applied to neutron stars, formula (11c) should be better used to BHs inside. Formula (11e) is a balance equation of a particle between gravitational potential energy and heat energy, it is not independent (α) is a coefficient depended on the state, structure and location in a BH. . Formula (11d) is the ideal (gas or ion plasma) state equation in BH. It will not need to know the microstructure in a BH in this article. The purpose of this article is to find out the simplistically special solution of formula (11c) in star-formed Schwarzchild's BH of spherical symmetry and to research the macro state or structure in BH.

Furthermore, five formulas come from the different theories. Thus, the explanations to BHs in this article are completely different with the conclusions of pure GTR.

Formulas (13aa), (11aa) below are derived from (13a), (11a) and have equally effective.

$T_b \times R_b = (C^3/4GM_b)(h/2\pi\kappa)(2GM_b/C^2) = Ch/4\pi\kappa \approx 0.1154$ cmk (13aa)

$M_b/R_b=m_o/r_o=C^2/2G\approx 0.675 \times 10^{28}g/cm\approx 10^{28}$g/cm, or $T_b \times M_b \approx 10^{27}$gk (11aa)

From formula (11aa), there is the equal potential energy in any BH with m_s = constant.

$P_b = P_o$ = constant, $P_b=m_sGM_b/R_b$, $P_o=m_sGm_o/r_o$ (13b)

P_o, m_o, r_o – parameters of a point in a BH (Figure 2),

Suppose the energy of each particle $\Delta E=\kappa T$, and $\Delta t \geq 2R/C$, R—Event Horizon of a BH,

$\Delta E \times \Delta t = \kappa T \times 2R/C$. Thus,

$T \times R \geq Ch/4\kappa\pi$ (13c)

(13aa) = (13c) (13d)

Formulas (13aa), (13d) express that the state on the Event Horizon of any BH exactly obeys the Uncertainty Principle of QM. The temperature (T_b) on the Event Horizon of a BH is too low. For example, to a BH of sun mass ($M_b=M_\theta$), $T_b= 0.4 \times 10^{-6}$ k.

(A). In any BH (mass = M_b), ($5M_0 > M_b > 10^{15}$g), there is always a small BH (m_o) inside,

In Figure 2 on above page, suppose a small BH in a BH, (M_b,T_b,R_b)--corresponding to mass, temperature and Schwarzchild's radius of BH; (m_o,r_o,t_o)--corresponding to mass, Schwarzchild's radius and temperature of the small BH inside.

Let $m_o=\beta_1 M_b$, $\beta_1 < 1$, β_1-coefficient,

$R_b = 2GM_b/C^2 = 2G \times m_o/(\beta_1 C^2)$ (13e)

If $R_b=r_o/\beta_1$, or $M_b/R_b= m_o/r_o = C^2/2G \approx 0.675\times 10^{28}$ g/cm can be proved, then BH (m_o,r_o,t_o) will be a really small BH (m_o) in BH (M_b).

First, from formulas (11a), if BH (m_o,r_o,t_o) were not a small BH in BH, two possibilities would happen. In case of $m_o/r_o > M_b/R_b$, so, $m_o/r_o > C^2/2G$, it is impossible, because $C^2/2G$ is the maximum. In case of $m_o/r_o < M_b/R_b$, as a result, the potential energy of m_s in BH (m_o) will be $P_o < P_b$ (potential energy of M_b). It indicates that all energy-matters in BH (M_b) will rush to its Event Horizon and lead to BH (M_b) disintegrated, that case is impossible too. Thus, the only way of a steady BH is $M_b/R_b= m_o/r_o = C^2/2G$, or $R_b= r_o/\beta_1$.

As a result, BH (m_o,r_o,t_o) is a really small BH in BH (M_b,R_b,T_b).

Second; Formula (11a) can be turned into

$m_sC^2/2=m_sGM_b/R$ (13f)

Formula (13f) indicates that, when a particle (m_s) drops onto the Event Horizon of a BH from infinity, its speed will attain the light speed (C), and its kinetic energy ($K_b=m_sC^2/2$) is equal to its potential energy ($P_b=m_sGM_b/R_b$), or $P_b=K_b$. However, after (m_s) enters inside of BH, (K_b) can keep only a constant with light speed (C). Thus, the potential energy (P_b) should keep a constant in BH too. The result in BH should be: $P_o=K_o$, or $m_o/r_o = C^2/2G = 0.675 \times 10^{28}$g/cm $= M_b/R_b$ or $R_b = r_o/\beta_1$. It is no doubt that (m_o,r_o,t_o) is a really small BH in BH (M_b,R_b,T_b).

The results above have also proved that formulas (11aa) and (13b) are perfectly correct.

The conclusion above is not relative to the Hawking's theory of BH.

It is said, according to pure GTR, once a BH (M_b) was formed, the various small BHs (m_o, r_o)would certainly appear in M_b. However, due to no way to obstruct $r_o \Rightarrow 0$, Singularity would inevitably appear in

BH. Besides, GTR can not solve the problems about temperature and lifetime of BHs.

$T_b=0.4\times10^{-6}M_\theta/M_b=0.4\times10^{-6}M_\theta(\beta_1/m_o)=\beta_1 t_o$ (13g)

$T_b \times R_b = (\beta_1 t_o)(r_o/\beta_1) = t_o \times r_o = 0.1154$cmk (13h)

Formula (13hd) expresses that (m_o, r_o, t_0) is a really small BH in BH (M_b) in accordance with Hawking's theory.

(B). According to Hawking's theory, in any small BH (m_o), a stable mini BH of ($m_{om}\approx10^{15}$g) can surely exist, it is a minimum BH.

First: According to Hawking's theory of BH, in the collapsing process of any star, its entropy always increased and its information capacity always decreased. Suppose Sm--original entropy before the collapse of a star, S_b--the entropy after collapsing, M_θ--mass of sun = 2×10^{33}g,

$S_b/S_m = 10^{18}M_b/M_\theta$ <2> (13i)

Jacob Bekinstein pointed out at the ideal conditions, $S_b = S_m$, or, the entropy did not change before and behind the collapse of a star, its mass M_b will be a minimum m_{om} of a mini BH.<2>

From (13i), $m_{om} = M_b/10^{18} = 2\times10^{33}/10^{18} = 10^{15}$g = mass of the mini BH, $\therefore\ m_{om} = 10^{15}$g (13j)

. Schwarzchild's radius r_{om} of m_{om} ($=10^{15}$g), $r_{om}=2Gm_{om}/C^2 =3\times10^{-13}$cm,(≈neutron radius),

$r_{om}=3\times10^{-13}$cm≠0, and r_{om} is the minimum size. Singularity cannot appear in any BH. Temperature t_{om} of m_{om}, $t_{om} = 0.1154/r_{om} = 0.38\times10^{12}$ k,

Second: The thermodynamic equilibrium between gravity (F) and pressure intensity (P) inside BH is gotten from the Newton's mechanics and thermodynamics.

From 2 page before, $dP/dR = -GM\rho/R^2$ (11c)

$P = n\kappa T = \rho\kappa T/m_s$ (11d)

From $M = 4\pi\rho R^3/3$, and from (13a),

$T = (C^3/4GM)\times(h/2\pi\kappa)$

$P = \rho\kappa T/m_s = (\kappa/m_s)\times(3M/4\pi R^3)\times(C^3/4GM)\times(h/2\pi\kappa) = 3hC^3/(32\pi^2GR^3m_s)$

$dP/dR = d[3hC^3/(32\pi^2GR^3m_s)]/dR = -(9hC^3)/(32\pi^2Gm_sR^4)$ (13ba)

$-GM\rho/R^2 = -(GM/R^2)\times(3M/4\pi R^3) = -(3G/4\pi R^3)\times(M^2/R^2)$,

from (11aa) $M_b/R_b=C^2/2G=M/R$,

So. $-GM\rho/R^2 = -3C^4/(16\pi GR^3)$ (13bb)

Take (13ba), (13bb) into (11c),

$(9hC^3)/(32\pi^2Gm_sR^4) = -3C^4/(16\pi GR^3)$

$\therefore\ 3h/(2\pi m_sR^4) = C/R^3$ (13bc)

$R = 3h/(2\pi Cm_s) = r_{om}$ (13bd)

$r_{om} = 3\times6.63\times10^{-27}/(2\pi\times3\times10^{10}\times1.67\times10^{-24})$

$\approx 0.63\times10^{-13}$cm

The numerical value of R is the same with the First section ($r_{om}=3\times10^{-13}$cm) above.

So, $R=0.63\times10^{-13}$cm ≈ $r_{om.}$= 3×10^{-13}cm = constant,

$T = 0.1154/R = 10^{12}$k = $t_{om.}$

From (11aa), (13aa),

$M = RC^2/2G = r_{om}C^2/2G = 0.43\times10^{15}$g ≈ $m_{om,}$

Formula (13bd) above is not relative to the mass of any BH (M_b). A sole value of (R) can be gotten in any BH, if any mass (mass > 10^{15}g) could collapse to become a BH. R= a constant ≈ r_{om} ≈ 0.63×10^{-13}cm**.** As a result, BH ($m_{om}\approx10^{15}$g) is the sole minimum BH in any BH and is a special solution to formula (11c). Except the mini BH, another points in BH cannot get the perfect equilibrium between the contracting gravity (F) and the pressure intensity (dP/dR). It is seen from formula (13bc), if (R) contracted to $R < r_{om}$, the result would be in mini BH, $dP/d(-R) > +GM\rho/R^2$, that case would be impossible to presence. Thus, in BH, $m_{om}=0.43\times10^{15}$g is the minimum BH. If $R > r_{om,}$ then $dP/d(-R) < +GM\rho/R^2$, the energy-matters in BH would have (13b1) the trend contracting to its center, but the mini BH (m_{om}) at the center as a solid core can counteract the surplus of the contracting gravity and obstruct the collapse of energy-matters in BH to become a Singularity. Thus, mini BH ($m_{om} = 10^{15}$g) is the smallest or minimum BH in any BH.

The lifetime τ_{om} of m_{om}, $\tau_{om}\approx10^{-27}\times m3om_{(S)}=10^{10}$ years.<2> Therefore, the mini BH ($m_{om}\approx10^{15}$ g) is very stable. Its lifetime of 10^{10} years is equal to the present age of our universe. In 1970s, many scientists endeavored to find out the primordial black holes of that size ($m\approx10^{15}$ g) coming from our baby universe, but their efforts were all in vain.

Density ρ_{om} of m_{om}, $m_{om} = 4\pi\rho_{om}r^3_{om}/3$, $\rho_{om}\approx10^{53}$g. The density of mini BH ($m_{om}\approx10^{15}$g) is very great. Thus, the mini BH cannot be formed from the direct collapse of a star in nature, but can only formed from the collapse of the energy-matters with great density in BH. It is said, mini BH was only formed closely after a BH had built up. It can only exist at the center of a star-formed BH with spherical symmetry, because the contracting gravities in Schwarzchild's BH are spherical symmetry.

The proton numbers n_{pom} of m_{om};

$n_{pom}=m_{om}/m_p=10^{15}/1.67\times10^{-24}=10^{39}$.

10^{39} = static electric force/gravitational force. It shows that 10^{39} neutrons broken up occupy the space of a present neutron. It is said, inside mini BH, the gravity between two closest particles is equal to the exclusive force of their electricity. The number 10^{39} is a mysterious number hidden in nature.

Third; Formulas (13aa), (11a) and (11e) as a group of simultaneous equations can be solved, and the sole solutions of M_b, T_b, R_b can be precisely gotten. From formulas (11e) and (11a), $\alpha\kappa T = m_sGM/R$, let $\alpha = 1$, then $R_b=2GM_b/C^2$, let T_b, R_b, M_b instead of T, M, R.

So, $T_b= m_sC^2/2\kappa =5.4\times10^{12}\ k = t_{om}$. (13be)

$R_b= 0.1154/T_b=0.2\times10^{-13}cm \approx r_{om},\neq o$. Thus, no Singularity can appear.

$M_b=R_bC^2/2G =0.13\times10^{15}g \approx m_{om}$.

The mini BH has the approximately equal numerical values of (m_{om},r_{om},t_{om}) in three sections above and is derived from six formulas of the different theories. ($\alpha = 1$) shows an ideal state. Formula (11e) expresses that the potential energy of a particle (m_s) ($P_{om}= m_sGm_{om}/r_{om}= m_sC^2/2$ = a maximum constant) in mini BH is exactly equal to its heat energy ($Q_{om}= \kappa t_{om}$) after its gravitational collapse. Thus, the heat energy (Q_{om}) is the highest one at the center of BH, and then ($m_{om}\approx10^{15}g$) is a minimum BH in any BH.

From formula (11e), if $\alpha < 1$, so $\kappa T > m_sGM/R$, that condition is the same with $dP/d(-R) > +GM\rho/R$.) above. If $\alpha > 1$, so $\kappa T < m_sGM/R$, that condition is the same with $dP/d(-R) < +GM\rho/R$ above.

(C). The space in BH (M_b) is full of energy-matters; the states and structures in BH

According to GTR, the space between Event Horizon of a BH and Singularity at its center is a pure vacuum. That corollary of pure GTR would be negated by the concepts in this article below.

Suppose another BH (m_o,t_o,r_o) in the space between the BH (M_b,T_b,R_b) and the mini BH $(m_{om},t_{om},r_{om},)$. Let $m_o= \beta_2 M_b$, β_2--coefficient, $\beta_2 < 1$. From formulas (11a), (13a) and (13aa),

$t_o = T_b/\beta_2$, $r_o = \beta_2R_b$, $to\times ro = (T_b/\beta_2)\times\beta_2R_b = T_b \times R_b = 0.1154cmk$,

The results above show that (m_o,t_o,r_o) is a real small BH between Event Horizon and the mini BH at the center. By the same method, it can be proved that there are innumerable small BHs full of the space in BH with the countless β_2. Every small BH composes a concentric sphere with the same radius and contains all smaller BHs in its Event Horizon. Therefore, the space inside Event Horizon of BH (M_b,T_b,R_b) is full of energy-matters and not a vacuum state.

The states and structure in a BH can be expressed by some parameters relative to the different radius r_o in BH (M_b). (suppose exterior BH --M_θ,R_b,T_b, mini BH--$m_{om,}t_{om},r_{om}$, medium BH--m_o,r_o,t_o, τ--lifetime, ρ--density,)

r_o in (M_θ), r_o= radius of m_o, $r_{om}\approx10^{-13}cm$, $R_b\approx3\times10^{5}cm$

mass, $m_o=(C^2/2G)\times r_{o,}$ $m_{om}\approx10^{15}g$, $M_\theta\approx2\times10^{33}g$

t_o of (m_o), $t_o = 0.1154/r_{o,}$ $t_{om}\approx10^{12}k$, $T_b\approx10^{-6}k$

ρ_o of (m_o), $\rho_o=(3C^2/8\pi G)/r_o^2$, $\rho_{om}\approx10^{53}g/cm^3$, $\rho_b\approx10^{17}g/cm^3$

τ_o of (m_o),$\tau_o=(10^{-27}C^6/8G^3)\times r_o^3$, $\tau_{om}\approx10^{10}$ yrs, $\tau_b\approx10^{65}$yrs

(D). How can the different temperatures (t_o) be changed with the different radius (r_o) in a star-formed BH in accordance with the Hawking's theory of BH?

The approximately equivalent numerical values of mini BH (m_{om}, $r_{om,}$ t_{om}) in above three sections of (B) are gotten under the condition of every particle possessed the same mass ($m_s=1.67\times10^{-24}g$ = mass of a proton or a nucleon,). Is it really? Why is it so? Will the mass of (m_s) be the maximum particles of long lifetime in any BH and in nature? (see 19th paragraph)

Firstly; If $m_s\neq$ a constant and particles m_s of different mass in nature were all stable particles of enough long lifetime, from formula (13aa) $t_o = 0.1154/r_o$, formula (13bd) $R= r_{om}=3h/(2\pi Cm_s) =0.63\times10^{-13}cm$, and formula (11aa) $m_{om}= r_{om}C^2/2G$. So, (r_{om}) or (m_{om}) or (t_{om}) of mini BH is decided only by every same (m_s) in BH. As a result, the different (m_s) in nature will lead to the formation of the different mini BHs (m_{om}) in BHs. That condition does not accord with reality.

However, the real condition in our universe is that m_s = mass of proton $=1.67\times10^{-24}g$ = constant. Protons are the largest and most stable particles in nature; its lifetime is over 10^{30}years. Thus, in our universe, at the center of all star-formed BHs, the same mini BH ($m_{om}\approx10^{15}g$) would certainly exist.

Suppose there were enough different kinds of stable particles m_o (mass $m_o < m_s$) other than m_s (= proton) in a star-formed BH, the real structure in BH should be: a mini BH ($m_{om}\approx10^{15}g$) formed by m_s at the center, particles m_o lighter than m_s would occupy the space between mini BH and Event Horizon. The lighter particles would locate the place of the bigger radius of BH r_o. The lightest particles are on Event Horizon. Thus, temperature t_o of any radius r_o in a BH could

accord with demand of Hawking's theory, because formula (11aa) shows, $t_o \times m_o = 10^{27}$gk.

Secondly; Under the condition of all $m_s=1.67\times10^{-24}$g = a constant = mass of a proton in a star-formed BH, mini BH (r_{om}) formed by enough m_s at the center has the highest temperature (t_{om}), and Event Horizon (R_b) has the lowest temperature (T_b). Thus, at different place of radius ($r_o > r_{om}$) in BH, surplus m_s except m_s in mini BH would spread in space between mini BH and Event Horizon. For attaining the demand of Hawking's theory to temperature t_o on different r_o, the bigger r_o is, the lower density ρ_o should have. Thus, the different temperature on different radius could accord with Hawking's theory.

Two conditions above may simultaneously exist in actual star-formed BHs.

(E). The exchange of energy-matters through Event Horizon, unstableness of the Event Horizon of BH

In any BH (M_b) ($5M_\theta > M_b > 10^{15}$g), energy emissions are extremely low. The exchange of energy-matters passed only through Event Horizon would lead to Event Horizon oscillated. From formulas (11a) $R_b = 2GM_b/C^2$, and (13aa) $T_bR_b = 0.1154$, If the temperature on Event Horizon is lower than environment outside, BH can take in energy-matters outside and simultaneously increase (M_b), lengthen (R_b) and lower (T_b). That condition will never stop until taking in all energy-matters outside. It is the same condition for a BH to take in materials outside or collide with the star objects. In addition, according to Hawking's theory, if the temperature on Event Horizon is higher than the temperature of its environment outside, BH can radiate energy-matters to outside. It leads to the decrease in (M_b), (R_b), and to the increase in (T_b) and (ρ_b) (density of BH). The process of radiating energy-matters is a contracting process onto the mini BH from Event Horizon.[1] A BH is composed by the infinite small BHs of concentric spheres with different r_o. If a BH nonstop radiates energy-matters to outside, its concentric spheres will be shrink and split off from Event Horizon to mini BH layer by layer. The finality of the disappearance of whole BH would be the last explosion of gradually shrunk mini BH with emitting the strongest γ-rays and x-rays.[1][4]

The character of any BH is always nonstop neither emitting energy to outside nor taking in energy-matters from outside until its final vanish, its Event Horizon would be oscillated nonstop.

According to Hawking's theory, the rate of radiating energy of a BH is:

$$dE/dt \approx 10^{46} M^{-2} \text{ erg/s}, \quad (13k)$$ [2]

Suppose $M = M_\theta = 2\times10^{33}$g, $dE/dt \approx 10^{-20}$ erg/s, based on such extremely tiny rate, a BH of sun mass (M_θ) needs about 10^{65}years to radiate out all its mass. Lifetime τ_b of a sun mass (M_θ) BH;

$$\tau_b \approx 10^{-27} M_b^3(s) = 10^{-27} M_\theta^3 = 10^{-27} \times (2\times10^{33})^3 \approx 8\times10^{72} \text{ s} \approx 10^{65} \text{ years}, \quad (13l)$$ [2]

In reality, the strong gravitational field of star-formed BH can almost absorb in energy-matters from its surrounding, and its radiation speed is extremely slow, BH mostly expands its size, except that its surrounding has become a vacuum state or the temperature of surrounding is lower than temperature of Event Horizon of BH.

Right now, whether BHs would emit energy-matters with other ways except Hawking's radiations remains a question.

(F). The formation of BH, its mass = M_b, , ($5M_\theta > M_b \geq 10^{15}$ g)

As above-mentioned, the stability and equilibrium in BH (M_b) of ($5M_\theta > M_b \geq 10^{15}$g) have been studied. It is no doubt that $M_b \geq (10^{15}\text{g} = m_{om})$ should be right. Why should ($M_b < 5 M_\theta$) be right too? For building up a star-formed BH, the density of BH must be greater than the density of the neutron star $\rho_n \approx 10^{15}$g/cm^3. Suppose the density of BH $\rho_b \geq \rho_n \approx 10^{15}$g/cm^3,

From formula (11a), $R_b = C[3/(8\pi G\rho_n)]^{1/2}$

$=0.423\times10^{-4}C$, $M_b = \rho_n R_b^3 4\pi/3 = 8.5\times10^{33}\text{g} \approx 5 M_\theta$

The simple calculation above shows that the density of a BH (mass $M_b < 5M_\theta$) would be $\rho_b > \rho_n \approx 10^{15}$g/cm^3. At that state, neutrons would be broken up and become quarks. That is to say, in the limits of ($5M_\theta > M_b \geq 10^{15}$g), there would be small BHs or quark stars inside or a mini BH at the center. Neutron stars cannot appear. Right now, it is uncertain whether quark stars could exist and have the quark degeneracy to resist the gravitational collapse, how quark star turns into BH and what limits of density should be had by quark stars. In any case, there is no Singularity at all.

14. The formation of BH (Mb) in limit of (105Mθ > Mb>5Mθ) (Suppose BH had established after nuclear fusion)

With the same analysis above, the density of the white dwarf is about $\rho_w \approx 10^6 g/cm^3$. The Schwazchild's radius R_b of BH with the density ρ_w is:

$R_b = C\times(3/8\pi G\rho_w)^{1/2} \approx 1.3C$, $M_b = 4\pi\rho_w R_b^3/3 \approx 2.65\times10^{38} g \approx 10^5 M_\theta$,

The simple calculations above express that in BH (M_b) of ($10^5 M_\theta > M_b > 5M_\theta$), either neutron star or BH might presence. If BH appeared, a mini BH would exist at the center, but the white dwarf would hardly appear. Probably, with taking in energy-matters from its surroundings, neutron star would become a quark star or a BH. Right now, it is not known what process and mechanism are necessary for the change from a neutron star into a quark star or into a BH.

15. The structure in BH (Mb) of ($105M\theta < Mb < 1023M\theta$) ($1023M\theta$ is the total mass of our present universe in its Event Horizon)

Such immense BH looks like our present universe. In our universal BH, the different locations can attain the different relative stability and equilibrium, which can obey the formulas (11a), (11e) and (13a). Everything except Singularity may appear and had existed in our universe. Singularity, which possesses the infinity of some physical quantities, is impossible to attain and keep the relative stability and equilibrium of its inside, so. Singularity has no possibility to appear.

Recently, many super-massive BHs of mass ($M_b \approx 10^9 M_\theta$) were discovered in universal space. According to calculation, its density on average is about $\rho_s \approx 0.0183 g/cm^3$. In such BH, the different location can get the different stability and equilibrium to accord with formula (11e) and formulas (11a), (13a). Thus, anything could appear in it; the dust clouds, nuclear fusion, white dwarfs, neutron stars, BHs, etc, except Singularity.

In any case, within the universal endless evolution, after all H_2 in universe burn away, everything in universe included white dwarfs and neutron stars will finally turn into BHs. Along with the establishment of a BH, a small stable BH would inevitably appear and exist inside BH as a solid core to obstruct the gravitational collapse of the energy-matters. Through the extremely long evolution, all BHs will disappear with the quantum vaporization (Hawking's radiation) according to Hawking's theory of BH.

16. The further explanations and two possible models of BHs

In above-mentioned paragraphs, formulas (13a), (13aa), (13i), (13k), and (13l) all come from Hawking's theory about BHs. All BHs collapsed from the mass of few stars and came from broken neutrons, which are in the state of subatomic particles or quantization. Thus, applying Hawking's formulas in this article should be correct and suitable.

In reality, without Hawking's theory of BH, according to deduction of pure GTR, the small BHs or the mini BH might appear and exist in any BH. [See sections (A) of paragraph 13 above].

There would be two possible models of BHs and two possible different destinies of BHs.

First, under the condition of that, no energy-matters radiate out permanently from BH (M_b), suppose the appearance of various small BHs (m_o, r_o, t_o) except Singularity appeared in a BH [see section (A) of paragraph 13], BH might permanently exist in nature. However, a BH could only increase its masses and size with taking in energy-matters or other objects from outside, after that, it would only become an absolutely bigger BH and keep the same size forever. Thus, all BHs would have the infinite lifetime and would be eternal beings in nature. Is it possible in universe? Another condition might be the appearance of Singularity in BH, it would lead to instant vanish of whole BH. Both conditions above have no possibility to appear in nature. Two wrong conclusions can be drawn from the principles of GTR, Newton's mechanics except Hawking's theory of BH.

Second, under the condition of that, the energy-matters can radiate out from BH, after the appearance of mini BH (m_{om}, r_{om}, t_{om}) except Singularity in a BH, mass of BH will decrease with energy-matters radiated out. Although BH could take in all energy-matters outside, after that, BH will gradually radiate out all energy-matters and disappear with the last explosion of mini BH. The limited lifetime of BH can be calculated from formula (13l). That result can be mainly gotten from Hawking's theory of BH and associated with Newton's mechanics, thermodynamics and GTR. In such a model of BH, the different radius (r_o) would have the different temperature (t_o). The new concepts in this article accord with the structures of above model.

17. Conclusions taken out from applying many current classical theories and formulas

(A). Mini BH [$m_{om} \approx 10^{15}$ g, $r_{om} = 3h/(2\pi C m_s)$] is a special solution of formula (11c) [$dP/dR = -$

$GM\rho/R^2$], which can be considered as the simplified Tolman-Oppenheimer-Volkoff's equation.[7]

The simple analyses above show that pure GTR has no way to solve problems in BH, especially Singularity. In substantiality, principles and equations of GTR are just the space-time geometry with four dimensionalities instead of gravity, and are without thermodynamic effect. Therefore, inside BH described by pure GTR, due to no antagonistic force produced by the thermodynamic effect, the gravitational collapse would inevitably lead to appearance of Singularity**.** If there had been no Hawking's theory about BH, there could be no way to find out the mini BHs (mass$\approx 10^{15}$g) possessing stability and long lifetime. Just such mini BH can obstruct the occurrence of Singularity in BH. A new formula [$r_{om} = 3h / (2\pi Cm_s)$…(13bd)] of mini BH as a special solution to (11c) can be precisely gotten [see paragraph 13 (B)]. Once thermodynamic effect had been applied to GTR equation, which would become TOV equation. However, TOV equation is too complicated and has no additional temperature restraints, it cannot be solved in BHs right now. In this article, formula (13a) [$T_b = 0.4\times 10^{-6}M_\theta/M_b$] is used as the additional temperature conditions to (11c), hence formula (11c) can be solved. Without Hawking's theory of BH, there could be no way to know the lifetime of any size of BHs, in addition, Hawking's formulas (13k),(13l) can insure the stability and long lifetime of mini BH. Just from Hawking's theories of BHs, it has been known that BHs can change its energy-matters with its surroundings. Now, BHs have become the living bodies from the dead bodies in the past.

The Hawking's theory about BH extricates the crisis of pure GTR about Singularity in BH. The same condition had already happened in atoms. Just Uncertainty Principle of Quantum Mechanics has obstructed all electrons in our universe from dropping into atomic nuclei so that we can live in an admirable present world.

(B). In any star-formed BH, the equilibrium between gravity and thermodynamics can certainly lead to the occurrence of a mini BH ($m_{om} \approx 10^{15}$g) formed by stable protons at its center, mass of mini BH is decided by mass of proton.

Mini BH is a perfect equilibrium body; it has extremely long lifetime (10^{10}years) and posses the greatest density. Mini BH would become a solid core to obstruct the collapse of energy-matters in BH to become Singularity. In nature, anybody has its solid core or its bone to support and attract the materials outside the core. There will be no exception for BHs. From formula (13bd)-- $3h/(2\pi Cm_s)$, the size r_{om} of mini BH is only decided by m_s (mass of proton). In nature, protons have the longest lifetime and stability. The lifetime of protons $L_p \approx 10^{30}$years >>the lifetime of mini BHs 10^{10}years, but L_p << the lifetime of star-formed BHs 10^{65}years. Right now, in the final analysis, the stability of mini BH may probably be decided by the stability of protons. The age of present universe is about 10^{10}years, it will not be known how will be the evolution of our universe after disappearance of protons.

From six formulas of different classical theories, the same values of every physical parameters of BHs have been exactly gotten. It is said, four physical parameters (m_{om}, t_{om}, r_{om}, m_s) of mini BH can be exactly gotten from four independent formulas below:

First, from formula (13i) [$S_b/S_m = 10^{18}M_b/M_\theta$], $m_{om} \approx 10^{15}$g can be got.

Second, from formula (11a) [$R_b = 2GM_b/C^2$], $r_{om} \approx 3\times 10^{-13}$cm can be got.

Third, from formula (13a) [$T_b \approx 0.4\times 10^{-6}M_\theta/M_b$], $t_{om} \approx 10^{12}$k can be got.

Fourth, from formula (13bd) [$r_{om} = 3h / (2\pi Cm_s)$], $m_s = 1.67\times 10^{-24}$g = mass of proton.

Here the value of m_s can be exactly calculated out. It has important significance. Formula (11e) can be used for checking the calculated figures m_s and t_{om} above, the results are exactly right and precisely accord with all calculated results. It has perfectly proved that, the actual existence of mini BH and its physical state in BH are completely consistent with all laws of classical theories applied before as well as the natural reality, i. e m_s = mass of proton = $1{,}67 \times 10^{-24}$g. If no mini BH at the center had successfully obstructed the collapse of gravity of energy-matter in star-formed BH, star-formed BHs would have no possibility to exist in nature.

It has clearly showed that, just protons (m_s) have excessive stability and long lifetime, the formations and existence of mini BHs are the inevitable result of gravitational collapse.

(C). In space of a star-formed BH, it is full of energy-matters, not a vacuum. That conclusion has important significance for mankind.

Structure of the star-formed Schwarzchild's BHs inside are composed by countless small BHs of concentrically sphere layer by layer, the mini BH (m_{om}

$\approx 10^{15}$g) is at the center. There are two completely different kinds of BHs in nature, one kind is star-formed BHs, another kind is gigantic BH, such as our universal BH and super-massive BHs. Now that the space in star-formed BH is full of materials, not a vacuum; the space of universal BH with very low density should more be full of materials. People cannot directly see BHs only from their outside, so, BHs are absolutely black bodies and so-called BHs. However, once mankind and energy-matters could live in the space of same character in a gigantic BH, that energy-matters would be visible for mankind. That is the reason that, mankind in the universal BH could have researched and detected the various interior states and structures of universe as a BH. It shows that the new concepts about BH in this article accord with the reality. Therefore, The inside of a BH is not black.

(D). Star-formed BH is a simple object in nature.

In all parameters of physical states of a BH ($M_b, T_b, R_b, \tau_b, \rho_b, \ldots$etc), once a parameter, such as M_b, is firstly decided, correspondingly, a sole value of all other parameters is decided by M_b. Thus, in reality, star-formed BH is a simple object in nature. BH is not the mysterious objects at all but only the object unknown by people in the past.

(E). Event Horizon of BH would be always oscillated.

A BH is always nonstop either to emit energy (Hawking's radiation) to outside, and to contract its size until its disappearance with last explosion, or to take in materials from outside and to increase in mass and size until outside become vacuum state. Thus, Event Horizon of BH would be always oscillated. BHs are very brisk objects and can be indirectly detected, but not the dead black bodies.

(F). Any BH would be a real BH forever until its final vanish.

Once a BH has formed, however the mass of that BH is, no matter whether it absorbs in materials from outside or radiates energy to outside, it would be a real BH forever until its final vanish.

18. The original universal small BHs (its mass = mass of mini BH) had no possibility to have existed

According to analyses above, the lifetime of mini BH ($m_{om} \approx 10^{15}$g, $r_{om} \approx 10^{-13}$ cm, $t_{om} \approx 10^{12}$ k) is about 10^{10}years, and equal to the present age of our universe. In 1970s, many scientists attempted to observe out such small BHs in universal space, but their efforts were in vain. Let's review our universal evolution at first. Look back the numerical values on figure (1) and chart 1 of Appendix A in part one, at the condition of temperature $T = 10^{12}$ k, corresponding time $t = 10^{-4}$ s, $\rho_c \approx 1.8\times 10^{14}$ g/cm^3. It was said, at that time, the whole expanding universe was like a gigantic neutron star. However, the density $\rho_{om} \approx 10^{53}$g/cm^3 of mini BH($m_{om} \approx 10^{15}$ g) is too high, such ultra-high density were impossible to exist in an expanding universe at time of $t = 10^{-4}$ s. At the another condition, when the evolution of our expanding universe was at the density of ($\rho_c \approx 10^{53}$ g/cm^3), the corresponding universal temperature $T \approx 10^{20}$ k and $t \approx 10^{-23}$ s, but the temperature (t_{om}) of mini BHs is about 10^{12} k, so, mini BHs ($m_{om} \approx 10^{15}$ g) had no possibility to appear at that time too. Where is the intersection between temperature T of the universal evolution and temperature T_b of the different BHs?

From formulas of BHs before, $M_b/R_b = C^2/3G$, $T_b \times R_b = 0.1154$, $M_b = 4\pi\rho_b R^3/3$. So,

$$\rho_b = (3C^2\times T_b^2)/(8\pi G\times 0.1154^2) \quad (18a)$$

In universal evolution of part one, $\rho_c = 3/(8\pi G t^2)$,

$$Tt^{1/2} = k_1 \approx 10^{10}, \text{ so, } \rho_c = 3T^4/(8\pi G k_1^4) \quad (18b)$$

In case $\rho_b = \rho_c$ and $T_b = T$, the double T 's solutions (T_1, T_2) can be gotten as below;

$$T^4/k_1^4 = C^2T_b^2/0.1154^2 \quad (18c)$$

$$T_1 = Ck_1^2/0.1154 = 3\times 10^{10}\times(10^{10})^2/0.1154 \approx 10^{32}$$

$$k(k_1 \approx 10^{10}) \quad (18d)$$

$$T_2 = 0 \quad (18e)$$

Formula (18d) [$T_1 \approx 10^{32}$ k] shows that, only under the condition of 10^{32}k, temperature of BHs T_b was equal to temperature of the universal genesis T, the states of the universal small BHs were exactly consistent with the states of universe at the beginning of Plank's Era. From part one, at that moment, all quantum micro BHs ($m_f \approx 10^{-5}$ g, $T_b \approx 10^{32}$ k, $r_b \approx 10^{-33}$ cm) had jointly obstructed appearance of Singularity at genesis of original universe. That is a sole intersection between T and T_b in the universal endless evolution. Formula (18e) [$T_2 = 0$] expresses no physical meaning or the intersection of T and T_b will be in the unlimited remote future, because ($T_2 = 0$) is almost impossible or inconceivable. Is that result a coincident or an inevitable?

Another conclusion is obvious. In universal endless evolution, it was no possible to cause and leave some kinds of originally small BHs in space firstly and then to take in matters outside growing up to a star. Thus, no

original universal small BHs could become embryos of stars or galaxies at all in the past.

19. The composition, the state and the vanishing process of mini BH (mom ≈ 1015g) in star- formed BH, the commonality between universe and BHs

According to analyses before, originally universal mini BHs ($m_{om} \approx 10^{15}$ g) would be impossible to exist in universe, mini BHs could only form and exist inside star-formed BHs. Mini BH ($m_{om} \approx 10^{15}$ g) is a body of perfect equilibrium between thermodynamics and gravity, it has very long lifetime. The space outside its Event Horizon is full of energy-matters. Mini BH not only emits energy through its Event Horizon into outside, but also absorbs in energy-matters from outside, so that mini BH can keep dynamical equilibrium with outside and its stability. However, the temperature on Event Horizon of a star-formed BH is too low($<10^{-6}$ k). Thus, star-formed BH would almost take in energy-matters from outside, increase in its size and mass. Only temperature on Event Horizon of star-formed BH is a little higher than temperature of outside, such a BH will nonstop radiate energy to outside and decrease in its size and mass until mini BH may become a naked body. According to above calculation, if a BH of mass = M_θ could emit energy-matter over (10^{65} – 10^{10}) years, its mini BH would be naked out. What will happen next? What will be the final destiny of mini BH? See analyses below.

(A). The composition of mini BH inside

Formula(13bd), $R_b=3h/(2\pi Cm_s)=r_{om}$ (13bd)

Formula (13aa), $T_b \times R_b \approx 0.1154$ cmk (13aa)

Formula (11aa), $M_b/R_b \approx 0.675\times10^{28}$ g/cm (11aa)

Formula (13l), $\tau_b \approx 10^{-27} M_b^{3}$ (s) (13l)

The values of physical parameters of mini BH have been gotten in 13th paragraph, $m_{om}\approx10^{15}$ g, $r_{om} \approx 10^{-13}$cm, $t_{om} \approx 10^{12}$k, $\tau_{om} \approx 10^{10}$yrs, $\rho_{om} \approx 10^{53}$g/cm^3, $m_s = 1.67\times10^{-24}$g. Those values are gotten under the condition of every particle ($m_s = 1.67\times10^{-24}$ g ≈ mass of a proton or a quark) in mini BH.

At the moment of formation of star-formed BH, neutrons in neutron star must be broken up before a BH formed. From (13bd), perfect equilibrium and stability between gravity and thermodynamics in mini BH is only depend on mass of m_s (quark or proton). The heavier m_s is, the smaller mini BH will be. Are there heavier particles > m_s in mini BH? Impossible. If by any chance heavier particles appeared, they would have shorter lifetime and disintegrate sooner. Thus, in mini BHs, particles of (mass ≈ proton) would steadily exist, its Event Horizon like a wall separated itself from its outside. Protons have extremely long lifetime($\approx10^{30}$yrs).

(B). The vanishing process of mini BHs

After all energy-matters outside Event Horizon of a mini BH were emitted away, mini BH would become naked. Now, we know no way can stop emitting energy (Hawking's radiation) to a naked mini BH, because its size is so small as a present neutron and its temperature is high to 10^{12}k. Thus, mini BH cannot choose but nonstop emit energy to outside, at the same time, its size and mass m_{om} are decreased and its temperature t_{om} are increased according to properties of BH. From (13bd), mass of particles m_s must grow up as the size r_{om} shrunk as to attempt keeping the equilibrium of shrunken mini BH. The characteristic of BH is that, once a BH had made up, no matter whether it enlarge or shrink, it would keep a BH forever until it vanished at the last moment. What is a last limit of size r_{om} shortened? The answer is: once mini BHs shrink to its mass of $m_{om} \approx 10^{-5}$g, i.e. $m_{om} = m_t \approx 10^{-5}$g, mini BH would shrink no more and vanish at a explosion, here m_t is the same one with original Quantum Micro Black Holes (QMBH) in part one of this article. Check up values of all parameters of m_t as below; $m_t \approx 10^{-5}$ g, $r_b\approx 10^{-33}$cm, $T_b \approx 10^{32}$ k, $\tau_b \approx 10^{-43}$ s, $\rho_b \approx 10^{92}$ g/cm^3. Applying formulas (13aa),(11aa),(13l), when mini BH ($m_{om} \approx 10^{15}$g) shrink to ($m_t \approx 10^{-5}$g), all values of other parameters of m_{om} after shrinking are respectively equal to that of m_t, such as $r_{om} = r_b\approx 10^{-33}$cm. Now calculating m_s in m_{om} from (13bd),

$m_s = 3h/(2\pi Cr_{om}) = 3\times6.63\times10^{-27}/(2\pi\times3\times10^{10}\times10^{-33}) \approx 10^{-5}$ g ≈ m_t,

Calculation above expresses that, once m_{om} shrinks to $m_t \approx 10^{-5}$ g, then, $m_{om} = m_s = m_t \approx 10^{-5}$ g. It is said, whole Quantum Micro Black Holes (QMBH) is just equal to single particle m_s. Thus, QMBH(m_t) would be impossible to shrink any more, according to (11aa), r_{om} would shorten with decease in m_t and lead increase in m_s, as a result, $m_s > m_t$, it is absolutely impossible. Could a leg of a person be heavier than his whole body? Thus, any particle ($m_s = m_t \approx 10^{-5}$ g) of $r_{om} \approx 10^{-33}$cm cannot choose but last vanish at an explosion in 10^{32}k. That is the last destiny of mini BH ($m_{om}\approx 10^{-5}$g) as well as all BHs. It has been proved once more that, universe absolutely was not born from Singularity and there would absolutely have no Singularity in any BH.

The vanishing conditions between mini BH after shrinking to $m_t \approx 10^{-5}$ g and the big contraction of pre-universe are completely different. Mini BH is just a single particle and emit energy to outside before its vanish, no new thing can be born after its explosion. However, collapse of pre-universe was extruded by countless particles between each other, and our new universe could emerge from ruins of pre-universe, no collection of enormous energy, no birth of our universe.

Analysis above indicates a possibly vanishing process of mini BHs or a possibly destiny of mini BHs. However, the age of our universe is about 10^{10}years. According to modern physical theory, once the age of our universe was beyond 10^{30} years, all protons would vanish with their decay. Is it true? How will be the state and structure of our universe after protons have disappeared?

(C). About the artificial bombs of mini BHs

Some Russian scientists had advertised to produce artificial bombs of mini BHs or so-called Oton. It was not known how they got the exactly calculated numerical values about such bombs. It had been pointed out before that, in reality, BHs are the simplest bodies, once one physical parameter of BH is decided, all others will be respectively and solely decided by the first. For example, according to the stipulation of Russian scientists, mass of 1 Oton = mass of 40 atoms = $40\times1.67\times10^{-24}$g $\approx10^{-22}$g = m_{ot}, correspondingly, from (13aa),(11aa),(13l),(13bd) above, $r_{ot} \approx 10^{-50}$cm, $t_{ot} \approx 10^{51}$k ($\approx10^{38}$GeV), $\tau_{ot} \approx 10^{-93}$s, but mass of particle $m_{sot} \approx 10^{14}$g. Utterly absurdly, ($m_{sot} \approx 10^{14}$g)>>($m_{ot} \approx 10^{-22}$g). In addition, could such bomb be well-done with values of any parameter above? Could such bomb exist with lifetime of 10^{-93}s? How could radiations of its energy be obstructed at temperature 10^{51}k? Otherwise, suppose a bomb of mini BH will be wanted to have lifetime $\tau_{30} \approx$ 30yrs, according to (13aa), (11aa), (13l), (13bd) $m_{30} \approx10^{12}$ g, $r_{30} \approx 10^{-16}$ cm, $t_{30} \approx 10^{17}$ k, mass of particle $m_{s30} \approx 10^{-21}$ g $\approx 5\times10^{2}$ GeV. How can mass of 10^{12}g be extruded to the size of 10^{-16}cm? How can control and stop its energy emission? They said, it will be the century of "Oton" after 50 ~60yrs. They also advocated that, mini BHs inside earth would ignite volcanic eruption, and mini BHs would lead to spontaneous combustion in human body, etc. It is really not known what are the scientific foundations about their talking to mini BHs.

(D). The commonality between universe and BHs,

For checking up the correctness of used theories, concepts and formulas about the birth of our universe and BHs before, the evolutionary process of a pretended mini universe as a example will be calculated below for reference to others who are interesting in this article.

Suppose a pretended mini universe out of ours was simultaneously born with our universe and both born from the same QMBHs ($m_t \approx 10^{-5}$ g), and the mini universe included N_m^{20} particles (QMBHs) of m_t. Thus, mass of mini universe $M_m \approx N_m^{20}\times10^{-5}g\approx10^{15}$ g. It is obvious, $M_m = m_{om} \approx10^{15}$ g, so, all other parameters of M_m are the same with m_{om}', $R_m\approx10^{-13}$ cm, $T_m\approx10^{12}$ k, $\tau_m\approx10^{10}$ yrs, $m_{sm}\approx1.67\times10^{-24}$g.

How long would be the expanded time (t_2) of mini universe from N_m^{20} of $m_t\approx10^{-5}$g to $M_m \approx10^{15}$g? Let us return back formula (1a) of part one, $R_1/R_2 = (t_1/t_2)^{1/2}$, here $R_1\approx10^{-33}$ cm, $R_2\approx10^{-13}$ cm, $t_1\approx10^{-43}$s, so, according to (1a), $t_2 \approx10^{-3}$ s. From calculation before, it is known the vanishing time of $m_{om} \approx 10^{15}$g in emitting energy would be 10^{10} yrs. Therefore, the whole lifetime of mini universe M_m from its birth to vanish would be equal to: 10^{10} yrs + 10^{-3} s.

However, the mass M_u of our universe in Event Horizon is 10^{56}g, numbers of QMBHs are ($N_o\approx10^{61}$) >>($N_m\approx10^{20}$). Are there any surplus mass outside M_u? Have dark energy existed inside Event Horizon of our universe? Does such dark energy have exclusive force? What are dark energy? Such many problems have not been known, no way can calculate out the expansible time of our present universe. At last**,** our universe would stop its expansion only with no energy-matters taken in from outside, and then instantaneously emit energy (Hawking's radiation) to outside to lose its mass gradually until it come to naught finally at an explosion.

Our universe was born from countless QMBHs and would finally vanish at an explosion of QMBHs, it is the same with BHs in essence. Both are all BHs and have all commonalties in BHs, but our universe is just a gigantic BH. The tremendous difference in mass between BHs would lead to the enormous differences in their structures, states, developments and lifetimes. The bigger the mass of BH is, the lower its temperature and density will be, and the much longer its lifetime is, the lifetime of a BH is proportional its mass[3]. Thus, the district of lower temperature in gigantic BH would have

enough time to evolve out intelligence living beings even mankind.

20. A few words of the writer

The demonstrations in this article are simple, rough and break down the old conventions. It probably will not be welcomed and convinced by the majority of scientists and professors, because of lacking new theory and complicated mathematical equations. However, the new concepts, inferences and all calculated results in this article are derived from many current classical theories, and are very closely consistent with the physical and natural laws in nature. The important contribution in this article is to have found out mini BH ($r_{om} = 3h/(2\pi Cm_s)$) as a special and simplified solution of formula (11c) [$dP/dR = -GM\rho/R^2$] and TOV equation applied in star-formed BH. Another contribution is to apply some rough and simplified methods to have effectively researched macro states, structures inside the star-formed BHs. Of course, many problems have been solved, much more complicated and knotty problems would have been left for others.

This article is separated into three big parts, the full text can be searched on website:
(http://www.sciencepub.org/nature/debate-001**).**

------ The End ------

References

[1] Jean-Pierre Luminet: Black Holes; Hunan Science-Technology Publishing House, China: Chinese Edition. 2000.
[2] Wang Yong-Jiu. Physics of Black Holes; Hunan Normal University Publishing House China. 2000.
[3] Dennis Overbye: Lonely Hearts of the Cosmos; 2002 by CITTC Publishing house, Beijing, China. Chinese Edition. 2002.
[4] John & Gribbin. Companion to the Cosmos; Hainan Publishing House, Hainan, China. 2001. Chinese Edition.
[5] He Xiang-Tao. Observational Astronomy; Science Publishing House, Beijing, China. 2002.
[6] Kip S. Thorne. Black Holes and Time Warps; Hunan Science & Technology Press, China, Chinese Edition. 2001.
[7] Wu Shi-Min. A Course in the General Theory of Relativity: Beijing Normal University Publishing House, Beijing, China. 1998. 8.

****

Author: Dongsheng Zhang, graduated in 1957 from Beijing University of Aeronautics and Astronautics of China, retired now. Permanent Address: Seventeen Pontiac Road, West Hartford, CT 06117-2129. Email: zhangds12@hotmail.com. Telephone: 860-869-0741.

This article had gotten number of Certificate of Registration TXu1-156-325, from UNITED STATE COPYRIGHT OFFICE.

Chinese edition of this article was published on "Aeronautical Education" magazine, June 2004, Beijing University of Aeronautics and Astronautics, China. Publication Number: ISSN1005-8176 | CN11-2548/G4.

****

Gene Transfer Technique

Hongbao Ma, Guozhong Chen

Michigan State University, East Lansing, MI 48823, USA, hongbao@msu.edu

Abstract: This article is describing the nine principle techniques for the gene transfection, which are: (1) lipid-mediated method; (2) calcium-phosphate mediated; (3) DEAE-dextran-mediated; (4) electroporation; (5) biolistics (gene gun); (6) viral vectors; (7) polybrene; (8) laser transfection; (9) gene transfection enhanced by elevated temperature, as the references for the researchers who are interested in this field. [Nature and Science. 2005;3(1):25-31].

Key words: DNA; gene; technique; transfer

1 Introduction

Gene transfer is to transfer a gene from one DNA molecule to another DNA molecule. Gene transfer represents a relatively new possibility for the treatment of rare genetic disorders and common multifactorial diseases by changing the expression of a person's genes (Arat, 2001). In 1928, Griffith reported that a nonpathogenic pneumoccocus strain could become pathogenic when it was mixed with cells of heat-killed pathogenic pneumoccocus, which hinted that the pathogenic genetic material could be transformed from the heat-killed pathogenic pneumoccocus to the nonpathogenic strain (Griffith, 1928). This is the first report for gene transfer observation. However, the transforming substance was not identified in these experiments. Up to 1944, Avery et al demonstrated that deoxyribonucleic acid (DNA) was the transforming substance (Avery, 1944). In 1952, Hershey and Chase showed that DNA was the only material transferred during bacteriophage infection, which suggested that the DNA is the genetic material (Hershey, 1952).

The basic technique for introducing DNA into E. coli have inspired procedures for the introduction of DNA into cells from a wide variety of organisms, including mammalian cells. Genetic engineering of food is the science which involves deliberate modification of the genetic material of plants or animals. Introduction of DNA into plants is of great agricultural potential and medical importance (Campbell, 1999; Uzogara, 2000; Lorence, 2004).

The gene transfer methods normally include three categories: 1. transfection by biochemical methods; 2. transfection by physical methods; 3. virus-mediately transduction. The gene transfer results can be transient and stable transfection.

Gene therapy can be defined as the deliberate transfer of DNA for therapeutic purposes. Many serious diseases such as the tragic mental and physical handicaps caused by some genetic metabolic disorders may be healed by gene transfer protocol. Gene transfer is one of the key factors in gene therapy (Matsui, 2003), and it is one of the key purposes of the clone (Ma, 2004).

Gene transfer can be targeted to somatic (body) or germ (egg and sperm) cells. In somatic gene transfer the recipient's genome is changed, but the change will not be passed on to the next generation. In germline gene transfer, the parents' egg and sperm cells are changed with the goal of passing on the changes to their offspring. Germline gene transfer is not being actively investigated, at least in larger animals and humans (Bordignon, 2003; Umemoto, 2005).

2 Transient and Stable Transfection

2.1 Transient transfection

In transient transfection, the transfected DNA is not integrated into host chromosome. DNA is transferred into a recipient cell in order to obtain a

temporary but high level of expression of the target gene.

2.2 Stable transfection

Stable transfection is also called permanent tran sfection. By the stable transfection, the transferred DNA is integrated (inserted) into chromosomal DNA and the genetics of recipient cells is permanent changed.

3 Transfection Methods

Generally, there are 9 ways for gene transfer: (1) Lipid-mediated method; (2) Calcium-phosphate mediated; (3) DEAE-dextran-mediated; (4) Electroporation; (5) Biolistics; (6) Viral vectors; (7) Polybrene; (8) Laser transfection; (9) Gene transfection enhanced by elevated temperature (Sambrook, 2001).

3.1 Lipid-mediated method

This method can be used for both transient and stable transfection, and it can be used for adherent cells, primary cell lines, and suspension cultures. For the following protocol, the Lipofectamine Reagent from Invitrogen Corporation will be used. Lipofectamine Reagent is a 3:1 (w/w) liposome formulation of the plycationic lipid 2,3-dioleyloxy-N-[2(sperminecardoxido)ethyl]-N,N-dimethyl-1-propanaminium trifluoroacetate (DOSPA) and the neutral lipid dioleoyl phosphatidylethanolamine (DOPE) in membrane-filtered water (Catalogue Number 18324, Invitrogen Corporation, Carlsbad, California, USA) (Hawley-Nelson, 1993; Shih, 1997).

(1) Put about 40,000 cells per well of a 24-well plate in 0.5 ml of the appropriate complete growth medium (add 10% serum if it needs).

(2) Incubate the cells at 37^{o}C in a CO_2 incubator until the cells are 50-80% confluent (about 20 hours, depending on the cells).

(3) Dilute 3 μg DNA into 25 μl medium without serum for each well and mix.

(4) Dilute 3 μl Lipofectamine Reagent into 25 μl medium without serum for each well and mix.

(5) Combine diluted DNA (Step 3) and Lipofectamine Reagent (Step 4) and incubate at room temperature for 30 min. In this step the DNA-liposome complexes are formed.

(6) Replace the medium in the cells with 0.2 ml transfection medium without serum.

(7) Add 0.15 ml medium without serum to the tube containing the complexes for each well.

(8) Incubate the cells with the complexes for about 10 hours at 37^{o}C in a CO_2 incubator. The incubating time will be flexible by the cell type.

(9) Add 0.4 ml growth medium containing double the 2× normal concentration of the serum without removing the transfection mixture.

(10) Replace the medium with fresh, complete medium at 20 hours following the start of transfection if continued cell growth is required.

(11) Assay cell extracts for transient gene expression at 24-72 hours after transfection, depending on the cell type and promoter activity.

(12) To obtain stable transfectants, passage the cells 1:10 into the selective medium after 72 hours of transfection for the reporter gene transfected.

3.2 Calcium-phosphate mediated

To get a better description, the following protocol is using the human interleukin-2 gene transfer into cultured rat myocytes as the example manual.

3.2.1 Rat heart muscle cells are primarily cultured:

(1) Adult rats are sacrificed by decapitation with a decapitator.

(2) Rat hearts are moved out and left atria are isolated under sterile condition.

(3) Tissue is transferred to a fresh sterile phosphate buffered solution (PBS) and rinse.

(4) Transfer to a second dish and dissect off unwanted tissue such as fat or necrotic material and chop finely with crossed scalpels to about 1 mm cubes.

(5) Transfer by pipette (10 – 20 ml with wide tip) to a 15-ml sterile centrifuge tube.

(6) Wash by resuspending the pieces in PBS, transfer the chopped pieces to the trypsinization flask, and add 1 ml trypsin solution (0.25%) per 100 mg tissue. Incubate the tissue in trypsin solution for 12 hours at 4^{o}C then wash with PBS for 3 times.

(7) Add 1 ml trypsin solution (0.25%) per 100 mg tissue, with 1 mg/ml elastase and 1 mg/ml collagenase then stir at about 200 rpm for 30 min at 36.5^{o}C.

(8) Allowing the pieces to settle, collect supernatant, centrifuge at approximately 500 g for 5 min, resuspending pellet in 10 ml medium with 10% serum (FBS) (Gibco BRL Life Technologies, Inc., Grand Island, NY, USA), and store cells on ice.

(9) Add fresh trypsin to pieces and continue to stir and incubate for a further 30 min. Repeat steps 6 – 8 until complete disaggregation occurs or until no further disaggregation is apparent.

(10) Collect and pool chilled cell suspensions, and count by hemocytometer.

(11) Dilute to 10^6 per ml in growth medium and seed as many flasks as are required with approximately 2 x 10^5 cells per ml or set up a range of concentrations from about 10 mg tissue per ml.

(12) Put into CO2 incubator with 36.5oC.

(13) Culture medium used is Medium 199 with 10% FBS. All the solutions used contain 0.1 mg/ml of anti-biotic ampicillin (Sigma, St Louis, MO, USA).

3.2.2 Bacteria Culture (Sambrook, 1989; Frederick, 1992)**:**

(1) Growth of *E. coli*: Dissolve *E. coli* in 0.3 ml LB plus tetracycline (2 mg/ml) medium, transfer it into a tube containing 5 ml LB plus tetracycline (2 mg/ml) medium, 37°C overnight, then freeze it at -70°C.

(2) Harvesting E. coli:

A. Streak an inoculum across one side of a plate. Resterilize an inoculating loop and streak a sample from the first streak across a fresh part of plate, then incubate at 37°C until colonies appear (overnight).
B. Transfer a single bacterial colony into 2 ml of LB medium containing tetracycline (2 mg/ml) in a loosely capped 15-ml tube. 37°C overnight with vigorous shaking.
C. Pour 1.5 ml of the culture into a microfuge tube. Centrifuge at 12,000g for 30 seconds at 4°C in a microfuge. Store remainder at 4°C.
D. Remove the medium by aspiration.

(3) Lysis of E. coli and purification of plasmid:

A. Resuspend *E. coli* pellet in 100 µl of ice-cold Solution I (50 mM glucose, 25 mM Tris-Cl, pH 8.0, 10 mM EDTA, pH 8.0).
B. Add 200 µl of freshly prepared Solution II (0.2 N NaOH, 1% SDS), inverting the tube rapidly 5 times. Do not vortex. Store at 4°C.
C. Add 150 µl ice-cold Solution III (5 M potassium acetate 60 ml, glacial acetic acid 11.5 ml, H_2O 28.5 ml), on ice for 3-5 min.
D. Centrifuge at 12,000g for 10 min, at 23°C .
E. Pour supernatant into QIAprep column (silicon gel column, Qiagen Company, USA).
F. Centrifuge at 12000g for 1 min and discard flow through.
G. Wash the column with 0.75 ml PE buffer (55 ml of 5 mM Mops-KOH, pH 7.5-7, 0.75 mM NaCl plus 220 ml of ethanol).
H. Centrifuge 1 min at 12000g and discard flow through.
I. Place column in 1.5 ml microcentrifuge tube.
J. Add 50 µl of the DEPC H_2O in the center of the column, stand for 1 min, centrifuge at 12000g for 1 min.
K. Take 1 µl of DNA (plasmid), add 99 µl of TE buffer, pH 8.0, measure DNA concentration at OD260 nm and OD280 nm (OD260 nm/OD280 nm should be >1.7).
L. Redissolve the DNA in 50 µl of TE (pH 8.0) containing DNAase-free pancreatic RNAase (20 µg/ml). Vortex briefly. Store at -20°C.
M. Calculate the concentration of the plasmid DNA: 1 $OD_{260\ nm}$ = 50 µg of plasmid DNA/ml. Store the DNA in aliquots at -20°C.

3.2.3 Transfer human interleukin-2 gene into rat heart muscle cells:

(1) Transferred gene: Human interleukin-2 (IL-2) gene cloned in plasmid pBR322 inserted in *E. coli* can be bought from American Type Culture Collection (ATCC, Rockville, MD, USA).

(2) Transfection: ~2×10^7 of heart muscle cells suspended in 0.2 ml medium are seeded into a tissue culture chamber. 48-72 hours later, remove medium and add 0.2 ml fresh medium, then add 0.5 µg of plasmid in 0.05 ml calcium phosphate-HEPES-buffered saline, pH 7.0, at 37°C.

3.2.4 Detection of interleukin-2:

12~48 hours after the addition of plasmid and incubation, the amount of interleukin-2 is measured with the indirect enzyme-linked immunosorbent assay (ELISA) in medium. Antibody of anti-interleukin-2 (human) can be gotten from Sigma (Sigma Chemical Co., St Louis, MO, USA).

3.3 DEAE-dextran mediated

DEAE-dextran (diethylaminoethyloethyl-dextran) was used to introduce poliovirus RNA and SV40 and polyomavirus DNAs into cells in 1960s (Pagano, 1965; McCutchan, 1968; Warden, 1968).

There are three points that DEAE-dextran mediated transfection differs from calcium phosphate coprecipitation. (1) It is used for transient transfection. (2) It works more efficiently with cell lines of BSC-1, CV-1 and COS, etc. (3) It is more sensitive.

The DEAE-dextran mediated transfection could be done by the following steps:

(1) Harvest exponentially growing cells by trypsinization and transfer then into 60-mm tissue culture dished at a density of 105 cells/dish.

(2) Add 5 ml complete growth medium.

(3) Incubate 24 hours at 37^{o}C with 5% CO_2.

(4) Prepare DNA/DEAE-dextran/TBS-D solution by mixing 2 mg of superoiled plasmid DNA into 1 μg/ml DEAE-dextran in TBS-D.

(5) Remove medium and wash tree times with PBS and twice with TBS-D.

(6) Add DNA/DEAE-dextran/TBS-D solution 250 μl.

(7) Incubate 60 min at 37^{o}C with 5% CO_2.

(8) Remove DNA/DEAE-dextran/TBS-D solution.

(9) Wash with TBS-D three time and PBS twice.

(10) Add 5 ml medium supplemented with serum and chloroquine (0.1 mM).

(11) Incubate 4 hours at 37^{o}C with 5% CO_2.

(12) Remove medium.

(13)Wash with serum-free medium three times.

(14) Add to cells 5 ml of medium supplement with serum, and incubate 48 hours at 37^{o}C with 5% CO_2.

(15) Harvest the cells after the 48 hours transferction.

(16) Analyze RNA or DNA by hybridization, or analyze expressed protein by radiommunoassay, immunoblotting, immuniprecipitation, or by enxzymoatic activity in cell extract.

3.4 Electroporation

Pulse electrical fields can be used to introduce DNA into cells of animal, plant and bacteria. Factors that influence efficiency of transfection by electroporation: applied electric field strength, electric pulse length, temperature, DNA conformation, DNA concentration, and ionic composition of transfection medium, etc.

Steps of the electroporation transfection:

(1) Harvest cells in the mid- to late-logarithmic phase of growth.

(2) Centrifuge at 500 g (2000 rpm) for 5 min at 4^{o}C.

(3) Resuspend cells in growth medium at concentration of 1 X 10^7 cells/ml.

(4) Add 20 μg plasmid DNA in 40 μl cells.

(5) Electric transfect by 300 V / 1050 μF for 1-2 min.

(6) Transfer the electroporated cells to culture dish and culture the cells.

(7) Assay DNA, RNA or protein and continuously culture the cells to get positive cell lines. .

3.5 Polybrene

Several polycations, including polybrene (1,5-dimethyl-1,5-diazaundecamethylene polymethobromide) (Chaney, 1986) and poly-L-ornithine (Nead, 1995), have been used in gene transfection with the DMSO enhancement. Normal steps are following:

(1) Harvest exponential cells by trypsinzationin and replate at a density of 5,000 cells/mm^2 in 10 ml MEM-α containing 10% fetal calf serum.

(2) Incubate 24 hours at 37^{o}C in 5% CO_2.

(3) Replace medium with 3 ml pre-warmed medium containing serum, 10 μg DNA and 30 μg polybrene (37^{o}C). Mix the medium before adding polybrene.

(4) Incubate 12 hours with a gent shake each hour.

(5) Remove medium and add 5 ml 30%^ DMSO in serum-containing medium.

(6) After 4 min incubation, aspirate the DMSO solution. Wash the cells twice with warmed (37^{o}C) serum-free medium, and add 10 ml complete medium containing 10% fetal calf serum.

(7) Incubate 48 hours at 37°C in 5% CO_2.

(8) Examine the cells everyday after the transfer-ction.

(9) For stable transfection, continue incubate 3 weeks with changing medium every 2 days.

3.6 Virus

Viruses are highly adapted to the process of gene transfer. Viral vectors have the ability to transfer DNA to a high fraction of cells, but using virus as the vector will be potentially arouse cancer leukaemia (Cavazzana-Calvo, 2004). Common vectors used for gene transfer in cell culture are derived from retroviruses. Adenovirus and other agents are used for the gene delivery.

3.7 Biolistics (Gene gun, or called microparticle bombardment)

Some cells, tissues and intracellular organelles are impermeable to foreign DNA, especially plant cells. biolistics, including particle bombardment, is a commonly used method for genetic transformation of plants and other organisms. To resolve this problem in gene transfer, the gene gun was made by Klein at Cornell University in 1987 (Klein, 1987; Kikkert, 2005). On the gene gun technique, Klein and Sanford et al published papers, obtained patents and formed a company called Biolistics (Klein, 1987).

The gene gun is part of the gene transfer method called the biolistic (also known as biobalistic or particle bombardment) method. In this method, DNA or RNA adhere to biological inert particles (such as gold or tungsten). By this method, DNA-particle complex is put on the top location of target tissue in a vacuum condition and accelerated by powerful shot to the tissue, then DNA will be effectively introduce into the target cells. Uncoated metal particles could also be shot through a solution containing DNA surrounding the cell thus picking up the genetic material and proceeding into the living cells. The efficiency of the gene gun transfer could be depended on the following factors: cell type, cell growth condition, culture medium, gene gun ammunition type, gene gun settings and the experimental experiences, etc.

Briefly for gene gun practice, the target cells or tissues on the polycarbonate membranes could be positioned in a Biolistic PDS-1000/HE Particle Delivery System (Bio-Rad Laboratories GmbH, München, Germany). Biolistic parameters are 15 in. Hg of chamber vacuum, target distance of 3 cm (stage 1), 900 psi to 1800 psi particle acceleration pressure, and 1.0 μm diameter gold microcarriers (Bio-Rad, USA). Gold microcarriers are prepared, and circular plasmid DNA is precipitated onto the gold using methods recommended by Bio-Rad with the following: 0.6 mg of gold particles carrying ~5 μg of plasmid DNA is used per bombardment.

The detail protocol for the gene gun transfection is described as follows:

(1) Prepare gold or tungsten particles: 60 mg gold or tungsten in 1 ml 70% ethanol, centrifuge at 10,000 rpm for 10 seconds and collect particles, and wash with H2O three times by centrifugation.

(2) Prepare DNA-coated particles: Mix 50 □l (about 3 mg) metal, 2.5 □l plasmid DNA (about 2.5 □g), CaCl2 50 □l (2.5 M), spermidine 20 □l (0.1M). Vortex and stand for 5 min. Centrifuge, remove supernatant, and add 140 □l 70% ethanol over the pelleted particles, and repeat the ethanol and centrifugation three times, then add 50 □l ethanol.

(3) Place a macrocarrier in the metal holder of gene gun and wash twice with ethanol.

(4) Vortex and spread 0.5 mg pellet slurry on the macrocarrier.

(5) Load the macrocarrier into the gene gun, and shoot it. Repeat the shoot until all the areas are shot. .

(6) For transient expression, examine cells 48 hours after the shooting, by immunology or other methods.

(7) For stable transfection, continue culture the transfected cells or tissues.

In our studies, we did gene transfection with the self-design CO_2 propelled gene gun (200 psi, distance 3 cm with 400 mesh nylon screen) using tungsten particle (600 nm diameter) coated with plasmid expressing anti-ampicillin gene, the plasmid with anti-ampicillin gene was transferred into E. Coli cells.

3.8 Laser transfection

As the example of our experiments, UV excimer laser (XeCl2, 308 nm) is used in the gene transfection (5 min by a 0.7 0.9, 1.4 or 2.0 mm diameter fiber with fluence of 45 and 60 mj/mm2 - real laser energy 2.3,

5.9, 13.1, 32.0 mj/pulse, 25 Hz) (CVX-300 Excimer Laser System, Spectranetics Corporation, Colorado Springs, CO, USA). Also, we used to make experiments with Nd:Yag, Ho:Yag in the gene transfection. All the methods of excimer, Nd:Yag and Ho:Yag laser transfection are effective.

3.9 Transfection enhanced by elevated temperature

Our studies show that high temperature enhances the gene transfection. In our experiments, rat heart muscle cells were cultured in medium 199 with 10% FBS and human aorta smooth muscle cells were cultured in F12K medium. Human interleukin-2 gene was transfected into rat heart cells and swine growth hormone gene was transfected into human aorta smooth muscle cells by calcium phosphate coprecipitation at various temperatures: 23ºC, 37ºC and 43ºC. Transfected interleukin-2 and swine growth hormone expressions were detected using an indirect ELISA. The heated cultured rat myocytes had a significantly higher expression of the transfected interleukin-2 gene. Ambient temperature rise to 43^{o}C for up to 30 min provided greater transient transfection of the interleukin-2 gene when compared to ambient temperatures at 37^{o}C and 23^{o}C ($p<0.01$). The greatest effects occurred within 10 min of incubation and persisted up to 30 min. These results suggest that even a few degrees of ambient temperature rise can significantly increase gene transfer into muscle cells. This may be of value when using gene therapy with transfection procedures (Ma, 2004b; Ma, 2004c).

3.10 Plant gene transfer

Agriculture and plant breeding relied solely on the accumulated experience of generations of farmers and breeders that is, on sexual transfer of genes between plant species. However, developments of plant molecular biology and genomics now give us access to knowledge and understanding of plant genomes and the possibility of modifying them. There are two most powerful technologies for transferring gene into plants: Agrobacterium-mediated transformation and biolistics. As plants have cell wall, the biolistics is very useful in the plant gene transfer (Rasco-Gaunt, 2001).

4 Discussion

The current century will bring tremendous changes to the science, technology, and the practice of medicine (Lushai, 2002). Gene therapy is part of a growing field in molecular medicine, which will gain importance in the treatment of human diseases (Gunther, 2005). As a critical topic, gene transfection gives people the hope to treat many diseases but it also could create dangerous species in the earth, so that it attracts plenty attention by the whole human society (Lanza, 2002). This simply means that the success of gene transfer technique will be benefit for the civilization, and also create the danger for the life in the earth either (Schiemann, 2003). Gene transfection procedures are used in the critic procedure animal clone (Chesne, 2002; Heyman, 2002), and the animal clone is challenged by the religious groups and ethnic extremists (Houdebine, 2003). As our personal views, no matter how big challenges from whatever aspects, the gene transfection and animal clone will develop quickly. The world is a complex place composed by different people. For the science and technology such as gene transfer and animal clone, no country can prevent other countries from the pursuing. We need to develop the technique even if the technique could be used in the danger action, and we need to consider the social effects of a technique when we develop it either.

Science development will be benefit to all the human society. As the gene therapy developing, many more desperate diseases could be cured and many human livings could be saved, such as the life of Pope John Paul II and Terri Schindler-Schiavo. Hope that the gene transfer techniques described in this article could be useful for the researches in the gene therapy field and help to advance the life science study.

Correspondence to:
Hongbao Ma
B410 Clinical Center
Michigan State University
East Lansing, MI 48824, USA
Telephone: (517) 432-0623
Email: hongbao@msu.edu

References

[1] Arat S, Rzucidlo SJ, Gibbons J, Miyoshi K, Stice SL. Production of transgenic bovine embryos by transfer of

transfected granulosa cells into enucleated oocytes. Mol Reprod Dev 2001;60(1):20-6.

[2] Avery OT, MacLeod CM, McCarty M. Studies on the chemical nature of the substance inducing transformation of pneumococcal types. J Exp Med 1944;79:137-58.

[3] Bordignon V, Keyston R, Lazaris A, Bilodeau AS, Pontes JH, Arnold D, Fecteau G, Keefer C, Smith LC. Transgene expression of green fluorescent protein and germ line transmission in cloned calves derived from in vitro-transfected somatic cells. Biol Reprod 2003;68(6):2013-23.

[4] Campbell KH. Nuclear transfer in farm animal species. Semin Cell Dev Biol 1999;10(3):245-52.

[5] Cavazzana-Calvo M, Thrasher A, Mavilio F. The future of gene therapy. Nature 2004;427(6977):779-81.

[6] Chaney WG, Howard DR, Pollard JW, Sallustio S, Stanley P. High-frequency transfection of CHO cells using polybrene. Somat Cell Mol Genet 1986;12(3):237-44.

[7] Chesne P, Adenot PG, Viglietta C, Baratte M, Boulanger L, Renard JP. Cloned rabbits produced by nuclear transfer from adult somatic cells. Nat Biotechnol 2002;20(4):366-9.

[8] Griffith F. The significant of pneumoccopal types. Hyg J 1928;27:113.

[9] Gunther M, Wagner E, Ogris M. Specific targets in tumor tissue for the delivery of therapeutic genes. Curr Med Chem Anti Canc Agents 2005;5(2):157-71.

[10] Hawley-Nelson P, Ciccarone V, Gebeyehu G, Jessee J, Felgner P. FOCUS 1993;15:73.

[11] Hershey AD, Chase D. Independent functions of viral protein and nuclei acid in growth of bacteriophage. J Gen Physiol 1952;36:39-56.

[12] Heyman Y, Zhou Q, Lebourhis D, Chavatte-Palmer P, Renard JP, Vignon X. Novel approaches and hurdles to somatic cloning in cattle. Cloning Stem Cells 2002;4(1):47-55.

[13] Houdebine LM. Animal transgenesis and Cloning. John Wiley & Sons, Inc. Hoboken, NJ, USA, 2003:34-73.

[14] Lanza RP, Dresser BL, Damiani P. Cloning Noah's ark, in Understanding Cloning. Scientific American, Inc. and Byron Press Visual Publications, Inc, 2002:24-35.

[15] Kikkert JR, Vidal JR, Reisch BI. Stable transformation of plant cells by particle bombardment/biolistics. Methods Mol Biol 2005;286:61-78.

[16] Klein TM, Wolf ED, Wu R, Sanford JC. Hugh-velocity microprojeectiles for delivering nucleic acids into living cells. Nature 1987'327:70-3.

[17] Lorence A, Verpoorte R. Gene transfer and expression in plants. Methods Mol Biol 2004;267:329-50.

[18] Ma H. Technique of Animal Clone. Nature and Science 2004(a);2(1):29-35.

[19] Ma H, Chi C, Abela GS. Increase in ambient temperature enhances gene transfer into human smooth muscle cells. FASEB Journal 2004(b);18(8):C293.

[20] Ma H, Chi C, Abela GS. Increased ambient temperature enhances human interleukin-2 gene transfer into cultured myocytes. Journal of Investigative Medicine 2004(c);52(2):S390.

[21] McCutchan JH, Pagano JS. Enchancement of the infectivity of simian virus 40 deoxyribonucleic acid with diethylaminoethyl-dextran. J Natl Cancer Inst 1968;41(2):351-7.

[22] Nead MA, McCance DJ. Poly-L-ornithine-mediated transfection of human keratinocytes. J Invest Dermatol 1995;105(5):668-71.

[23] Pagano JS, Vaheri A. Enhancement of infectivity of poliovirus RNA with diethylaminoethyl-dextran (DEAE-D). Arch Gesamte Virusforsch 1965;17(3):456-64.

[24] Rasco-Gaunt S, Riley A, Cannell M, Barcelo P, Lazzeri PA. 2001. Procedures allowing the transformation of a range of European elite wheat (*Triticum aestivum* L.) varieties *via* particle bombardment. J Exp Bot 2001;52(357):865-74.

[25] Sambrook J, Russell DW. Molecular cloning: a laboratory manual. Cold Spring Harbor Laboratory Press, Cold Spring Harbor, NY, USA. 2001;3(16):16.1-16.62.

[26] Schiemann J. New science for enhanced biosafety. Environ Biosafety Res 2003;2(1):37-41.

[27] Shih PJ, Evans K, Schifferli KP, Ciccarone V, Lichaa F, Masoud MJ, Hawley-Nelson P. FOCUS 1997;19:52.

[28] Umemoto Y, Sasaki S, Kojima Y, Kubota H, Kaneko T, Hayashi Y, Kohri K. Gene transfer to mouse testes by electroporation and its influence on spermatogenesis. J Androl 2005;26(2):264-71.

[29] Uzogara SG. The impact of genetic modification of human foods in the 21st century: a review. Biotechnol Adv 2000;18(3):179-206.

[30] Warden D, Thorne HV. The infectivity of polyoma virus DNA for mouse embryo cells in the presence of diethylaminoethyl-dextran. J Gen Virol 1968;3(3):371-7.

Research and Analysis on 211 Cases of Toxic Disease of Chinese Domestic Rabbits

Zilin Gu [1,2], Yangang Hao [1], Baojiang Chen [1], Wenshe Ren [1], Chao Zhao [1], Yuting Huang [1]

1. Mountainous Areas Research Institute of Agriculture University of Hebei, Baoding, Hebei 071001, China;
2. Animal Science & Technology College, Northeast Agricultural University, Harbin, Heilongjiang 150030, China, hebaugzl@sohu.com

Abstract: In this paper induction and analysis was carried out concerning toxic diseases of domestic rabbits reported in China from 1994 to 2002. 78 papers were adopted, involving 212 cases of toxic events of domestic rabbits and 23 kinds of poisonous types. 34558 rabbits were poisoned in all and 8551 ones died. The mortality was 24.74% (with 19 cases not providing the particular number of poisoned rabbits). Among 212 cases, 145 cases were caused by diet, 41530 rabbits were poisoned and 2595 died; 67 cases were caused by drug, 13028 rabbits were poisoned and 5956 died. The mortality of each kind was 12.05% and 45.75% respectively. In addition, there were a good few pregnant rabbits with abortion or stillbirth. Among diet poison cases, there were 35 cases caused by fungi toxins, 12 cases by plant toxins, 88 cases by organic phosphorous insecticide and 10 cases by other factors. The number of poisoned rabbits was 17626, 1047, 1609 and 1248 separately. The number of dead rabbits was 602,542, 885 and 566 separately. The mortality of each kind was 3.42%, 51.77%, 55.00% and 45.35% separately. Among medicine poison cases, there were 9 cases caused by anti-bacterial medicine, 48 cases by anti-coccidium medicine (of which 46 cases were Maduramicin), 4 cases by acaricide and 6 cases by other drugs. The number of poisoned rabbies was 1646, 11084, 136 and 162 respectively. The number of dead poisoned ones was 230, 5629, 26 and 71 respectively. The mortality of each kind was 13.97%, 50.78%, 19.12% and 43.83% respectively. [Nature and Science. 2005;3(1):32-36].

Key Words: domestic rabbit; toxic disease; diet poison; drug poison; fungi toxin; plant toxin; Maduramicin

1 Introduction

Domestic rabbit is a small animal, which has weak resistibility against diseases, and its metabolism is easy to be confused to cause diseases in some way. In practice, great importance tends to be given to the prevention of contagious diseases and little to the administration and the influence of poisonous, pernicious stuff to the health of the rabbit so as to cause great loss in the production.

The paper analysed the relationship between animal feed poison and feeding pattern, toxin poison and mortality, drug poison and mortality, medicine poison and way of application.

According to the analysis of these articles, it was suggested that scale rabbit farms should pay attention to fungi toxin resulted from mouldy roughage fodder, rabbit farms in the country should mainly prevent poison caused by organic phosphorous insecticide, it was prohibited to use Maduramicin as the anti-coccidium medicine of rabbits and important to popularize the knowledge of scientific use of rabbits feed and medicine towards lots of rabbit-keepers. The author organized and studied the documents from 1994 to 2002 on the rabbit's toxic diseases of China and give some suggest to prevent these diseases effectively.

2 Investigation and analysis

Exploit the bank of Chinese periodical full-text, search the relative documents by the searching words of rabbit and toxication on the basis of the respective segment of topic, key words, abstract and full-text and then consult the above documents one by one. All the documents on the report of cases are listed as the material for consultation. The adopted documents then are listed, classified according to the toxication genre, case load, ingredients of toxin, feeding quantity, feeding time, numbers of toxication, numbers of death, main symptom, pathological dissection, diagnostic, treating measures, treatment result, source of document.

There are two categories of toxication: by feed and by drug. The toxication by feed is further divided into four parts: roughage, concentrate, total mixed ration and succulence; among the toxic ingredients are mycotoxin, plant toxin (such as gossypol, oleandrism, hydrocyanic acid, alkaloid and etc.) and the others (such as fluorine, alcohol, urea, estrogen, sulfite and nitrite; among the toxication by drug, the drugs are divided into four categories: antibacterial drug, anticoccidial drug, anti-mite drug and others (such as patulin). According to the usage , the drug can be divided into oral drug, external drug and others (such as toxication by misusing rodenticide). The following is the analysis of the above respectively.

3 Results

3.1 Distribution of the toxication

457 relevant articles were searched and 78 were adopted. 212 cases of rabbit toxications were involved, the number of the toxic rabbits is 34558(19 cases gave no concrete numbers of the toxic rabbit), the number of death is 21530 and the death rate is 24.74%. Among which there are 145 cases of toxication by feedstuff, accounting for 68.4%,and the number of the toxic rabbits is 21530,with 2595 dead and the death rate is 12.05%, accounting for 35%of the total dead; there are 67 cases of toxication by drug, accounting for 31.60% of the total cases, and the number of the toxic rabbits is 13028, with 5956 dead, and the death rate is 45.72%, accounting for 69.65% of the total dead. Moreover, there are large numbers of doe abortion and dead embryos.

3.2 Toxication by diet

Categories of the feed

There are 22 cases of roughage toxication , 14 cases of concentrate toxication, 6 cases of total mixed ration toxication and 103 cases of succulence toxication, the toxication rate is 15.17%, 9.66%, 4.14% and 71.03% respectively; the respective number of the toxic rabbits is 17022, 2226, 31 and 2251, accounting for 79.06%, 10.34%, 0.97% and 50.33% of the total feedstuff toxication; the number of death is 632, 632, 25, and 1306 respectively and the death rate is 3.71%, 28.39%, 80.65% and 58.02%, taking up 24.35%, 24.35%, 0.97 and 50.33% of the total dead.

Ingredients of the toxin

There are 35 cases of rabbit toxication by mycotoxin, 12 by plant toxin, 88 by organic phosphorus toxin and 10 cases by others, accounting for 24.14%, 8.27%, 60.69% and 6.90% of the total cases of the rabbit toxication; the number of toxicated rabbits is 17626, 1047, 1609 and 1248 respectively, taking up 81.87%, 4.86%, 7.47 and 5.80 of the total toxication by feed; the number of death is 602, 542, 885 and 566 respectively, and the death rate is 3.42%, 51.77%, 55.00% and 45.35%, the proportion being 23.20%, 20.89%, 34.10% and 21.81% of the total dead by drug toxin.

Table 1. Stat of ingredients of the toxin

	Item	Cases of toxication		Number of toxication		Number of death		Proportion to the total death
		case	%	number	%	number	%	
Categories of feedstuff	Roughage	22	15.17	17022	79.06	632	3.71	24.35
	Concentrate	14	9.66	2226	10.34	632	28.39	24.35
	Total mixed .	6	4.14	31	0.14	25	80.65	0.97
	Succulence	103	71.03	2251	10.46	1306	58.02	50.33
	Total	145	100.00	21530	100.00	2595	12.05	100.00
ts en	Mycotoxin	35	24.14	17626	81.87	602	3.42	23.20

	Plant toxin	12	8.27	1047	4.86	542	51.77	20.89
	Organic insecticide	88	60.69	1609	7.47	885	55.00	34.10
	Other toxins	10	6.90	1248	5.80	566	45.35	21.81
	Total	145	100.00	21530	100.00	2595	12.05	100

3.3 Toxication by drug

Categories of drugs

There are 9 cases of toxication by antimicrobial drug, 48 cases of anticoccidial drugs（among which there are 46 cases of maduramicin toxication）, 4 cases of mite-killing drug toxication and 6 cases of others, accounting for 13.43%, 71.64%, 5.97% and 8.96% respectively; the respective of the toxic rabbit number is 2646, 11084, 136 and 162, accounting for 12.65%, 85.08%, 1.04% and 1.24%; the number of death for toxin is 230, 5629, 26 and 71 respectively, and the death rate is 13.97%, 50.78%, 19.12% and 43.83%, accounting for 3.86%, 94.51%, 0.44% and 1.19% of the total death by drug toxication respectively.

Usage of drug

There are 61 cases of toxication for taking drug orally, 4 cases for using drug externally, 2 cases for misusing drug, accounting for 91.04%, 5.97% and 2.99% respectively of the total cases of toxication by drugs; the number of the toxic rabbits is 12828, 136 and 64 respectively, taking up 98.47%, 1.04% and 0.49% of the total number of the toxication; the number of death for toxication is respectively 5889, 26 and 41, and the death rate is 45.91%, 19.12% and 64.06% respectively, accounting for 98.88%, 0.44% and 0.68% of the total dead for toxication by drug.

Table 2. Stat of toxication by drug

Item		Cases of toxication		Number of toxicated rabbit		Number of death		Proportion to the
		case	%	number	%	number	%	total death（%）
Categories of drug	Antibacterial	9	13.43	1646	12.65	230	13.97	3.86
	Anticoccidial drug	48	71.64	11084	85.08	5629	50.78	94.51
	Killing mite Drug	4	5.97	136	1.04	26	19.12	0.44
	Others	6	8.96	162	1.24	71	43.83	1.19
	Total	67	100.00	13028	100.00	5956	45.72	100.00
Usage for taking drug	Oral drug	61	91.04	12828	98.47	5889	45.91	98.88
	External drug	4	5.97	136	1.04	26	19.12	0.44
	others	2	2.99	64	0.49	41	64.06	0.68
	Total	67	100.00	13028	100.00	5956	45.72	100.00

4 Analysis and discussion

4.1 Wide spread of rabbit toxication

In the articles published in China from1994 to 2002, there are 212 cases relevant to rabbit toxication, in the reports, the number of the toxic rabbits being 34558, the number of death being 8551. Among which there are 145 cases of toxication by feedstuff, the number of death is 2595; there are 67 cases of toxication by drug, the number of death is 5956, all these brings a great loss to the production. In fact, in China, the figure can be greater for there are cases unreported for unknown reasons and some cases of toxication undiagnosed for the lacking of relevant equipments. For example, in this article, only three cases of olaquindox toxication are introduced (among which there is only a case of toxication simply by olaquindox and two cases by furalzolidone), being mixed with olaquindox, nevertheless in production, the cases of olaquindox toxication that the author diagnosed and handled can amount to more than 20, which caused great numbers of doe abortion and dead embryos; moreover, the categories of toxications involved in the article only include about 23 kinds, such as mycotoxin、estrogen、oleandrism、urea、hydrocyanic acid、fluorine, alcohol, urea, sulfite and nitrite gossypol, olaquindox, Robenidine, maduramicin, oxytetracycline and rodenticide，and other categories of toxications such as the toxications of NaCl, rapeseed cake, organic chlorine, sulfanilamide, salinomycin, NH_3, CO are not reported, which the author once met with in the rabbit study and production. From the above facts, it is easily understood that there is a widespread phenomenon of rabbit toxications, even more serious in some rabbit farms.

4.2 Toxication by feed and feeding ways

Of the 145 cases of toxication by feed, roughage, concentrate, total mixed ration and succulence account for 15.17%, 9.66%, 4.14% and 71.03 of the total cases respectively and succulence toxication takes up two thirds of the total. But the number of the toxic rabbit is 17022, 2226, 31 and 2251 respectively, which clearly shows that the succulence toxication most likely appears in small rabbit farms, especially the small household rabbit farms in the villages, while the roughage toxication in large scale. It is also reflected that the household rabbit farms of small scale share the larger part of China's market, and the weak technological sense and the feeding technology of the rabbit breeders need improving. As to the relationship between the categories of feedstuff and the ingredients ,of all the cases of toxication of roughage, refined feedstuff and mixed feedstuff, 83.33 is toxication by mycotoxin, while of the toxication by succulence , 85.44% of the cases is the toxication by organic phosphorus, 10.68% is by plant toxin. Here we can notice that the toxication for moldy feedstuff easily takes place in rabbit farms of large scale while the toxication for mis-eating the succulence sprayed by the organic phosphorus insecticide easily takes place in the household rabbit farms of small scale in the villages.

4.3 Categories of toxins and death rate

The death rate of toxication is relevant to the ingredients of toxins and the absorbed quantity, as well as the physiological condition of the domestic rabbits. The death rate of mycotoxin, plant toxin, organic insecticide and other toxins is 3.42%, 51.77%, 55.00% and 45.35 respectively, and the death rate of the last three is very high. In different toxin ingredients, the death rate of toxication for oleandrism is 100%, the death rate of toxication for hydrocyanic acid amounts to 86.52% and that for nitrous salt is 28.73%. Though the death rate of toxication for mycotoxin is relatively low, it acts as one of the chronic sediment, affecting the stud rabbit in its multiplying period, and characterized by doe abortion and stillbirth, which not only causes certain death rate, but also brings danger to human's health due to the internal toxin sediment.

4.4 Toxication by drug and death rate

Of all the toxication by drug, the death rate of the toxication for antibacterial, anticoccidial drug, mite-killing drug and other drugs is respectively 13.97%, 50.78%, 19.12% and 43.84%, of which the highest death rate comes to anticoccidial drug and other drugs (mainly misusing rodenticide). As to the anticoccidial drug, there are 46 cases of toxication for maduramicin, taking up 68.66% of all cases of toxication by drug, and the number of death is 5347, accounting for 89.76 of death for toxication by drug. There are 2 cases of toxication for Robenidine, with 282 rabbits dead , death rate 25.64%; there are 2 cases of toxication for rodenticide, with 41 dead, death rate 64.06%. From the above facts, one can see the necessity to articulate to the rabbit breeders the toxicity of maduramicin to domestic rabbits and the urgency to control its use.

4.5 Toxication by drug and the usage

Of all the toxication by drug, except for the rabbit's sensitivity to maduramicin, most toxication is caused by the abuse of other drugs. Firstly, an overdose of drug, not according to the instruction, for example, in some cases, olaquindox was overdosed in the feedstuff to 1000 milligram per kilo ; secondly, an extended use, not according to the period of treatment, for example, in some rabbit farms, in order to prevent diarrhea, some breeders add furazolidone to the feedstuff for as long as half a year; thirdly, using drugs without identifying objects, for example, when preventing coccidiosis, baby rabbits are its object, but all rabbits are involved, with the result of toxication of lactating does; fourthly, disproportional stirring of feedstuff, especially in rural household rabbit farms, there being no stirring equipments, and disproportional stirring of feedstuff easily takes place.

4.6 Toxication and treatment

Most toxications have their particular clinical symptoms and diagnostic, pathological changes, the two charts that the article introduces can help diagnose the toxication in production. But large numbers of cases of toxication have no specifics, and generally the allopathy and backup treatment are adopted. Therefore, spreading feedstuff science and medicine science is the key to lower the toxications of rabbits.

In one word, animal toxications not only cause loss to production but also bring danger to the environment as well as human's health. So, lowering and preventing the happening of toxications of rabbits are the duty and responsibility of our technological workers on rabbit study. Through the analysis of the cases of toxications of rabbits in China, one can conclude that the happening of toxication is a widespread phenomenon, and to solve the problem of the feedstuff molding is one of the difficulties; controlling the use of organic phosphorus insecticide in grains and using biologic drug as the substitute are the key to preventing the toxication of organic phosphorus insecticide in rabbit household farms of small scale; spreading the knowledge of rabbit breeding to breeders and identifying the difference between toxic plants and the feedstuff are effective measures to lower the happening of toxication by feedstuff; domestic rabbits are very sensitive to maduramicin, so it shouldn't be used as anticoccidial drug for rabbits, it is suggested that relevant producers should give the warning "rabbit forbidding" in the marked place of the commodity package.

References

[1] Chang Fujun.. Treatment on DDG toxication of rabbit. J of China Rabbit 2000;6:33

[2] Cai Kuizheng. Study on meat and bone meal toxication of rabbit. J of China Vet 1999;4:46-7.

[3] Feng Tao. Diagnosis on maduramicin toxication of rabbit. China Vet Science 2001;3:37-8.

[4] Gao Aiping Study of maduramicin toxication of meat rabbit. Husbandry of Vet 2001;3:47

[5] Gao Yue. Study on maduramicin toxication of Rex rabbit. J of China Rabbit 2002;5:11-2.

[6] Gu Zilin. Investigation and treatment on maduramicin toxication of rabbit. J of Economic Animal 1999;3:1-4.

[7] Gu Zilin. Study on weak and limp disease of rabbit. J of Feed Research 2002;2:38-43.

[8] Gu Zilin. Study on dead fetus of rabbit. J of Feed Industry 2001;10:43-5.

[9] Gu Zilin. Report on a rare case of breed rabbit sterility. J of China Rabbit 1996;3:32-4.

[10] He Zhongqing. Study of rabbit toxication on rice straw. J of China Rabbit 1998;1:38

[11] Hu Taiwen. Diagnosis and treatment onoxytetracycline toxication of meat rabbit. J of animal Science and Vet of Yunnan Province 1997;2:43.

[12] Jin Zhaojiang. Study on nitrite toxication of rabbit J of Husbandry and Vet 2000;2:46.

[13] Li Yongbin. A case of carrot vine toxication of rabbit. J of China Rabbit 1998;6:36-7.

[14] Li Zhengxian. Urea toxication of rabbit. J of China Vet 1998;9:31-2.

[15] Liang Kexing. Study on olaquindox toxication of meat rabbit. J of Economic Animal 4:60.

[16] Lu Shaoda. Study on morning glory vine of rabbit. J of China Rabbit 2000;3:37.

[17] Lu Xiaochun. Toxication and treatment of maduramicin of Meat Rabbit. J of China Rabbit 2001;1:38.

[18] Pang Xianhua. Prevention and treatment on dichlorvos toxication of rabbit. Report of Agricultural Science and Technology 2002;5:22.

[19] Shi Chuanlin . Report on norfloxcia toxication of rabbit. Modern Husbandry 2001;6:23.

[20] Wang Cairtu. Study on mildew toxication of rabbit. J of China Vet 2000;9:42.

[21] Wei Yulie. Study on furazolidone toxication of meat rabbit. J of Animal Husbandry and Vet 2001;3:30.

[22] Wen Jian. Study on "Qiushasi" toxication of fur rabbit. J of China Rabbit 1994;6:42.

[23] Wu Zhengming . Study on cottonseed toxication of rabbit. J of China Vet 1999;7:53.

[24] Xu Hanxiang. Prevention and treatment on flavomycin toxication. Agricultural Science of Jiangsu Province 1994;3:57-8.

[25] Yang Guoliang. Experience on drug toxication of rabbi. J of China Medicine 1997;2:28-9.

[26] Zheng Zengyi. Study on fluorin toxication of rabbit. J of Economic Animal1997;1:3.

[27] .Zhao Yuantong . Treatment on moldy feed toxication of rabbit. J of Guangxi Animal Science 2000;6:28-9.

[28] Zhao Hengliang . Prevention and treatment of cottonseed cake of rabbit. J of China Rabbit 2000;3:11-2. .

The Molecular Biological Application of the Theory of Stochastic Resonance: The Cellular Response to the ELF AC Magnetic Field

Hsien-Chiao Teng

Department of Electrical Engineering, Chinese Military Academy, Fengshan, Taiwan 833, Republic of China, scteng@cc.cma.edu.tw; 011886-7747-9510 ext 134

Abstract: The cultured rat liver epithelial cells in vitro initiates noisy magnetic fluctuation, which can be measured and provides a basis for signal amplification to transmit of weak signal along the possible signaling pathways in cell despite low signal-to-noise ratio of the primary cellular response for external stimulus. By using power density spectrum analysis of noisy magnetic fluctuation, the signal-to-noise ratio (SNR) of the possible intrinsic periodical extremely low frequency signals can be depicted. The calculation reveals that 7 Hz is an intrinsic signal for rat liver epithelial cell system. Exposing cultured rat liver epithelial cells into a constant extremely low frequency (ELF) alternating current (AC) magnetic field 150 mG at 7 Hz for 60 minutes, 20% promotion of the gap junction intracellular communication (GJIC) was observed from Lucifer yellow fluorescence microscopic image while comparing with the control. Cellular response is experimentally found at 7 Hz, which agrees with the mathematical analysis under the theory of stochastic resonance. [Nature and Science. 2005;3(1):37-41].

Key words: signal to noise ratio; gap junctional intracellular communication (GJIC); power density spectrum; stochastic resonance

1 Introduction

The theoretical calculation of a periodically driven stochastic process has been developed for two decades and applied to a wide variety of naturally occurring and computer simulation processes (McNamara and Wiesenfeld, 1989; Jung, 1993; Jung et al., 2005; Schatzer and Weigert, 1998; Schmid et al., 2004). The possibility of amplification of weak

signal in cellular system and the modulation of grating properties of membrane K+ and Na+ channels by external signals were proposed under the assumption of existence of stochastic resonance (Schmid et al., 2004). However, the gap junctional intracellular communication (GJIC) within the cells may induce the surface-current instead of trans-membrane voltage upon the cultured cells (Hart, 1996). In cell, six connexin 43 subunits oligomerze in the Golgi apparatus into a connexon, called hemi channel and be transported to plasma membrane of the cell. Before pairing process, hemi channels are closed to avoid leakage of cellular contents and entry of extra-cellular materials. During the pairing of connexons and aggregation into plaques at the plasma membrane, connexin 43 is phosphorylated at least twice and connexons are attracted to those located on the adjacent cells. Two connexons join in an end-to-end manner to form a complete channel. The channels aggregate into large gap junction plaques open to connect two cells for cell-to-cell communication and is called gap junctional intracellular communication (GJIC), which can be modulated by environmental factors, such as drugs, X-ray, electromagnetic fields etc. Since the function of the GJIC, cultured cells coupled together in vitro except the stem cells and cancer cells (Trosko et al., 1990). In this article, we introduce the magnetic field fluctuation induced by GJIC surface-current of the cells. We apply the concept of periodically driven stochastic processes to a model consisting of hemi channels and Lucifer yellow fluorescence diffusion. Scrape loading dye transfer of Lucifer yellow is a technique to observe and measure the diffusive range of Lucifer yellow fluorescence (Upham et al., 1998). The varied diffuse range of Lucifer yellow fluorescence can express the cellular response under the exposure of ELF at the intrinsic-resonance frequency ω. Since GJIC is affiliated with many pathological endpoints (Trosko et al., 1990; Upham et al., 1998; Trosko et al. 2001), GJIC modulation can be used as a biological response factor to evaluate the ELF reaction for cellular system.

2 Theory

Electronically, the magnetic fluctuation can be acquisitioned to oscilloscope voltage V(N) for N times measurement per second.

$$V(N)=\{V_1,V_2,\ldots..V_{N-1}V_N\}; \quad (1)$$

$$R_q=\left(\frac{1}{N}\right)\sum_{p=1}^{N}V_pV_{p+q} \quad (2)$$

$$S_k = \sum_{q=1}^{N} R_q e^{\frac{i2\pi}{N}kq} \quad (3)$$

$i = \sqrt{-1}$. Equation (3) is the power density component at frequency $\omega_k = \frac{2\pi}{N}$ k (fundamental frequencies), the unit of S_k is watt per hertz for each V_p. To assess the magnitude of amplification of a signal, we take the surface diffusive current fluctuation of the cultured cells through N measurements per second. Begin from a simple open-close gap junctional connexin 43 channel assumption, whose close state and open state specified by c-state and o-state respectively, the rate of changing of c-state and o-state affects the surface diffusive current fluctuations across the cells. However, we must propose the state of the channel be either fully open or close. The probabilities P^o and P^c represent the states, which is either in c-state or in o-state respectively (Galvanovskis et al., 1997). Then, the diffusive current equation for connexin 43 channels can be written as

$$<I> = \sum_{k=1}^{m} kP(k) \quad (4)$$

where probability P(k) indicates total m channels is taken into account for opening k channels from all cell-to-cell communications on the surface of the cell mono layer. Therefore,

$$P(k) = \frac{m!}{k!(m-k)!}(P^o)^k (P^c)^{m-k} \quad (5)$$

$$\frac{dP^o}{dt} = r^c P^c - r^o P^o \quad (6)$$

$$\frac{dP^c}{dt} = r^o P^o - r^c P^c \quad (7)$$

where r^c is the rate of changing from c-state to o-state and r^o is the rate of changing from o-state to c-state of the connexin 43 channels activating totally on the cells mono layer surface. Generally, r^o does not have to be same with r^c since the life times of the o-state and c-state may vary. To clarify the physical meaning, we further assume the current through an open channel as i. The diffusive current caused by GJIC channels can be rewritten as

$$<I> = m\, i\, P_S^o \quad (8)$$

where P_S^o is the modulated probability for o-state by external ELF field signal. According to theory of Jung (1993), the power spectral component originated from the signal is given by

$$S_k = \frac{(m\,i)^2}{2} \sum_{q=1}^{\infty} \left| C_q \right| \delta(\omega - q\omega_k) \quad (9)$$

C_q is the Fourier expansion coefficients of P_S^o.

In Comparison with equations (3) and (9), the signal-to-noise ratio (SNR) of the characteristic frequency of the cell system can be depicted (Galvanovskis et al., 1997).

$$SNR = \left| \frac{\text{signal amplitude}}{\text{background amplitude}} \right|^2 = A^2 \left| \sqrt{m \frac{\pi}{\Delta\omega} \frac{r^o r^c}{(r^o + r^c)}} \right|^2 \quad (10)$$

where m is the number of channels, A is the amplitude and $\Delta\omega$ is the bandwidth of the external ELF field signal.

3 Materials and Methods

Fitting 3.5 cm diameter cell culture dish, a solenoid was made by a simple 5-cm diameter plastic cylinder tube 2 cm in height wrapped with single layer 200 turns 0.45-mm diameter cooper string connecting a function generator to provide ELF field signals for rat liver epithelial cells *in vitro*. The solenoid was placed in an incubator so called ELF incubator controlled the environment at 5% CO_2 at 98% relative humidity. Another sham field chamber was exactly same as the ELF incubator only with no ELF provider. The cell culture dishes were placed within the solenoid parallel to the normal direction of the cross-section. The function generator generated the ELF signal through the solenoid perpendicularly to the cells in the center of the solenoid for sixty minutes.

3.1 Cell Culture

The rat liver epithelial cell line *in vitro* was obtained from the Fisher Scientific (WB344) (Hampton, NH, USA). It was derived from normal liver and maintained in D-medium (Formula 78-5470EF, GIBCO, Grand Island, NY, USA), supplemented with 10% fetal bovine serum (GIBCO) and 50 μg/ml gentamicin (Quality Biological, Inc., Gaithersburg MD, USA). The cells were incubated at 37°C in a humidified atmosphere containing 5% CO_2 and 95% air and were fed or trypsinized every two to three days.

3.2 SNR Spectrum

By using of the probe of Gauss-meter, we took rat liver epithelial cells-induced magnetic fluctuation $\{B_i^c\} = \{B_1^c, B_2^c \ldots\ldots B_{2000}^c\}$, which may contain the

cellular response signal to the external ELF magnetic field reaction. The sampling time was 0.0005 second and the probe was at the distance 10^{-4} m perpendicularly to the center of single layer of the cells. The Gauss-meter was manufactured by F.W. Bell Company (series of 9550) in Florida of USA. Oscilloscope was manufactured by Agilent Company (54621A) and be able to convert $\{B_i^c\}$ to voltage sequence $\{V_i^c\}$. Matlab and Fortran programming were used for power density spectrum analysis of these voltage sequences. Medium control group $\{B_i^m\}$ was also taken at 2000 times per second at the distance 10^{-4} m perpendicularly to the bottom of culture plate only with medium in it. In the mean time, geo-field control group $\{B_i^n\}$ was taken with the same sample rate at the distance 10^{-4} m perpendicularly to the bottom of empty culture plate for recording local geomagnetic field fluctuation. The $\{V_i^m\}$ and $\{V_i^n\}$ voltage sequences were recorded in the same way as $\{V_i^c\}$ did previously. Further more, we must take a series trial signals for separating the characteristic frequencies from the background. Those signals were defined as $\Omega_i(n)=A_i\times\sin(\omega_i n)$, $1\text{Hz} \le \omega_i \le 60\text{Hz}$, where $A_i = F\times V_{.,\max}^{i}$, F is the adjustable fraction factor and $V_{.,\max}^{i}$ is such, for instance, $V_{.,\max}^{i}$ = MAX($\{V_i^c\}$), as to the maximum value of the sequence. By taking into consideration of signal amplitudes $A_{0.7} = 0.7\times V_{max}$, $A_{0.4} = 0.4\times V_{max}$, $A_{0.03} = 0.03\times V_{max}$ for a given trial signal at ELF ω_i ($1\text{Hz} \le \omega_i \le 60\text{Hz}$), we computed the Fourier transforms of the autocorrelation function of $\{V_i^c + \Omega_i(n)\}$ to obtain the signal-to-ratio ratio $SNR\omega_i$ (0.7), $SNR\omega_i$ (0.4) and $SNR\omega_i$ (0.03) respectively. The SNR spectrum for $\{V_i^c + \Omega_i(n)\}$ at frequency ω_i could be simply a second order equation as $a \times (SNR\omega_i(F))^2 + b \times (SNR\omega_i(F)) + c = 0$. Accordingly, substituting the SNR values into the equation, we can solve unknowns a, b and c

$a(SNR\omega_i(0.7))^2 + b(SNR\omega_i(0.7)) + c = 0$; (11)

$a(SNR\omega_i(0.4))^2 + b(SNR\omega_i(0.4)) + c = 0$; (12)

$a(SNR\omega_i(0.03))^2 + b(SNR\omega_i(0.03)) + c = 0$ (13)

Equations (11), (12), (13) involved three equations and three unknowns, a, b and c. Therefore, a, b and c values could be solved. If c-value is bigger than zero, which means the SNR of the intrinsic signal peaked at ELF ω_i is detected. In the paper by Galvanovskis (1997), $SNR\omega_i(F) = (F\times V_{max})^2 \times m \times Q \times \frac{2\pi}{\omega_i(\tau_o + \tau_c)}$, the theoretical value of c is approximately 0.09 when the life time of c-state and o-state equal to 10^{-6} second. Under optimal condition, the quality factor $Q = \frac{\omega_S}{\Delta\omega}$ approximately equals to 100 at 60Hz with bandwidth $\triangle\omega = 0.6$Hz, F = 0.6 respectively. The numbers of GJIC channels are approximately taken 1000 per cell (Galvanovskis et al., 1997).

3.3 Bioassay of GJIC

The scrape load/dye transfer (SL/DT) technique was used to measure the GJIC within cells. After exposure to ELF at intrinsic frequency, the cells were rinsed with phosphate buffered saline (PBS), and a PBS solution containing 4% concentration Lucifer yellow fluorescence dye is injected into the cells by a scrape using a scalpel blade. Afterwards the cells were incubated for 3 min and extra cellular dye was rinsed off and fixed with 5% formalin. We then measured the area of the dye migrated from the scrape line using digital images taken by an epifluorescent microscope and quantitated with Nucleotech image analysis software (Upham et al., 1998) for the GJIC images.

4 Results

Figure 1 depicts the plot of V_i^c. Figure 2 depicted the SNR fitting curve of ELF at 7Hz such as to confirm if the intrinsic frequency situated. When the intrinsic ELF is present at 7 Hz, GJIC modulation can then be used to observe the biological effect of ELF provided externally. Figure 3 shows the GJIC fluorescent images. Since the GJIC of cells was quantified with the measurement of the average distance of dye migration, GJIC was reported in this article as a fraction of the control (FOC) in Figure 4. An FOC value equals to 1.0 indicates normal GJIC. The FOC value more than 1.0 indicates excitation.

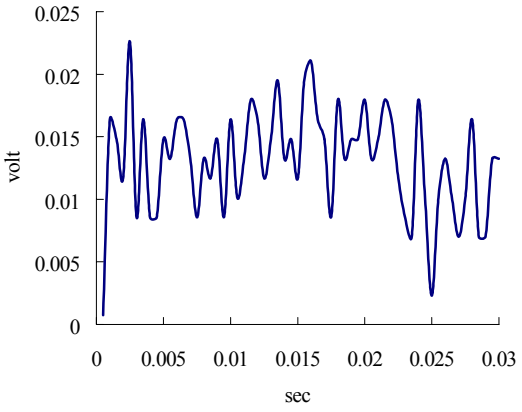

Figure 1. V_i^c schematic drawing

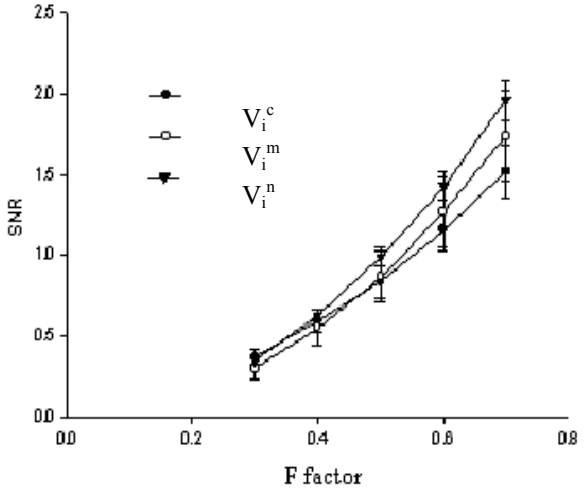

Figure 2. SNR of the trial signal at 7 Hz

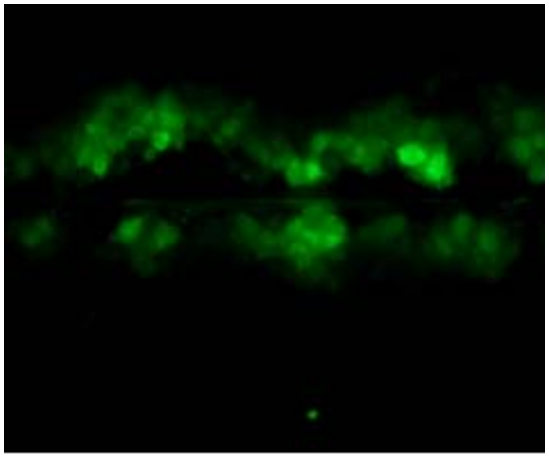

Figure 3. The GJIC imagine

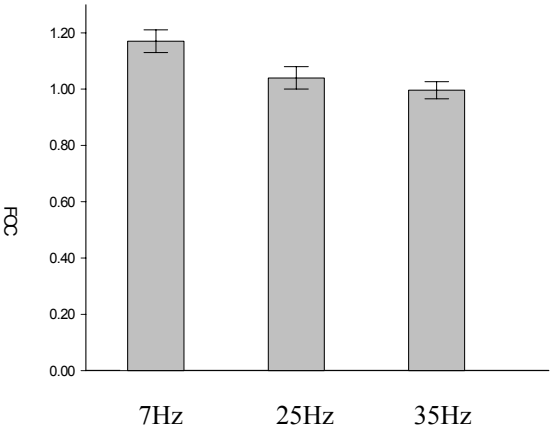

Figure 4. The fraction of control of the GJIC Assay at different ELF exposure

5 Discussion

Experimental results depicted that the GJIC within cells relates to both the background noisy magnetic field fluctuation and the intrinsic ELF signal. In the paper by Hart, the GJIC affects the cell-surface current, which is about 10^{-9} Amp (Hart, 1996) under the background noisy magnetic fluctuation within confluent cells in culture. Thus, the GJIC would also affects cell surface electrical current simultaneously when the SNR of the intrinsic signal adjusts the changing rate of the GJIC channel in o-state. The varying amplitudes of trial signal were used to determine the intrinsic signal and its SNR buried in the power density spectrum of $V_i^c(t)$.

6 Conclusion

The main feature of our research introduced is $V_i^c(t)$ relating to the change in the probability of GJIC channels being in o-state or c-states. The $V_i^c(t)$ expression for cell induced GJIC current flow into and out of the two states, o-state and c-state *in vitro* under the background magnetic fluctuation has been identified by specific external ELF ac magnetic field signal at 7 Hz, which modulates the GJIC 20% within the cells. Based on the application of stochastic resonance, which predicts the existence of the intrinsic ELF signal, our study depicted that we were able to obtain the corresponding level of the SNR expression for illustrating that the external ELF ac magnetic field signal can modulate 20% GJIC promotion within the cells at 7 hertz.

Correspondence to:
Hsien-Chiao Teng
Department of Electrical Engineering
Chinese Military Academy, Fengshan, Taiwan 833
Republic of China
Email: scteng@cc.cma.edu.tw
Telephone: 011886-7747-9510 ext 134

References

[1] Hart F. Cell culture dosimetry for low frequency magnetic fields. Bioelectromagnetics 1996;17:48-57.
[2] Galvanovskis J, Sandblom J. Amplification of electromagnetic signals by ion channels. Biophysical Journal 1997;73:3056-65.
[3] Jung P. Periodically driven stochastic systems. editor: I. Procaccia, Physics Reports (Review Section of Physics Letters) 1993;234(4,5);175-295.
[4] Jung J., Alexander N, Muhammad KN, Afghan N, Suhita, Ghanim U. New Journal of Physics *2005;*7:17 (http://www.njp.org/)
[5] McNamara B, Wiesenfeld K. Theory of stochastic resonance. Physical Review A 1989;39(9):4854-69.
[6] Schatzer L, Weigert S. Solvable three-state model of a driven double-well potential and coherent destruction of tunneling. Physical Review A 1998;57(1):68-78.
[7] Schmid G, Guychok I, Hanggi P, Zeng S, Jung P. Stochastic resonance and optimal clustering for assemblies of ion channels.

Fluctuation and Noise Letters 2004;4(1):L33-L42.
[8] Trosko JE, Chang CC, Madhukar BV. Modulation of intercellular communication during radiation and chemical carcinogenesis. Radiation Research 1990;123:241-51.
[9] Trosko JE, Chang CC. Role of stem cells and gap junctional intercellular communication in human carcinogensis. Radiation Research 2001;155:175-80.
[10] Upham BL, Deocampo ND, Wurl B, Trosko JE. Inhibition of gap junctional intracellular communication by perfluorinated fatty acids is dependent on the chain length of the fluorinated tail. Int J Cancer 1998;78:491-5.

Fundamental Study on Relevance of Retail Format Structure and Average Profit Rate of Assets

Fengge Yao, Yan Zhao, Minming She

Harbin University of Commerce, Harbin, Heilongjiang 150028, China, zhaoyan2000@yahoo.com.cn

Abstract: There are insufficient researches done on the field of retail format structure at present both at home and abroad, and most of these researches focus on qualitative analysis. We put forward that the essence of good and bad structure is an equilibrium problem, and set up the evaluation criterion of the retail format structure according to the equilibrium theory in the paper. We analyze the relevance between the retail format structure and the average profit rate in China, in that we draw a conclusion that the analysis based on format structure equilibrium is an optimal one. [Nature and Science. 2005;3(1):42-44].

Keywords: retail format; retail format structure; correlation coefficient; profit rate of the assets

1 Foreword

Retail format structure is mainly used to describe retail format state under some certain circumstance. At present, there is not a definite and intact definition. We put forward that the definition of retail format structure should be in two aspects: narrow sense and broad sense, through our summing up and study on a large number of articles at home and abroad. The so-called definition of retail format structure in narrow sense encompasses the numbers of all retail format assets, incomes, profits, every kind of retail format and the according proportional relationship under a specific economic social environment. In broad sense, it defines as all kinds of retail format shops, assets, incomes and profits in every retail format, the according proportional relationship and the space structure of every retail format. It includes kinds and numbers of retail format and their proportional relationship and arrangement relationship. Its epitaxy includes quantity structure, assets structure, sales structure (market structure), profit structure and space structure.

In the following the paper is focused on the relationship between evaluation criterion and average profit rate, which involves improving the retail competitiveness of a district or a nation.

2 Foundation of the evaluation criterion of retail format structure

First, an evaluation criterion of retail format structure should be set up. We think that an equilibrium format structure is good according to the equilibrium theory. The essence of structure evaluation is to evaluate the equilibrium of format structure.

The paper is predominantly based on the equilibrium of Goshen's second theorem, whose basic content is that a consumer must make the utility by spending the last unit of money on each good equal maximize his utility and pleasure with his limited income. Mathematical method can also express the theorem. Suppose there are good A, good B, good C with their marginal utilities and prices M_{uA}, M_{uB}, M_{uC}, P_A, P_B, P_C respectively. Then the theorem can be written as follows:

$$\frac{M_{uA}}{P_A} = \frac{M_{uB}}{P_B} = \frac{M_{uC}}{P_C} \cdots$$

It is obvious that we can substitute a nation for a consumer, national format investment for consumer's purchasing behavior and the purpose of consumer's utility maximization equals national profit maximization. Therefore, the nation can get its maximum profit.

According to the above thought, we propose the correlation between each format asset structure and profit structure as an evaluation criterion of format structure, i.e., correlation coefficient. The more approximate the correlation coefficient is near 1, the

more balanced and the better the format structure is.

Correlation coefficient comes from clustering analysis. In clustering analysis we need classify not only samples but variables as well by using the tool of correlation coefficient. The general definition is as follows:

Suppose that V is a variable set and c is a real function from $V \times V$ to $[1 \times 1]$. If

(1) $c_{xy} = \pm 1 \Leftrightarrow x = ay, a \neq 0$ (constant)

(2) $\forall x, y \in V, |C_{xy}| \leq 1$;

(3) $\forall x, y \in V, c_{xy} = c_{yx}$

then c_{xy} is the correlation coefficient of x and y. The more approximate $|c_{xy}|$ approaches 1, the more closely the relation between x and y is and the larger the correlation is. The most frequent correlation is included angle cosine. Suppose n observed values of index variables I_i and I_j form n-dimension vectors $x_i = (x_{1i}, x_{2i}, \cdots, x_{ni})^T$ and $x_j = (x_{1j}, x_{2j}, \cdots, x_{nj})^T$. We define the correlation coefficient is

$$C_{ij}(I) = \cos(x_i, x_j) = \frac{(x_i, x_j)}{\|x_i\| \|x_j\|} = \frac{\sum_{k=1}^{n} x_{ki} x_{kj}}{\sqrt{\left(\sum_{k=1}^{n} x_{ki}^2\right)\left(\sum_{k=1}^{n} x_{kj}^2\right)}}$$

The correlation coefficient method in the paper is that we create structure vectors according to the theorem and then work out the correlation coefficient of every format asset vector and profit vector. After that we evaluate format structure development through observing correlation coefficient. The more approximate the coefficient approaches 1, the more correlated the asset and profit vectors are, the better and the more balanced the structure is. On the contrary the structure is out of balance.

3 Empirical analysis on the correlation of retail format structure and average profit

According to the equilibrium theory above, we can evaluate retail the format structure in every district. First we evaluate retail format structures in the whole country (China) and 9 districts and then set up the following index variables.

(meaning of signal: GM_i for the *ith* format assets; LY_i for the *ith* format profit; t for time)

1. Asset structure vector $\overrightarrow{GM} = \{GM_1, GM_2, GM_3, GM_4\}$

2. Profit structure vector $\overrightarrow{LY} = \{LY_1, LY_2, LY_3, LY_4\}$

3. $C(GL)_t = \cos(\overrightarrow{GM}, \overrightarrow{LY})_t$ ($C(GL)_t$ for the correlation coefficient of asset and profit)

According to the study on the cross-section data of retail format in each district in 1999, we get the correlation coefficients between the format assets and profits as follows:

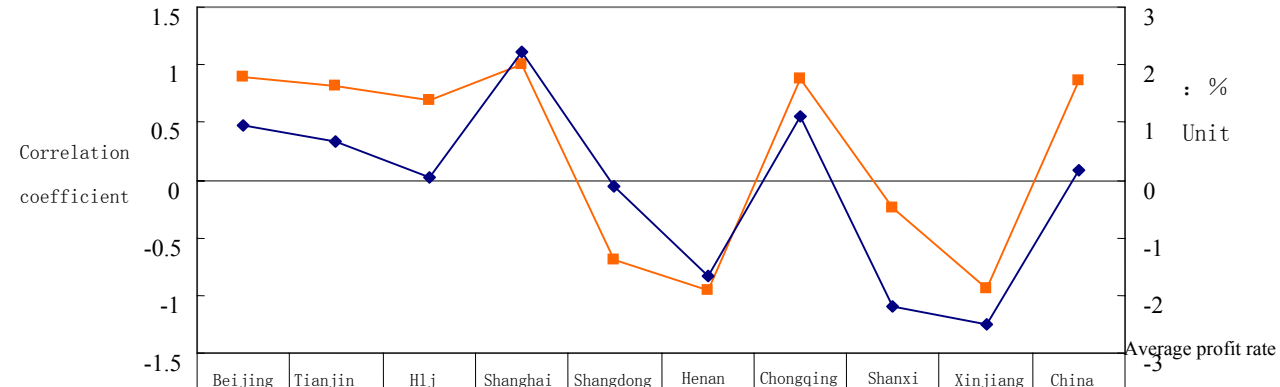

	Beijing	Tianjin	Hlj	Shanghai	Shangdong	Henan	Chongqing	Shanxi	Xinjiang	China
coefficient	0.88774	0.823604	0.698298	0.997067	-0.69391	-0.9584	0.874489	-0.24119	-0.94378	0.861635
Average profit rate	0.963011	0.656408	0.039404	2.229749	-0.1009	-1.65246	1.08913	-2.18539	-2.49562	0.17263

Figure 1. Retail format structure and profit rate in 9 districts in 1999

But does structure equilibrium really mean high profit rate? We make our further empirical research on correlation between format structure and average profit rate and we get correlation coefficient between format structure and average profit rate $r = 0.83214$ $t = \frac{0.83214\sqrt{10-2}}{\sqrt{1-0.83214^2}} = 4.24$. When the level of significance is 0.01, $t_{\alpha/2} = 3.3554$, $t > t_{\alpha/2}$, which means that *r* passes significance test, i.e. the correlation coefficient between format structure and average profit rate is highly linearly dependent.

4 Conclusion

Through our research, we verify the essence of whether a structure is good or bad is the problem of structure equilibrium. Balanced format structure can create higher profit rate. Consequently it is optimum one. Afterwards we can judge whether the retail format structure in a district is good or bad through measuring its correlation coefficient and then adjust it to improve retail industry competitiveness in the district.

Correspondence to:
Fengge Yao,Yan Zhao, Minming She
Harbin University of Commerce
Harbin, Heilongjiang 150028, China
E-mail: zhaoyan2000@yahoo.com.cn

References

[1] Li Few *Retail Revolution* [M] Economic Management Publishing House 2003.
[2] Wei Hongsen, Zeng Guoping *System Theory—System Science Philosophy* [M] Tsinghua University Press 1995.
[3] Xia Chunyu *Retail Format Vicissitude Theory and New Development* [J]Contemporary Economics Science 2002.
[4] James·M·Henderson *Intermediary Microeconomics Theory — Mathematical Method* [M] Peking University Press 1989.
[5] GRADY D. BRUCE. The ecological Structure of Retail Institutions. Journal of Marketing Research 1969;6:48-53.

Study On Sunlight Greenhouse Temperature And Humidity Fuzzy Control System

Lishu Wang[1], Guanglin Yang[1], Qiang Fu[2], Xiangfeng Xu[1]

1. School of Engineering, Northeast Agricultural University, Harbin, Heilongjiang 150030, China
2. School of Water Conservancy & Civil Engineering, Northeast Agricultural University, Harbin, Heilongjiang 150030, China, wanglishu@neau.edu.cn

Abstract: Through establishing fuzzy control system model, designing on fuzzy controller, controlling sunlight greenhouse temperature and humidity, we designed temperature and humidity fuzzy control system, and then studied on input and output parameter in fuzzy controller, analyzed membership function of inputting and outputting parameter, then designed fuzzy control operation. The greenhouse has the best entironment for crop growing. [Nature and Science. 2005;3(1):45-48].

Key words: greenhouse; fuzzy control; temperature; humidity

Introduction

The sunlight greenhouse is a kind of new-type, highly-efficient, controllable agricultural production facility. For years, people regard sunlight greenhouse as research object, making further investigation on various kinds of produce factor, which can influence produce control in the hope of obtaining the best benefit (Yu, 2002). Because the sunlight greenhouse is a non-linear system with big inertia, in addition influence factor are numerous, it is very difficult to describe the production process with the mathematics model. The crop-grow fuzzy control system designed in this paper is a kind of automatic control system, which based on the knowledge of fuzzy mathematics and fuzzy language knowledge expression. It also regards fuzzy logic regular reasoning as the theoretical foundation, and it is a numerical control system adopting the computer numerical control technology of the closes-ring structure form one of feedbacks passageway.

1 Systematic Design Thought

The sunlight greenhouse production process is very complicated, especially the extreme fuzzy in the requisition for environmental parameter. So this paper researches on it with the fuzzy control theory (Zhong, 2001). The basic principle of fuzzy controls is: to compare ideal value of controlling quantity with the measuring value t transient, receive input parameter (deviation E), and calculate declination variation rate ΔE, turn E and ΔE into fuzzy quantity e and Δe, and then make a decision by fuzzy control regular R and e、Δe, get fuzzy control parameter u, finally turn the fuzzy control one into accurate quantity, act on the target under controlled, circulate like this, and realize the fuzzy control of the target. The fuzzier the fuzzy target that controls is, the more superiority this kind of control method reflects than the other methods they are. So that it is very suitable for the control of the environmental system of the greenhouse.

2 Temperature and Humidity Fuzzy Control ystem

The frame diagram of fuzzy control system is as Figure 1 shows.

2.1 Study on input and output parameter in fuzzy controller

Input parameter is an external variable of the fuzzy controller, and its numeric equals difference between measurement T(t)、H(t) and ideal T0、H0 of moment t. That is

$$E_{\mathrm{T}} = T(t) - T_0 \quad \text{（Temperature deviation）（1）}$$

$$C_H = E_{\mathrm{H}} = H(t) - H_0 \quad \text{（Humidity deviation）（2）}$$

Quantitative temperature deviation set X_1 11 grade, then X_1={-5，-4，-3，-2，-1，0，1，2，3，4，5}.

Quantization factor of the temperature deviation $K_{eT}=\frac{C_T}{1}=5$。

E_H fuzzy control area establishes less than ±5%, C_i value as {*NB*，*NM*，*NS*，*ZO*，*PS*，*PM*，*PB*}, Quantization is grade 11, X_3={-5，-4，-3，-2，-1，0，1，2，3，4，5}. Quantization factor of the t humidity deviation $K_{eT}=\frac{C_T}{1}=5$.

In the temperature and humidity control, it does not merely make temperature rise to the heating of the greenhouse, but also can increase the greenhouse moisture evaporation. It makes the humidity rise too. When arranged wetly at the same time, it will make temperature change too. The coupling phenomenon is named cross between the temperature and humidity. To introduce solving coupling parameter α_1， α_2，it receives the equation of outputting.

$$U_T=(1-\alpha_1)\times C_T+\alpha_2\times C_H$$

$$U_H=(1-\alpha_2)\times C_H+\alpha_1\times C_T \qquad (\alpha_1、\alpha_2 \in [0\sim 1]) \quad (3)$$

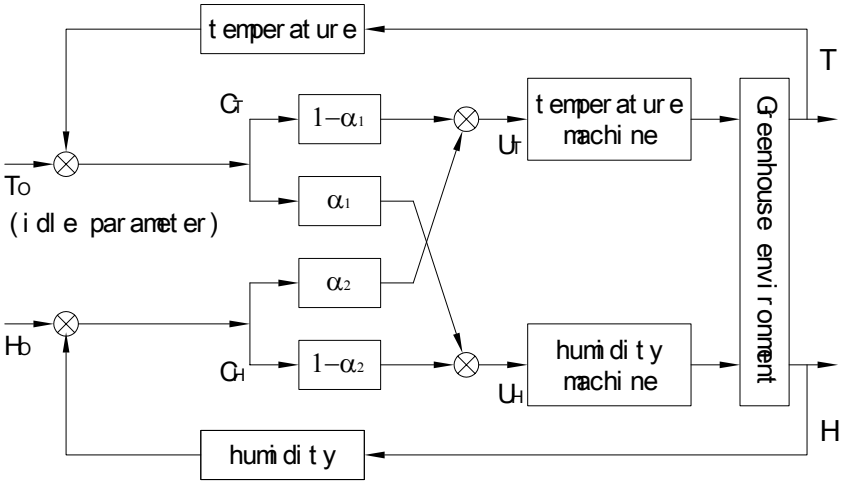

Figure1. The frame diagram of fuzzy control system

2.2 Outputs quantity described

Output variable is endogenous variable of fuzzy controller for adjust temperature and wet machine it is input variable. Because it is coupling output of the input information, its variable classification corresponds to variable of inputting grade.

U_T is temperature control exporting parameter. Its fuzzy subset E_i value is {*NB*，*NM*，*NS*，*ZO*，*PS*，*PM*，*PB*}. Among them *PB* (heat completely): The proportion valve is opened maximum. *PM* (mild heat): proportion 1/2 valve turn on degree, *PS* (little to heat). 1/3 of proportion valve is opened degree. *ZO* (not rise or low the temperature): The proportion valve closes and the skylight does not open. *NS* (the little drop in the temperature): The skylight opened 1/3 degree. *NM* (mild lowers the temperature): The skylight opened 1/2 degree. *NB* (lower the temperature completely): The skylight is opened maximum.

U_H is humidity control exporting parameter. Its fuzzy subset F_i value is {*NB*，*NM*，*NS*，*ZO*，*PS*，*PM*，*PB*}，among them *PB* (the whole humidification): All hydrant open. *PM* (mild humidification): hydrant open of half, *PS* (little humidification): hydrant turn on 1/3. *ZO* (no increase or lower humidification): hydrant close and skylight close. *NS* (little lower temperature): 1/3 of skylight is opened. *NM* (mild lowers the temperature): 1/2 of skylight is opened. *NB* (lower the temperature completely): The skylight is opened biggest. Quantification output amount 11 grade, so X_6={-5，-4，-3，-2，-1，0，1，2，3，4，5}.

Obviously, when α_1 and α_2 are all 0, $U_T=C_T$，$U_H=C_H$，equal to two single circuits control at this moment. When they are all 1, $U_T=C_H$，$U_H=C_T$，then it is limit coupling at this moment （Zhang 2002）. The real α_1 and α_2 are among 0~1. The concrete

methods are to hypothesize α_1 and α_2 to be equal to 0 and carry on the experiment to the greenhouse. Whenever heat or eliminate damp, it will make the temperature and humidity in the greenhouse have greater fluctuations. Then gradually increase α_1 and α_2, it makes the fluctuation reduce, achieve the goal of solving coupling, thus get the optimum value.

2.3 Membership function of inputting and outputting parameter

Membership function is always gotten by experience, so it has greater random. The choice of the fuzzy variable Membership function has certain influence on the functions of the fuzzy controller（Liu, 2001）. Generally speaking, the steeper the form of Membership function is, the higher the resolution ratio is and the higher sensitivity of the control is. On the contrary, the slower the form of Membership function is, the characteristic control is gentle, and systematic stability is fine. The form of Membership function adopts the triangle or bell has small influence on control function, we choose the triangle form of Membership function for the purpose to achieve simplified calculation.

Temperature and humidity deviation Membership function, the Membership functions of temperature and humidity controlled output are shown in Figure 2 and Figure 3. Stability is fine. The form of Membership function adopts the triangle or bell has small influence on control function. We choose the triangle form of Membership function for the purpose to achieve simplified calculation (Ren, 2001). Temperature and humidity deviation membership function, the Membership functions of temperature and humidity controlled output are showed in Figure 2 and Figure 3.

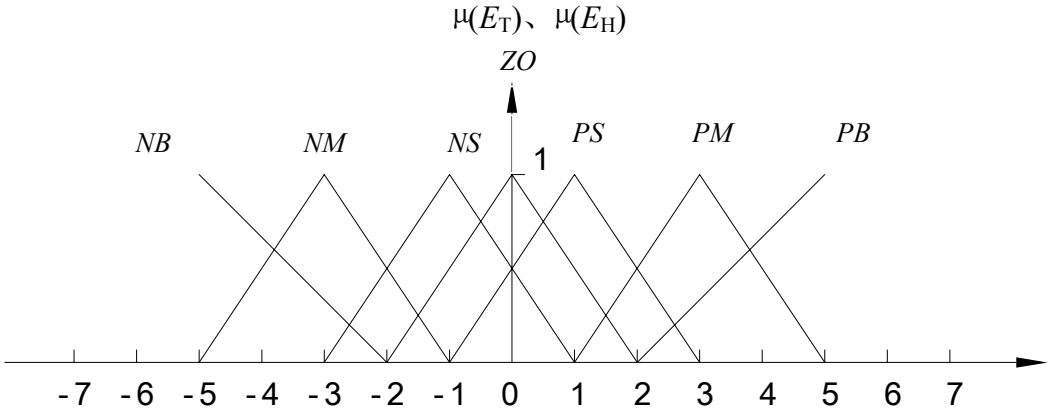

Figure 2. The temperature and humidity deviation Membership functions

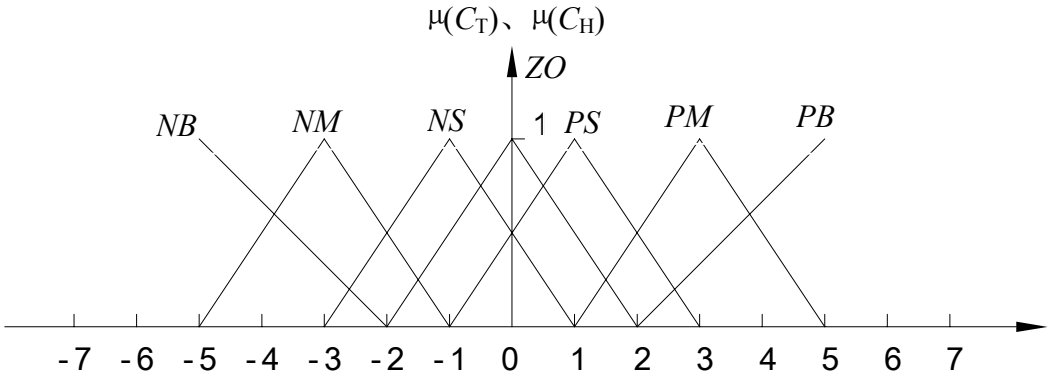

Figure 3. The Membership functions of temperature and humidity controlled output

3 Design of Fuzzy Control Operation

In the fuzzy control operation design, control operation of the execution according to outputting variable information. When the error is less, besides wanting the error of dispelling, should consider systematic stability, prevent system produce unnecessary exceeding adjusting even shock. When E_T is *NS or ZO*, the groundwork is turned into the stability problem. In order to prevent exceeding adjusting, making the system steady as soon as possible, it will confirm the controlling amount according to the concrete conditions that temperature will be changed soon at this moment, and it will choose the corresponding control rule. If ΔE_T is plus then indicating the temperature change has the tendency to reduce, so the fuzzy control system should fetch the smaller control amount. The same principle when deviation is plus or minus, the corresponding symbol carries on the change（Xu, 1987）. The humidity fuzzy control rule in line with when the error is greater the controlling amount does the best to make the error reduce rapidly. When the error is less, besides wanting the error of dispelling, should consider systematic stability.

4 Conclusion

This paper has put forward a train of thought and method in connection with the sunlight greenhouse on temperature and humidity fuzzy control. Through fuzzily controlling and regulating the crop growth environment of the sunlight greenhouse, it will play a enormous role to improve the output and quality of the crops.

Acknowledge

The financial support is provided by the Department of Education of Heilongjiang Province Programme (No. 10531018): “Optimization design on intelligence sunlight greenhouse moisture and temperature entironment automatism surveillance and control”.

Correspondence to:
Lishu Wang, Guanglin Yang, Qiang Fu
School of Engineering
Northeast Agricultural University
Harbin, Heilongjiang 150030, China
Telephone: 01186-451-8997-1785
E-mail: wanglishu@neau.edu.cn

References

[1] Liu Shuguang, Wei Junmin, Zhu Chao. Fuzzy Control Technology. China Textiles Press, 2001:81-2.
[2] Ren Zhen Hui, Zhang Shu Guang, Xie Jing Xin, et al. Development of Intelligent Monitoring and Managing System of Environment Parameters for Solar Greenhouse . Transactions of the CSAE 2001;17(2):107-10.
[3] Xu CW, Zailu Y. Fuzzy Model Identification and Self-learing for dynamic Systems. IEEE Trans. on Syst, Man, Cybem,1987;17(4):683-9.
[4] Yu Yongchang, Hu Jiandong, Mao Pengjun. Fuzzy Control for Environment Parameters in Greenhouse Transactions of the CSAE［M］. Beijing: 2002;18(2):72-5.
[5] Zhang Rui Hua. Automatic measurement and control system of greenhouse. Computer and agriculture［M］. 2002, the second issue: pp 8-10.
[6] Zhong Yingshan, Yang Jiaqiang, Deng Jinlian. Multivariable Fuzzy Control of Temperature and Humidity in a Greenhouse. Transactions of the agricultural machinery［M］ 2001;32(3):75-8.

Research on Mode of Ranges Control by Farm and Lateral Ditches

Liquan Wan[1], Zhangchun Yao[2], Zhengmao Liu[2]

1 Water Service of General Bureau of Reclamation, Harbin, Heilongjiang 150091, China, nkjl@163.com
2 Heilongjiang Agricultural Reclamation Exploration Survey and Design Institute, Jiamusi, Heilongjiang 154002, China

Abstract: it is abundant in water resource in Heilongjiang province and the level of agricultural mechanization is high, but the disasters such as flood, waterlogging, alkalization and drought are more serious too, at present, the waterlogging in the Sanjiang plain and alkalization in the Songnen plain are the most serious. Because the project quantity of salinization control is large and a lot of investment is needed, the salinization control has not been put the agenda of controlling plan. If the ranges control by farm, lateral ditches is combined with the present project and the operation of modern family farms, the leap development of salinization and waterlogging control can be realized, the new innovation of bringing water conservancy technology into house. At present, two ranges-controlling demonstration areas have been constructed. [Nature and Science. 2005;3(1):49-58].

Keywords: waterlogged disaster; salinization; mechanization; family farm; rainfall drainage and storage for irrigation; ecological water conservancy; bringing science and technique into house

1 Environmental features of water resource in Heilongjiang province

①Heilongjiang province is situated in northeast china and is one of the most important granary areas of China. there are two larger plains — Sanjiang and Songnen plain in Heilongjiang, the former lies in the center and the latter lies in the west, both of the two plains are main agricultural areas of Heilongjiang. Heilongjiang lies in the humid and sub humid mesothermal climate zone and is slightly abundant in water resource. In Heilongjiang, the average annual precipitation ranges from 400 mm to 700 mm, while the water demand of dry farming agriculture is only about 450 mm, the relationship between water supply and demand is balanced, which is the greatest predominance for agricultural development of Heilongjiang. However, because the inter-year and inner-year distribution of rainfall is not uniform in time and space, again influenced by topographical feature, land form, soil, geological structure and other meteorological and hydrological factors, disasters such as flood, waterlogging, waterlogged, drought, alkalization often take place. According to statistics data, the drought and waterlogging disasters account for 55% of all kinds of disasters in the world, among which water disasters (flood, waterlogging, waterlogged, salinization) account for 40% and drought disasters account for 15%, the ratios mentioned above are in accord with those of Heilongjiang. From above, we can see that the flood disaster is more serious than the drought disaster, especially in area where rainfall is above 500 mm. So, the drainage should be attached extra importance to.

②In the Sanjiang plain, the largest daily rainfall that can reach 60mm only takes place once every five years, the largest daily rainfall that can reach 90 mm only takes place once every ten years, and the runoff yield is only about 20 mm and 30 mm separately under good draining conditions. Compared with the domestic standards that regard the daily rainfall reaching 100 mm as light waterlogging, daily rainfall reaching 150 mm as medium waterlogging and the daily rainfall reaching 200 mm as heavy waterlogging. The damage degree caused by waterlogging disasters that take place once every five to ten years in the Sanjiang plain is even below that of the light disaster. The Sanjiang plain is an area of little or hard runoff yield under saturated storage. In the Sanjiang and Songnen plain, because of the flat surface relief, the sophisticated micro relief, the high organic-bearing soil and the freezing and thawing phenomenon, it is easy to form plenty of surface residual water and perched water, which will make soil excessively humid and finally cause waterlogging and saline-alkali disaster. The flood and waterlogging is relatively lighter

than the waterlogged and alkalization in the Sanjiang and Songnen plain. At present, control of waterlogged and alkalization has not been attached much importance to and has not been put on the controlling agenda of Heilongjiang. This is the second feature.

Not only does the excessive moisture of soil influence the growth of crop, but also it can make dryland crop die from suffocation. The high soil viscosity and the formation of soil cold slurry decreases the soil bearing capacity and cause great influence on the management of tillage, especially on the large-scale mechanized tillage of modern agriculture. All of above will cause zero yield locally and yield reduction globally and will finally form vicious circle of agricultural operation loss. Salinization can make slick spot of green farmland and is the main cause of land desertisation in Heilongjiang. This is the third feature.

Because it is abundant in water resource in Heilongjiang province and the relationship between water supplies and demands is balanced, so, the drainage should be combined with storage and irrigation to make reasonable use of water resource such as return water, runoff and so on in control. This is the fourth feature.

Table 1. Water supply and demand in Sanjiang and Songnen plain

Area	Songnen plain	Sanjiang plain
Climate	Sub humid mesothermal climate zone	Humid mesothermal climate zone
Quantity of precipitation (mm)	400-700	500-600
Farmland density (mu/km^2)	464	325
Residential density (people/km^2)	130	46
Value of industrial output (RMB/km^2)	90000	20000
Water supply (m^3/km^2)	50000	55000
Average water supply (m^3/people)	400	722
Modulus of water demand (m^3/km^2)	50000	30000
Average water demand (m^3/people)	300-600	600
Evaluation	Balance between supply and demand	Surplus of supply

2 Difficulties in waterlogging and salinization control

At present, only controlling measures such as the flood and waterlogging drainage, drought-resistance irrigation and so on have been taken in Heilongjiang, while the control of waterlogged and salinization which are the main contradictions and disasters has not been put on the agenda. By analyzing the reason, the problem of subjective cognizance is the main reason, there also exists an important objective reason that the control of waterlogged and salinization disaster is hard to be done and need a lot of investment.

① The drainage modulus is too large. In Heilongjiang, the surface residual water and groundwater with excessively high level (including perched water) cannot be drained horizontally and the upright drainage such as evaporation is the only way that can be depended on, which will cause the excessive moisture of soil and surface salt accumulation. Because the surface is not flat, the residual water can reach 30~50 mm (including paddy field with flat land accuracy ± 35 cm), plus the gravity water, the quantity of water is larger. Through analyzing data of the subsurface drainage test that was made in Baoqing county in the Sanjiang plain in 1981, we can find that the largest drainage modulus can reach above 60 mmd (Table 2, Figure 1), which is equal to the largest drainage modulus 60 mm ($q_{max} \approx 3R$) that can be formed by 20 mm runoff caused by the largest daily rainfall that happens once every five years. From Figure 1 and Figure 2, we can see that the subsurface drainage degree is large and the time of drainage is long, the changing rate of surface drainage degree is small and the drainage time is short (normally less than one day), the drainage process is under the control of subsurface drainage, the drainage process has the features that the obvious

controlling stages of surface, subsurface and evapotranspiration drainage are formed (Figure 2.), which is different from that of abroad and domestic areas with plenty of rainfall. The modulus is six times as large as the average one that is about 10 mmd (0.124 $m^3/s.km^2$) and formed under condition that one-day's rainfall can be drained in two days.

Table 2. . Degree of groundwater drainage (1981, Baoqing Farm of Heilongjiang province)

Time 6/month	28/9	29/9	30/9	1/10	2/10	Demo
Average modulus of drainage /mm • d^{-1}	41.26	15.64	11.42	10.40	9.93	Embedded depth of concealed gutter1.0 m, interval 10 m

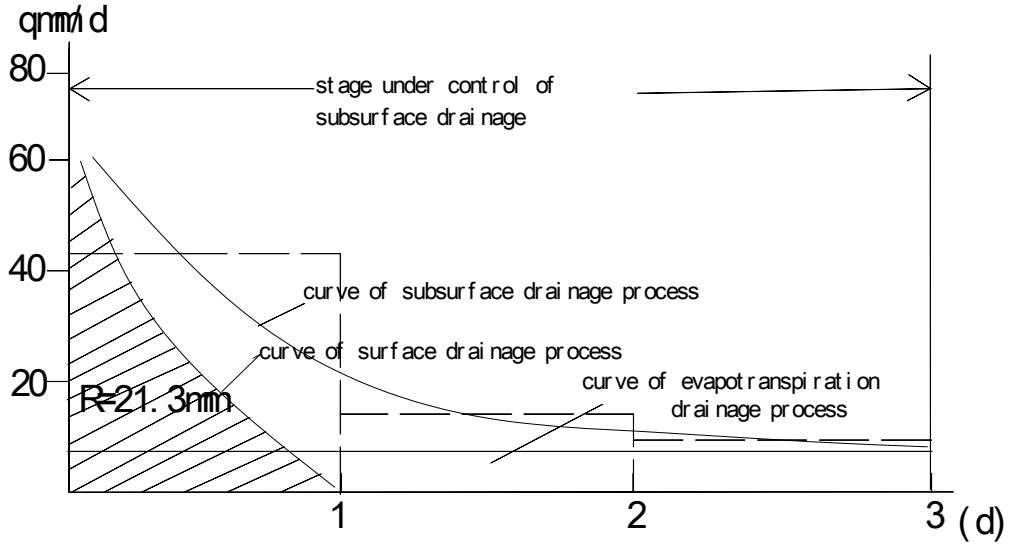

Figure 1. Diagram of surface and subsurface drainage degree in Sanjiang plain

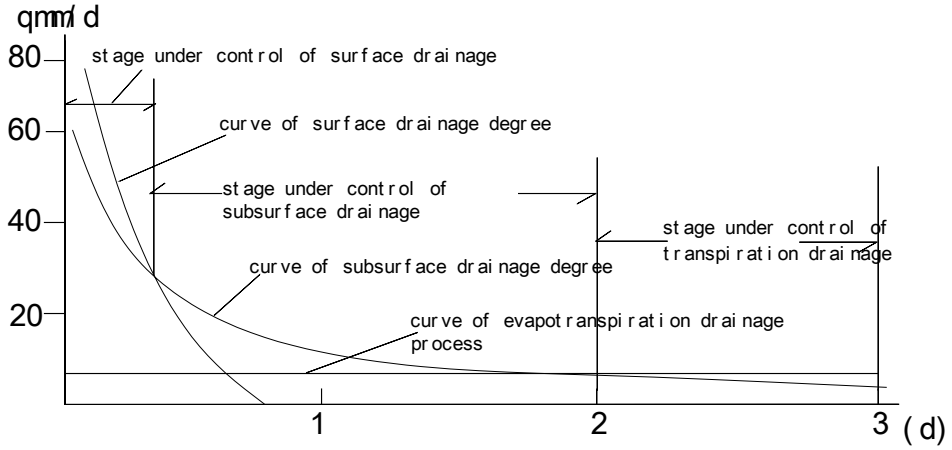

Figure 2. Diagram of standard drainage degree in area with plenty of rainfall

② The designed water level should be lower. Generally, the reference water level of drainage in waterlogged and salinization control should be the lowest surface elevation, and the groundwater embedded depth in waterlogged control should be 0.8~1.0 m deep below land surface and the groundwater embedded depth of salinization control should be 1.2~1.5 deep below land surface. Only thus, can thedemand of mechanized operation and controlling salinization drainage be met. however, the reference water level in farm ditch design is 80%~90% of surface elevation in the past, the designed water level is equal to or 0.2~0.3 m less than the demand. So, the designed water level should be much lower than that in the past in order to meet the demand of mechanized operation and salinization control.

③The ditches of draining system are deep and the project quantity is too large. By adopting the largest modulus of 60mmd and area factors in the cross-section design of farm, lateral and branch ditches (Table 3.), we can get the depth of farm ditch should be 1.5~2.0 m, lateral 2.0~2.5 m, branch 3.0~3.5 m (Table 4.). So, the main ditch should be deeper and project quantity is usually very large, the project is hard to be carried out. The authors had ever carried out ranges control by branch ditches in Dongxie general drainage system of 4^{th} branch of Friendship Farm. Sluice stations were built at the branch ditches exit to force drainage, the water flow into Dongxie main ditches (the compound cross-section that flood can pass on the surface is adopted in the design of Dongxie main ditch).

Table 3. Factors of area used for discharge calculation of drainage ditch (reference to manual of USA)

Area /hm^2	20	50	100	200	500	2000	4000
C	1	0.86	0.75	0.64	0.5	0.4	0.38

Table 4. Longitudinal and cross section Design of farm, tributary and lateral ditch

Ditch	Control area /hm^2	Discharge /m^3/s	Slop /i%	Slop factor	Bottom width /m	Designed water depth	Reference ditch depth /m	
							Waterlogged control	Saltern control
Farm ditch	20	0.138	1/2000	1.25	0.8	0.32	1.5	2.0
Lateral ditch	200	0.880	1/4000	1.5	2.5	0.56	2.0	2.51
Branch ditch	2000	5.71	1/5000	2.0	4.0	1.22	3.0	3.5

3 Modes of ranges control

With the advance of science and technology and the development of agricultural economy, in Heilongjiang province, the draining and irrigating power and equipments are kept at large and the family farms are operated prevalently, among which the area of little and middle-scale family farms is 10-20 hm^2 and the area of large-scale family farms is about 100-200 hm^2, which are both the right scales that can be controlled by farm ditches and lateral ditches. Ranges control by farm and lateral ditches can be designed with the waterlogged and alkalization control as main aim (including the high-standard control such as field buried pipe drainage, laser land grading and so on), and the trunk and branch ditches only need slight remaking (the water level of trunk or branch ditches can be above the land surface temporarily if conditions permit), thus, the project quantity and investment can be greatly decreased, which is of great advantage for promotion and application in practice. It is a leap development in drainage standard and controlling stage to stride into high standard waterlogged controlling stage from

low-standard water logging stage. Combined with well irrigation and low-water-level operation, it will form the water conservancy mode of drainage of precipitation and storage for irrigation or water conservancy of water diversion, drainage of precipitation and storage for irrigation, which will form ecological water conservancy consisting of disaster-resistance type, resource type and environment type water conservancy. Because the ranges-controlling scale matches with the scale of family farm, it can be regarded as water conservancy mode of science and technology into house, briefly called water conservancy-into-house mode (Figure 3), the key lies in that the farm ditches and lateral ditches are designed with waterlogged control as main task.

To achieve the combination of drainage and irrigation and good order between precipitation and storage, deep ditches of flat bottom and adverse slope should be designed in ranges, at the exit of which sluice stations should be built. The deep ditches (the inner ditches are deeper than the outer ditches) can be used for waterlogging control during flood period. Besides gravity drainage by keeping the sluice opened, forced drainage by keeping the sluice closed can be made to keep the water level staying below the exit of buried pipe. Diversion can be made by keeping the sluice opened to coordinate with well irrigation. As usual, the sluice can be closed to store water, when the water level should be less than 1 m. Thus, the functions of drainage, precipitation, storage and irrigation are performed. The sluices used for water retaining and diverting are the gates of controlled ranges. By taking farm ditches for examples, ϕ250～300 continuous culvert pipe can be buried, in which the wooden plugs can be used as sluice gate, the ϕ350～300 axial-flow pump of 500～1000 T/h flow rate and 12～15 horsepower can be used in sluice stations, it can be used both for pumping irrigation and tillage. Ditches can be used for irrigating farmland and draining water out of controlled ranges. If area of ranges controlled by farm ditches reaches 20hm^2, it should be under one farmer's control; if area of ranges controlled by lateral ditches reaches 100～200 hm^2, it should be under control of a large-scale family farm. The new ranges-controlling mode will cause leap development in water conservancy science and technology and will become the leading demonstration mode of ecological water conservancy construction in Heilongjiang. Combined with "bringing science and technology into family", it will become a domestic technology innovation of "bringing water conservancy in to family".

4 Ranges-controlling practical examples and its operating feedback information

4-1 Introduction about ranges-controlling examples

Besides ranges-controlling mode adopted by 4th branch of Friendship Farm, there are two more regular ranges-controlling examples in farm-ditch scale, i.e. ranges-controlling demonstration area in 14th group of 850 Farm and ranges-controlling demonstration area of Qingfeng seeds company. The area of the two demonstration areas both is 25 hm^2 or so. The comprehensive controlling measures such as gate, pump, ditch, channel, well, pipe, culvert, joint, land grading, slope making and trench construction are all taken in the two demonstration areas, and the main aim of which is waterlogging control. In the two demonstration areas, the central ditches are all designed to be in connection with hydro projects by adverse grade ditches. Thus, the forced irrigation and forced drainage can be made and the water separation between outer and inner, free water retaining and diversion, combination of drainage and irrigation. Storage is also achieved. Figure 4 and Figure 5 are layouts of two demonstration areas; Table 5 and Table 6 are project quantity and cost of engineering construction and equipment.

4-2 Benefit and operation

①Since the construction of ranges-controlling demonstration area in 14th group of 850 Farm was completed in 1998, it has experienced serious waterlogging disasters in 2000 and 2002 (annual rainfall reached 726 mm and 660 mm separately) and drought disasters in 1998 and 2001 (the annual rainfall reached 441.3mm and 450.2mm separately).But, the yield of dryland and paddy field increased stably. During the period of 1998~2004, on land that could not be tilled in the past, the unit yield of beans ranged from 2250 to 2400 kg/hm^2, the unit yield of rice ranged from 7500~9000 kg/hm^2. especially in 2003, because the market price of beans was high, the net profit of 12hm^2 dryland reached 60 thousand Chinese Yuan, these lands become middle or high-class lands.

Because of the combination of draining and irrigation, the good order between precipitation and storage and the associated use of surface water and groundwater, the comprehensive utilization of local water resource is achieved (Table 7).

②The ranges-controlling demonstration area of Qingfeng seeds company was constructed in 2002, after two year's operation, three everlasting waterlogging and low-lying barren lands died away and three-year continuous waterlogging disasters which had happened during the period of 2002~2004 were conquered. The special area is made of prohibited area for agriculture. The zero-yield land in the past become high-yield land, and the yield increased by more than 15% compared with that on high flat land (table8. table 9). Not only has the diversion, drainage and irrigation been done well, but also the good order between precipitation and storage and the comprehensive utilization of local water resource are achieved. The ecological water conservancy consisting of water conservancies of disaster-resistance type, resource type and environmental type was formed.

4-3 Problems and countermeasures

①Being short of detailed research on waterlogged disaster control, a situation comes into being, in which the design lacks theorization and standardization, the implementation lacks regularization, the measures lack synthesis and some completed projects even lack corollary facilities. This makes the benefit in ranges unstable in time and space. In 2004, the science and technology park was caught by disasters too, the yields on some lands decreased by more than 70%.

②The technique and method of monitoring and construction is not advanced, especially that the laser technology is not used in the survey of spoil leveling, land grading, slope making and trench building and the surveys lack accuracy control and are mostly made by visual observation, which results in a lot of man-made secondary closing low-lying land. During the process of buried pipe construction, sometimes the depth is too large and sometimes the bottom slope is not flat, which combined with lack of control over quality of filler and filter material greatly influences the benefit and effect of project.

③The two ranges-controlling demonstration areas are both separately operated by several different farmers, the operating management is not made much of , the operating contradiction between drainage and irrigation and new argument on water conservancy come into being. The paddy field farmers usually attach much importance to water storage and irrigation, and the dryland farmers usually attach much importance to precipitation and drainage, sometimes, even no adjustment is made. It is hard to perform the general comprehensive ranges-controlling function, sometimes the disorder between precipitation and storage is caused, and the advantages change into disadvantages.

④There also exists phenomenon of making much of irrigation and little of drainage. Generally, the positivity of irrigation is high, but the farmers know little about draining precipitation, especially about the forced drainage. In operation, the forced draining machines are rarely used to drain water during flood period.

New countermeasures should be taken to solve the problems mentioned above.

- enhance research on techniques, standards and measures of controlling waterlogged and salinized fields.
- elaborately carry out the planning and designing of ranges control.
- attach more importance to utilization of high-new practical technology such as using laser for land leveling , buried pipe construction and ditches digging.
- elaborately carry out implementation of systematic project and comprehensive controlling measures and its operation management and updating.
- attach more importance to using small scientific satellite for data collection, survey, monitoring and control.
- adjust operating mechanism to make the scale of ranges control match with the scale of family farm.

Only thus, can we truly achieve the rapid development of hydro science and technology and practice in Heilongjiang province, and we can make this new water conservancy technology used in family farm.

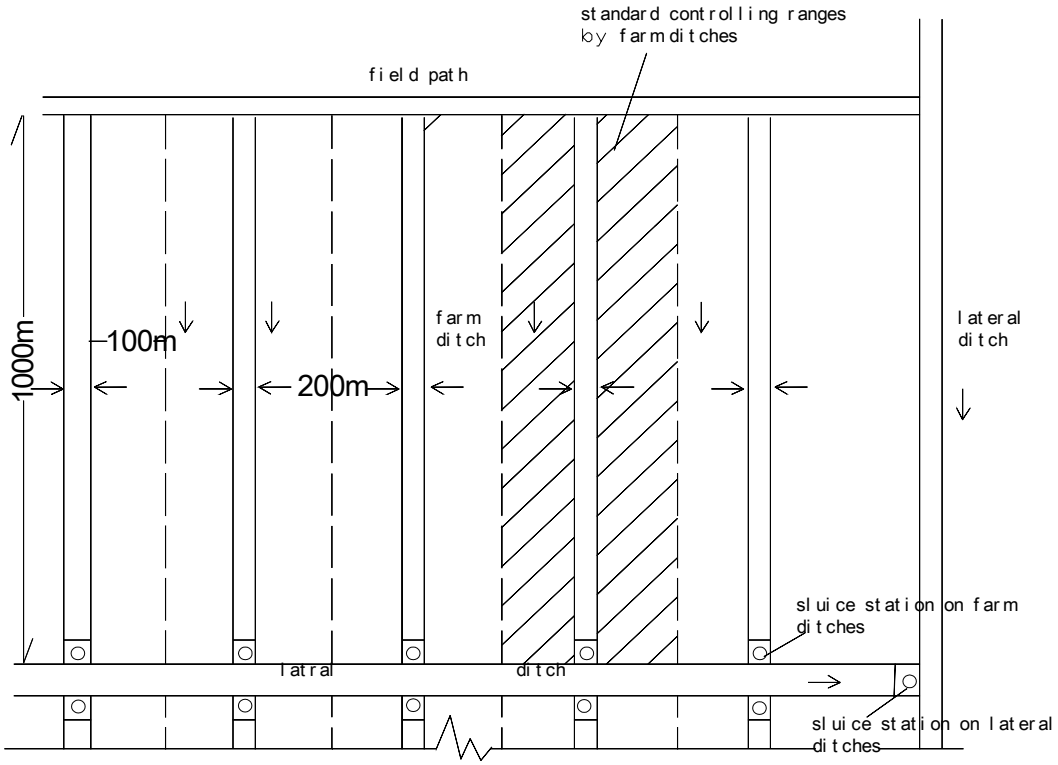

Figure 3. Program of ranges control of farm, tributary and lateral ditches.

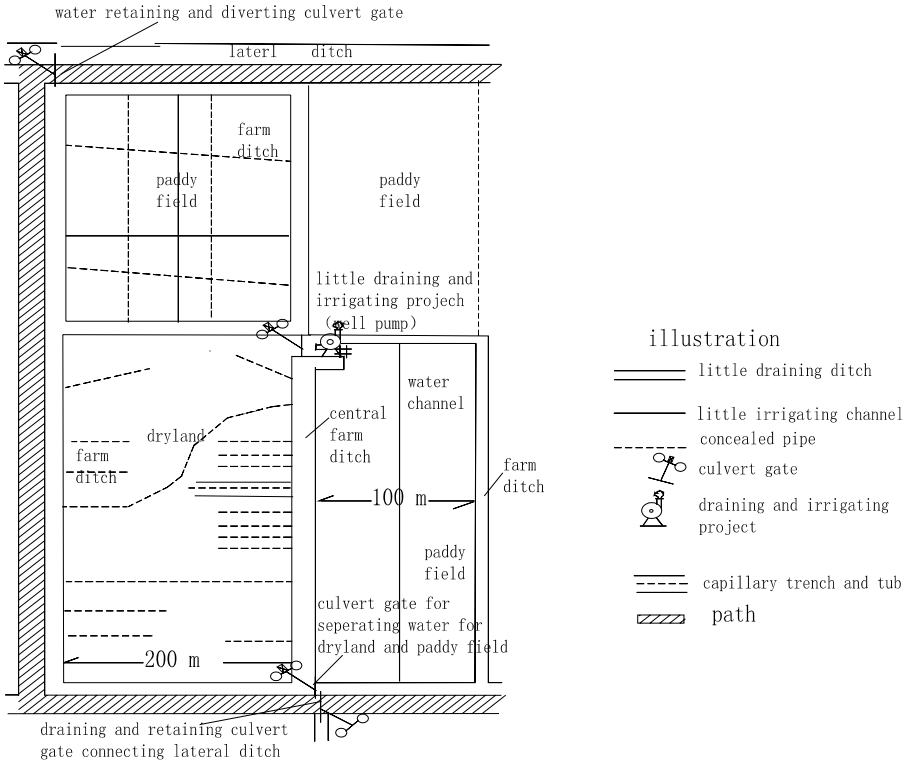

Figure 4. Schematic drawing of ranges control demonstration area in 14th group of 850 Farm

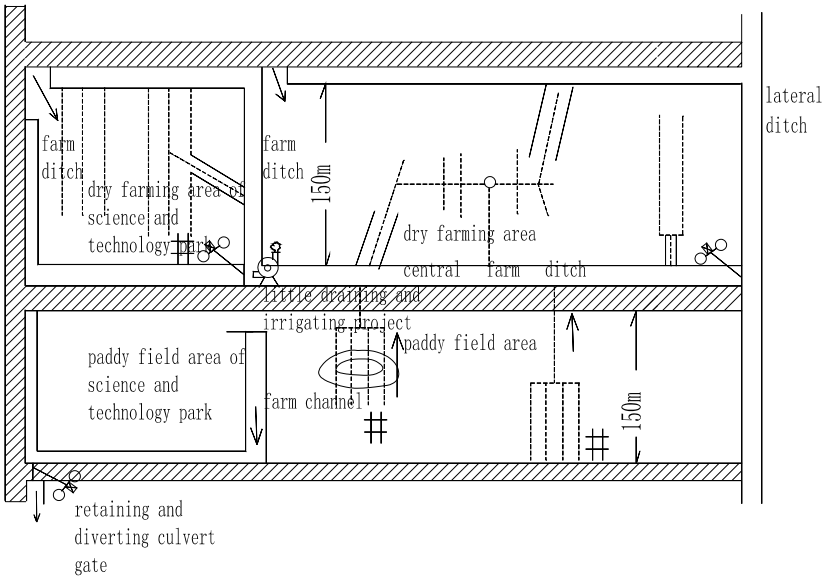

Figure 5. Ranges-controlling schematic drawing of demonstration area of Qingfeng farm's seed company on Sanjiang plain

Table 5. Constructing cost of ranges-controlling project in ecological water conservancy demonstration area in 14th group of 850 Farm

Project	Kind	Volume	Unit cost /RMB	Constructing cost/10^4yuan	Demo
Farm ditch	Earthwork	$1.85\times10^4m^3$	2.0	3.70	
Flat land trench	Earthwork	$0.9\times10^4m^3$	2.0	1.80	Flat Paddy field is not included
Concealed pipe	Dryland	0.15×10^4m	20	3.00	Sand and gravel filler
	Paddy field	0.09×10^4m	20	1.80	
Mole channel	Dryland	12hm2	300	0.36	
Culvert gate	Dryland	4	1000	0.40	
	Paddy field	1	10000	1.00	
Draining and irrigating equipment	Pump	2	0.3×10^4	0.60	
	Well	1	0.3×10^4	0.30	
Total				12.96	26.67 hm^2

Table 6. Constructing cost of ranges-controlling project in ecological water conservancy demonstration area of 14th group of 850 Farm.

Project	Kind	Volume	Unit cost /RMB	Constructing cost/10^4yuan	Demo
Farm ditch	Earthwork	$1.55\times10^4m^3$	2.0	3.1	
Flat land trench	Earthwork	$1.20\times10^4m^3$	2.0	2.4	Flat Paddy field is not included
Concealed pipe	Dryland	0.20×10^4m	15	3.00	Rice crust filler
	Paddy field	0.18×10^4m	15	2.70	
Mole channel	dryland	$12hm^2$	300	0.36	
Culvert gate	Culvert gate	3	1000	0.60	
Draining and irrigating equipment	Culvert Pump	4	0.3×104		
	Well	3	0.3×10^4	0.90	
Total				14.96	Area24hm2

Table7. Surface and groundwater Utilization in ranges-controlling area of 850 Farm

Year	Well water		Ditch water		Gross volume	Irrigating quota (paddy field/$m^3(hm^2)^{-1}$
	Time/h	Uolume/m^3	Time/h	Volume/m^3		
1998	356.3	28500	141	29880	58380	7960
1999	271.5	21720	213	54900	76680	8737
2000	342	27360	443	66450	93750	7800

Table 8. Yield measurement of Qingfeng Seeds Company ranges-controlling demonstration area (Beans, 2004)

Treatment	Plant height /cm	Legumen's amount /plant$(m^2)^{-1}$	Granules /Legumen	Empty rate /%	Unit yield In theory /kg $(hm^2)^{-1}$	Rate /%	Demo
Typical low-lying land	125	28	32.1	84	4236	121	
High flat land	84	27	29.4	72	3501	100	

Table 9. Yield measurement of Qingfeng Seeds Company ranges-controlling demonstration area (Rice, 2004)

Treatment	Plant height /cm	Legumen's amount /plant $(m^2)^{-1}$	Granules /Legumen	Empty rate/%	Unit yield In theory /kg $(hm^2)^{-1}$	Rate /%	Demo
Controlled low-lying land	85	662.58	63.44	6.24	10.25	116.5	
Low-lying land	86.5	520	72.84	10.70	8.79	100	

③Through the preliminary analysis on the two practical examples above, we can get that the average investment is 5546 Yuan/hm^2 and the average benefit is 1208 Yuan/hm^2, the cost can be covered in five years, it is feasible in economy.

Correspondence to:
Liquan Wang
Water Service of General Bureau of Reclamation,
Harbin, Heilongjiang 150091, China,
Telephone: 01186-451-55196667
E-mail: nkjl@163.com

References:

[1] Jia Qing-feng, Liu Yong-fan, Wang Bin. Analysis on benefit and problems of waterlogged area control on Qingfeng Farm on Sanjiang plain. Journal of Heilongjiang Hydraulic Engineering College 2004;4:10-3.

[2] Wang Bin, Yin Jian-guo, Chen Jie. Special area for agriculture is made of prohibited area. Journal of Heilongjiang Hydraulic Engineering College 2004;1:26-7

[3] Yao Zhang-chun, Sun Yuan-feng. New research on draining methods of project draining and controlling waterlogged area. Northeast Water Conservancy and Hydropower 1996;12:44-9.

[4] Yao Zhang-chun, Yan Xue-yi, Research on partial improvement of waterlogged area on Sanjiang plain. Technology of Water Conservancy and Hydropower 1996;1:34-9.

[5] Yao Zhang-chun, Xia Guang-liang, KONG Ling-bo. Mode of comprehensive control and reasonable utilization of water resource on Sanjiang plain. Journal of Heilongjiang Hydraulic Engineering College 2001;3:5-8.

[6] .Zhu Chun-kai, Liu Xin-an, Liu Wen-feng. Secondary discussion on precipitation's drainage and storage for irrigation. Journal of Heilongjiang Hydraulic Engineering College 2002;3:29-31.

Mathematical Analysis of Root Growth in Gamma-irradiated Cashew (Anacardium occidentale L.) and Mangosteen (Garcinia mangostana L.) Using Fractals

Klarizze Anne M. Puzon

Quezon City, Philippines, klarizze@gmail.com

Abstract: Root growth is related to the acquisition, distribution, and consumption of water and nutrients of plants. As a vital organ, roots directly take the effect of environmental change and its behavior is closely related to the growth of the whole plant. With such, the importance of root systems has motivated botanists to seek a better understanding of root branching complexity. This complexity, which has been difficult to comprehend using simple Euclidean methods (i.e. lines and circles), is important to the survival of plants, especially when the distribution of resources in the environment is scarce. Mathematical models using fractals and computers can be applied to accurately understand the growth and form complexity of plant root systems. This study was conducted to analyze the root growth of gamma-irradiated cashew and mangosteen using fractals. [Nature and Science. 2005;3(1):59-64].

Key words: fractals; root growth; cashew; mangosteen; mathematical model

1 Brief Summary

Seeds of cashew (n=360) gamma-irradiated at 0 Gy, 150 Gy, 300 Gy, 450 Gy, 600 Gy and 750 Gy, and mangosteen (n=75) gamma-irradiated at 0 Gy, 10 Gy, 20 Gy, 30 Gy, and 40 Gy were germinated in perlite plots. The plants' primary root lengths were measured. Image analysis using *Fractal Dimensions* software was conducted to determine the fractal dimensions, D, of the plant roots.

Findings for mangosteen reveal that as the gamma-irradiation dose increases, the primary root length decreases and the root D increases. Roots irradiated at 40 Gy showed the highest average D at 1.657. This implies greater root branching complexity which results to better plant nutrient exploitation efficiency. For cashew roots, D did not vary significantly with increasing gamma-irradiation dose. However, cashew seeds irradiated at 150 Gy exhibited the highest germination rate, highest average primary root length, and an average D of 1.613. General trends also reveal that cashew roots' D increased with time.

This study demonstrates that fractal dimension can be a useful tool in characterizing the complex branching characteristics of root systems. This may pave the way for further applications of fractals in other areas of research. The findings from this study can also be used to improve the production of cashew and mangosteen which are the two of the world's most economically valued fruits.

2 Brief introduction

As people's views on using modern means such as computers extend, it has been difficult to use traditional methods like simple lines and circles to comprehend biological systems. Biological systems, like root branching, display fragmentations that cannot be modeled and comprehended by simple shapes alone. Mathematical models using fractals have recently been applied to explore the relationship between plant growth and structure.

A. Problem

Complexity in root systems, which reflects nutrient exploitation efficiency, is important for plant survival, especially when the distribution of resources in the soil environment is scarce. However, root complexity is difficult for scientists and researchers to study.

B. Objective

This research study was conducted to analyze and compare the root growth branching patterns of gamma-irradiated cashew and mangosteen using fractals.

C. Significance

- The study addresses the real-world problem of making accurate quantitative observations regarding root growth. The fractal dimensions may reflect the plants' root branching complexity and reflect nutrient uptake efficiency.
- Since radiation causes genetic mutations, fractal analyses of root patterns in gamma-irradiated cashew and mangosteen provide information on the growth mechanisms of these plants. Data from this study can be used to improve the agriculture and production of

cashew and mangosteen which are economically valued fruits.

3 Detailed introduction

A. Background of the Study

The emergence of forms in the growth process, like root branching, is one of the most exciting problems in biology. Most biological systems, like root branching, are difficult to comprehend, displaying fragmentations which cannot be easily modeled by simple shapes (Kaandorp, 1994). Mathematical models using fractals have recently been applied to explore relationship between growth and form (Kenkel & Walker, 1996). Cashew (*Anacardium occidentale L.*) and mangosteen (*Garcinia mangostana* L.) are one of the most recognized tropical fruits. Both have universal appeal and high economic values because of their quality in color, shape and flavor.

B. Statement of the Problem

The demand on cashew and mangosteen often exceeds supply. Further studies about the growth and agriculture of both are needed. Also, the qualitative characteristics of cashew and mangosteen root systems are already known, the problem is to make accurate quantitative observations on their root growth. The major objective, therefore, of this study is to analyze and compare the root growth patterns of irradiated cashew and mangosteen using fractals.

C. Significance

This study would be a means of new knowledge about root branching growth of cashew and mangosteen. The fractal analysis of the root patterns of irradiated cashew and mangosteen can help understand their growth dynamics. The fractal dimensions would reflect their branching complexity and growth velocity. Moreover, a comparison of the fractal models and the actual growth forms can be used to detect the effects of slow changes in the environment, like gamma radiation.

D. Scope and Limitations of the Study

This study focuses on having quantitative observations on the root systems of the samples, not on their already known qualitative characteristics. One limitation of this study is that the root structure being three dimensional will be modeled using a two dimensional fractal analysis software due to the inavailability of a three dimensional fractals software to the author.

4 Review of related literature

A. Cashew

The cashew tree is a medium-sized tree with oval blunt alternate leaves (Grieve, 2004). The cashew nut is defined botanically as the fruit. It grows externally in its own kidney-shaped hard shell at the end of this pseudo-fruit, or peduncle. It is commonly found in Brazil and in other tropical countries. Besides being a popular food export, it is now being used as an alternative medicine against asthma, diabetes, fever, and the like.

B. Mangosteen

The mangosteen fruit, usually found in tropical countries, is 2-3 inches in diameter and has a thick reddish-purple rind that covers the segmented pulp (Morton, 1987). It is usually eaten fresh, but can be stored successfully for short periods of time. It is also canned, frozen, or made into juice, preserves, and syrup. Mangosteen is also used as a pharmaceutical.

C. Fractals

Fractals are unusual geometric structures that can be used to analyze many biologic structures not amenable to conventional analysis (Richardson & Gillepsy, 2000). Mandelbrot introduced the term 'fractal', from the Latin *fractus*, meaning 'broken', to characterize spatial or temporal phenomena that are continuous but not differentiable (Kenkel & Walker, 1996). Fractals possess properties that include scale independence, self-similarity, complexity, and infinite length or detail. Fractals have been recently used to analyze the root architecture of some plants. Correlations between fractal dimension and topology of root systems of legume plants grown in root boxes were studied (Tatsumi & Takagai, 1996). It was suggested that when roots develop under favorable conditions, D is a good indicator for estimating the system's size and root branching.

5 Methodology

The method used is summarized by the FLOWCHART (Figure 1).

PLANT

5.1 Plant materials and seed germination

Cashew seeds were obtained from University of the Philippines Los Banos- Agriculture Department. The 360 seeds were randomly divided into 3 blocks with 6 groups containing 20 seeds each. All groups were soaked in water for 48 hours and were randomly irradiated at 0 gy, 150 gy, 300 gy, 450 gy, 600 gy and 750 gy. The seeds were germinated in plots with perlite. For four weeks, the length of the primary roots of the samples was obtained. The plant materials for mangosteen were obtained at the Philippine Nuclear Research Institute. The same preparation were to mangosteen, but the radiation doses were 0 gy, 10gy, 20 gy, 30 gy, and 40 gy.

5.2 Fractal analysis

Roughly once a week, 9 cashew root samples per radiation dose (3 from each block) were digitally photographed. Then, 3 from 5 samples per radiation

dose of mangosteen root pictures were randomly chosen. After such, the pictures were turned into monochrome format. Then, fractal analyses using the Fractal Dimensions software's box-counting method were done. The data from the fractal counting were tabulated and plotted on a log-log plot graph. A linear regression was done to find the best fit line. The fractal dimension was calculated. It is equal to 1 minus the slope of the best fit line, relative to 1 or simply D=–slope.

6 Data and results

A. Mangosteen and Cashew Root Growth Observations (Figures 2-4)

B. Fractal Analysis of Mangosteen and Cashew Root Growth Patterns (Figures 5-7)

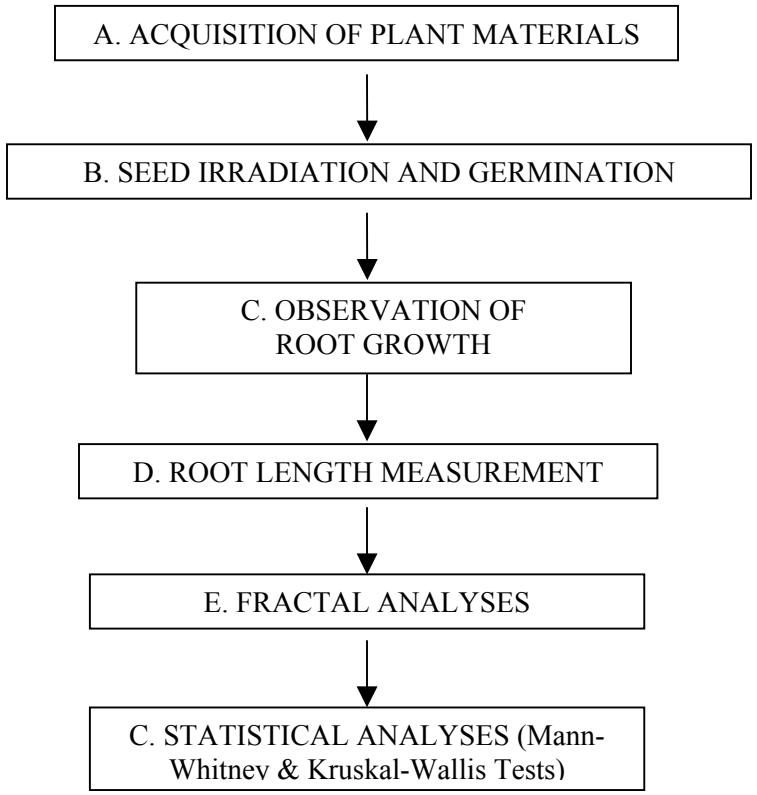

Figure 1. Flowchart

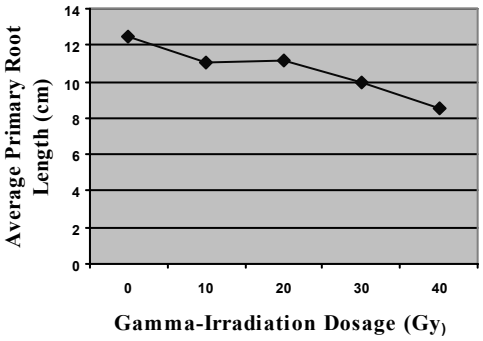

Figure 2. Average primary root length of mangosteen at increasing gamma-irradiation doses

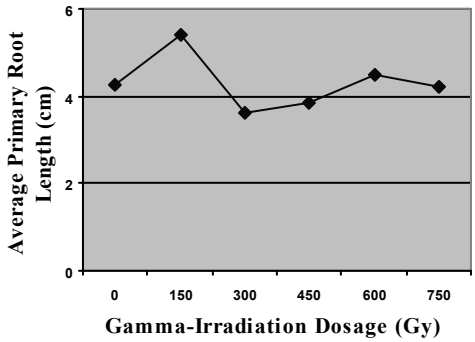

Figure 3. Average primary root length of cashew at increasing gamma-irradiation doses

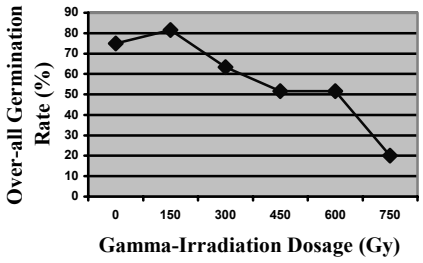

Figure 4. Changes in cashew (*Anacardium occidentale* L.) seed germination rate at increasing gamma-irradiation doses.

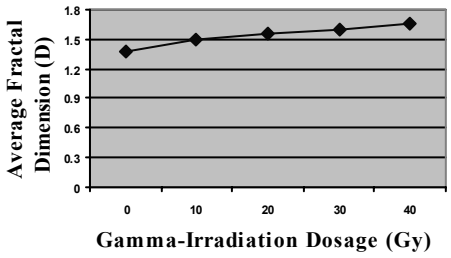

Figure 5. Changes in average fractal dimensions of mangosteen roots at increasing gamma-irradiation doses

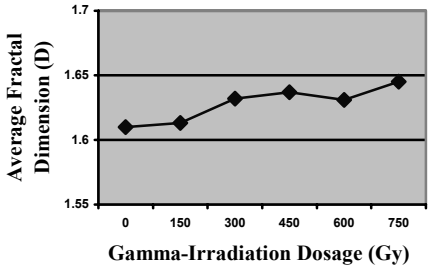

Figure 6. Changes in average fractal dimension of cashew roots at increasing gamma-irradiation doses

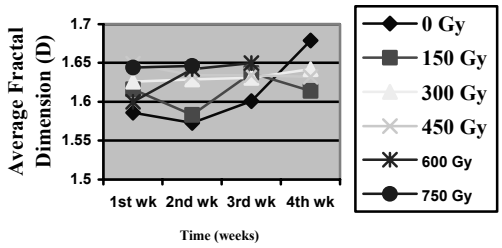

Figure 7. Changes through time in the fractal dimensions of cashew roots

7 Analysis and discussion summary

- For mangosteen roots, fractal dimension, D, decreased as the primary root length increased. The highest gamma-irradiation dose for mangosteen, 40 Gy, resulted in the highest D, 1.657. This high value implies greater root complexity, which in turn could result to enhanced efficiency for soil nutrient exploitation.
- For cashew roots, D did not vary significantly with increasing radiation dose. However, primary root length measurements (5.40 cm) and germination rates (81.6%) revealed that cashew grows best at 150 Gy. Such results might have happened maybe because cashew is less radiosensitive compared to mangostee.
- From a cellular perspective, gamma-irradiation might have altered chromosomal structure (e.g. introduction of transitions, deletions, and frameshifts in the genetic material) of mangosteen and cashew root cells. The radiation might have also affected transmission of the genetic material through inhibition of cell mitosis. It is hypothesized that these alterations in genetic makeup might have led to the changes in root cell growth, which in turn affected the root systems' complexity.

8 Conclusions and recommendations

- Fractals are useful in analyzing complex biological systems accurately. The fractal dimension (D) served as the summary statistic of the branching characteristics of cashew and mangosteen roots.
- The best gamma-irradiation dose for mangosteen was 40 Gy, which showed the highest root fractal dimension. While the best dose for cashew was 150 Gy.
- In this study, the process of determining fractal dimensions of gamma-irradiated roots and correlating it to primary root lengths showed that variations in D exist due to plant differences brought about by genetic makeup (e.g. species) and/or environmental factors (e.g. radiation dose).
- The fractal dimension could be of interest to botanists because it is directly correlated with the efficiency at which the roots exploit soil resources. The use of other types of plant species and the application of other forms of environmental stress,

like drought and mineral deficiency, is recommended.

- This study may pave the way for further applications of fractals in other areas of research, especially in agricultural engineering, computer science and biology. Data from this research can also help the Philippines achieve its goal of attaining efficiency in crop production for sustainable development and global competitiveness.

Acknowledgements

- Harvard-Massachusetts Institute of Technology Health Sciences and Technology Division, especially to Dr. George Moody, and Dr. Dani Widawsky of Boston University for the 2-d fractals software and tutorials kit.
- U.S.A. Department of Agriculture, especially to Dr. Yakov Pachepsky for e-mailing me references regarding crop growth, fractal geometry, and computer applications in biology.
- Philippine Nuclear Research Institute for the gamma-irradiation of the seeds and perlite plots.
- Dr. Ricardo del Rosario, former chairman and professor of the University of the Philippines Mathematics Department for all the consultations and paper editing.
- Dr. Jessamyn Yazon, my science and technology research adviser, for her guidance during the experimentation process.
- Dr. Rafael Saldana of Ateneo de Manila University & Dr. Yongwimon Lenbury of Thailand Mahidol University for their appreciation of my study.
- My family and relatives, friends, classmates, and my other teachers in Philippine Science High School, for their support and encouragement.
- And most of all, God, for without Him, this could not be achieved.

Remarks

- The research won 3rd Award in the 2005 Taiwan International Science Fair, 1st Place in the Philippine Science High School- Main Science and Technology Fair (YMSAT 2005), 2nd Place in the Intel Regional Fair and was a finalist in the UP Alchemes Fair. It was conducted when the author was in 4th year high school.
- The author is a graduate of Philippine Science High School- Main Campus and a BS Mathematics freshman at the University of the Philippines- Diliman.

References

[1] Bin FW. Maohua, Senwen Z. Application of fractal image simulation in plant root growth. Proceedings of an international conference on agricultural engineering. December 1999. Beijing, China. pp. 6-9.

[2] Bonsol MF, Lasiste JM, Quinio MF. The effects of varying concentrations of growth regulators benzyladenine and naphthalene acetic acid and gamma irradiation on the gross plantlet morphology of *Garcinia mangostana* L. Quezon City, Philippines. Philippine Science High School Research Paper. 2004:4-6.

[3] Campbell N, Reece J, Mitchell L. Biology. 5th ed. New York. Addison-Wesley Pub., Inc. 2000.

[4] Cheema A, Atta B. Radiosensitivity studies in Basmati rice. Pak J Bot 2003;35(2):197-207.

[5] Deering W, West BJ. Fractal physiology. IEEE Engin Med Biol 1992;11:40-6.

[6] Dertinger H, Jung H, Zimmer K. Molecular radiation biology: The action of ionizing radiation on elementary biological objects. New York. Springer-Verlag Pub., Inc. 1970.

[7] Diggle AJ. Root map—a model in three-dimensional coordinates of the growth and structure of fibrous systems. Plant and Soil Journal. 1988;105:169-78.

[8] Eghball B, Ferguson B, Gotway CA, Hergert GW, Varvel GE. Fractals: a bridge to future of soil science. 1998. http://www.ars.usda.gov/is/AR/archive/apr98 /frac0498.htm?pf=1 (28 September 2003).

[9] Eghball B, Settimi JR, Maranville JW, Parkhurst AM. Fractal analysis for morphological description of corn roots under nitrogen stress. Agronomy Journal 1993;85:287-9.

[10] Erickson ET, Atmowidjojo AH. "Mangosteen." 2001. http://www.gears.tucson.ars.aq.gov/book/chap5/mangosteen.htm 2001;l (6 June 2004).

[11] Eshel A. On the fractal dimensions of a root system. Plant, cell, and environment. 1998;21(2):247.

[12] Faucon P. "Mangosteen." *Mangosteen (Garcinia mangostana L.)*. 2003. http://www.desert-tropicals.com/plants/guttiferae/garcinia.html (6 June 2004).

[13] Fitter, A.H. and T.R. Strickland. Architectural analysis of plant root systems. II. Influence of nutrient supply on architecture in contrasting plant species. New Phytologist 1991;118:383-9.

[14] Fitter AH, Strickland TR, Harvey ML, Wilson GW. Architectural analysis of plant root systems. I. Architectural correlates of exploitation efficiency. New Phytologist. 1991;118:375-82.

[15] Glenny RW, Robertson HT, Yamashiro S, Bassingthwaighte JB. Applications of fractal analysis to physiology. J Appl Physiol 1991;70:2351-67.

[16] Goldberger AL, Rigney DG, West BJ. Chaos and fractals in human physiology. Sci Am 1990;262(2):42-9.

[17] [17] Grieve M. "Cashew nut." *A modern herbal.* http://botanical.com/ botanical/mgmh/c/casnut 29.html#des. (6 June 2004).

[18] Kaandorp JA. Fractal modelling: growth and form in biology. New York. Springer-Verlag Pub., Inc. 1994.

[19] Kenkel NC, Walker DJ. "Fractals in biological science." 1996. http://www.umanitoba.ca/faculties/science/botany/labs/ecology/fractals.htm.(13 September 2003).

[20] Lethen J. "The Kruskal-Wallis Test for *K* Independent Samples". 1996. http://stat.tamu.edu/stat30x/notes/node151.html (29 Nov. 2004).
[21] Lowry R. "Mann-Whitney Test". 2001. http://faculty.vassar.edu/lowry/utest.html. (29 Nov. 2004).
[22] Morton, J. "Mangosteen." 2004. http://www.hort.purdue.edu/newcrop/ morton/mangosteen.html (6 June 2004).
[23] Morton J. Cashew apple. Fruits of warm climates 1987;1(1):239-40.
[24] Ng M, Lau R, Tsang L, Wells K. "The fractal dimension of leaves." 1999. http://www.midwoodscience.org (28 September 2003).
[25] Pizzarello D, Witcoski R. Basic radiation biology. Boston. Lea and Febiger, Publishing, Inc. 1967.
[26] Prove PC. "Mangosteen: general crop management." *Horticultural and fresh produce.* 2004. http://www.dpi.qld.gov.au/horticulture/5447.html (6 June 2004).
[27] Richardson ML, Gillepsy T, III. "Fractal analysis of trabecular bone."2000.http://www.rad.washington.edu/exhibits/fractal.htm l (21 September 2003).
[28] Ritz K, Crawford J. Quantification of the fractal nature of colonies of *Trichoderma viride*. Mycol Res 1990;94:1138-52.
[29] Salisbury F, Ross C. Plant physiology. 4th edition. California. Wadsworth Publishing Company. 1992.
[30] Stanley HE, Taylor EF, Trunfio PH. Fractals in science: an introductory course. New York. Spring-Verlag Publishing Inc. 1994.
[31] Sylianco C, Wu L. Modern biochemistry. 5th edition. Quezon City. Papi Publishers. 1994.
[32] Taylor L. "Cajuiero." *Anacardium occidentale.* 2004. http://www.rain-tree.com/plants.htm (6 June 2004).
[33] Tatsumi J, Takagai K. "Fractal characterization of root system architecture in legume seedlings." 1996.http://www.kingston.ac.uk/fractal/abstr97.html (20 September 2004).
[34] Umaly R, Roderos R. Lecture notes on molecular genetics. Manila. 24K Printing Corp., Inc. 1988.
[35] Venkatachalam M, Teuber S, Roux K, Satne S. "Effects of gamma-radiation in antigenicity of almonds, cashew nuts, and walnuts."2002. http://ift.confex.com/ift/2002/techprogram/paper_11317.htm (6 June 2004).
[36] Weier T, Stocking C, Barbour M, Rost T. Botany: An introduction to plant biology. 6th ed. Quebec. John Wiley and Sons. 1982.
[37] West BJ, Goldberger AL. Physiology in fractal dimensions. Am Sci 1987;75:354-65.
[38] Wiebel J, Chacko EK, Downton WJ, Luedders P. Influence of irradiance onphotosynthesis, morphology, and growth of mangosteen (*Garcinia mangostana* L.) seedlings. Tree Physiology 1994;14 (3):236-74.
[39] World Scientific Publishing Company. "Fractal dimension and self-similarity in *Asparagus plumosus*." 2002. http://www.worldscinet.com/fractals/10/ sample/s0128348X 0200 1439. html. (20 September 2003).

Empirical Analysis of Cash Dividend Payment in Chinese Listed Companies

Shulian Liu, Yanhong Hu

School of Accounting, Dongbei University of Finance and Economics, Dalian, Liaoning, China, 0086-411-8471-2716, msy8895@sohu.com, 01186-411-82392135, sparrowhu@yahoo.com.cn

Abstract: This paper empirically analyzed the dividend policy of Chinese listed companies from the factors of the abilities in cash payout and investment opportunity of the companies, especially studied how cash flow (FCFE, ONCE, NCE) impacted on cash dividend. The study answered the following questions: (1) Why cash dividend and free cash flow to equity are not equal; (2) What is the relationship between cash dividend and ability of cash payout and also the opportunity of investment; (3) What are the features of cash dividend payout in different industries. [Nature and Science. 2005;3(1):65-70].

Key Words: cash dividend; free cash flow; investment opportunity

1 Research Background

Dividend policy, one of the three corporation financial decisions, has been concerned among theoreticians and practitioners. John Lintner (1956) brought forward a model of dividend adjustment.[1] According to the model, a firm that is currently paying dividends at the rate of DPS_t, and that has a target payout ratio of POR, will adjust (ADJ) its dividend rate, but less than fully, as its earnings per share (EPS) changes. Modigliani and Miller (1961) argued that dividend policy has no effect on either the price of a firm's stock or its cost of capital, in a perfect world, the dividend policy is irrelevant to shareholders wealth. This proposition has laid a solid theoretical foundation for the dividend policy. After that, economists have offered explanations in different ways about dividend payment, such as effect of taxes, dividend signaling, agency costs issues and transaction costs. Over decades, economists could not come to an agreement. Thus, Black, Fischer (1976) gave it a name "dividend puzzle".

In China, the dividend policy of listed companies has its unique characteristic in the strong emerging market economy if comparing the type of dividend payment in China with the type used in developed countries. In addition to cash dividend and stock dividend, several mixed types of dividend payment derive from cash dividend and stock dividend such as mix of bonus issues and dividend, mix of rights issues and dividend, According to China Securities Journal's relative statistical data, there are more listed companies who adopted the pattern of stock dividend in 1993 which were 36%, and more listed companies adopted cash dividend policy during 1994 and 1995 which were 40% and 36% respectively. The companies that paid no dividends account for 35%, 54%, 59% and 62% respectively during the period of 1996 and 1999. The proportion of total listed companies that adopted cash dividend increased from 47% to 54% during 2000 and 2001.

In this situation, in order to resolve the "dividend puzzle", many Chinese scholars have done a number of empirical studies. Two main approaches were taken in these studies:

First, using event study method to analyze the influence of different dividend policy on share price and the value of a firm. Wei Chen et al (1999) empirical analyzed the dividend policy of Shanghai stock market by the method of Cumulative Abnormal Return (CAR) and study the existence and character of the signaling effect of dividend policy in this market. This study showed that the degree of CAR was very different from different dividend policy. The CAR of right issue was higher than cash dividend but lower than bonus. Yu Qiao et al (2001) found that there was evidential positive statistical relationship between the dividends and mix dividend policies of firms on the stock market. But their study showed that the market was not sensitive with cash dividends. This phenomenon is opposition with the result being observed in developed countries' mature markets. Gang Wei (2000) found that dividend policy often signal the information of

long-term earnings about a firm for investors.

Second, based on diversified dividend policy theories, analyzers analyzed dynamic reasons of dividend policy, and tried to find impact of dynamic factors (such as ownership structure, the size of assets, profitability, ability of growth, ability of repayment, consumer preference and agency problem, etc) and influencing extent on dividend policy of firms. Different point of view offered different significant conclusions. For example, cash dividend may be affected by currency balance and retained earnings, and has positive relationship with them (Yang, 2000); different size of firms choose different pattern of dividend: small firms tend to choose stock dividend, while large firms prefer cash dividend (Yan, 2001; Zhao, 2001). If the firms have lower proportion of holding state shares and corporative shares and the stronger self-growth and development of firms, the firms enjoy the higher stock dividend payment, and also the lower cash dividend payment (Lu, 1999).

Domestic theoretic and empirical researches based mostly on profit flow (net income, EPS or retained earnings) investigated the dividend policy, and ignored the effect on cash flow. In fact, cash dividend distribution not only depends on profitability of firms, but also depends on free cash flow to firm. Compare profit flow with cash flow, the latter not only express the value which has been created by firm, but also express how many value that has been realized. From the point of view of cash flow to analyze it , it can patch the faults of profit flow (accounting policy choice, earning management), and declare real relationship between cash flow and the ability of cash payout.

Recently, more and more investors prefer cash flow, because of the idea that “cash is king” which have become many managers’ conception. Therefore, this paper seeks to analyze the problem of cash dividend payment from the cash flow point of view, and three questions answered in this paper: (1) How much cash will be distributed to shareholders by paying a cash dividend after all expenses. What is the actual dividend? (2) Why is the cash dividend payment higher or lower than cash flow? What are the factors that affect cash dividend payment? (3) What are the features of cash dividend payment in different industries?

2 Assumptions

When we analyze dividend policy of listed companies, there are two key clues: whether the firm has sufficient cash to pay a dividend; whether the cash flow of firm has another way to enhance the value of firm. There are two assumptions in this paper:

Assumption 1: the ability of dividend payment. The dividend policy is measured by dividend payout ratio (dividend/EPS). This assumption suggests that dividend is a part of EPS, but EPS is not the only source of cash dividend. According to accounting standard, cash dividend is an item in the statement of cash flows, and a residue given back to shareholders. In this case, free cash flow to equity (FCFE) is the measure of the cash that is available to shareholders after the payment of business expensive, interest and tax, which is for distribution in the form of dividends or for reinvestment in our business. It is usually measured from earning, through a series of adjustment to cash flow, it can also be measured by equation, assets = debt + equity, directly get free cash flow to equity. Ordinarily, free cash flow is the source of cash dividend, and also the maximum of cash dividend. If the cash dividend is less than FCFE, it means a firm has residual cash or increase cash storage; if cash dividend is over FCFE, it means a firm needs financing by issuing new shares etc, in order to meet the requirement of the payment of cash dividend.

Assumption 2: the investment opportunities. Instead of the method of repaying back cash to shareholders is reinvestment. Thus, reinvestment opportunities become another analytic rule of dividend policy. We assume listed companies’ dividend policy accords with the model that dividend payout ratio depend on EPS. If there is good investment opportunity in future, listed companies will reduce the rate of dividend payment; oppositely, if the investment opportunities of the firm are lack in the future, they will raise the level of cash dividend payment.

3 Variables and sample

In this empirical study, we have designed 12 variables as seen below, in order to analyze the relationship between cash dividend of listed companies and other factors, relative variables and definitions (Table 1).

Table 1. Table of variables

Variable name	Measure of variables	Definition of variables
Earnings per share (EPS)	Net profit/ total shares	Profitability
Return on equity (ROE)	Net profit/ total equity	Investment opportunity
Operating net cash flow (ONCF)	Operating cash flow/ total shares	Ability to pay out of cash flow
Free cash flow to equity (FCFE)	Free cash flow to equity/ total shares	Ability to pay out of cash flow
Net cash flow (NCF)	Net cash flow/total shares	Ability to pay out of cash flow
Dividend per share (DPS)	Dividend/total shares	Ability to cash dividend payment
Cash dividend-to-EPS ratio (EPSR)	Cash dividend/EPS	Ability to cash dividend payment
Cash dividend-to-ONCF ratio (ONCFR)	Cash dividend/ONCF	Ability to cash dividend payment
Cash dividend-to-FCFE ratio (FCFER)	Cash dividend/FCFE	Ability to cash dividend payment
Debt-to-asset ratio (BAR)	Total debt/ total assets	Ability of financing
Non-outstanding stock proportion ratio (NPR)	Non-outstanding stock /total shares	Concentration of large shareholders
Total assets (TA)	Logarithm total assets	Size of assets

In order to estimate the ability of cash dividend payment, the variable we choose not only the index of profitability such as ROE, EPS but also the index of cash flow, such as FCFE, ONCF and NCF. The last two variables (ONCF, NCF) belong to real cash flow of a company during current period; they are additional remarks for the analytic results of FCFE. The net operating cash flow associated with the cash flow creates during current period. The higher of the ONCF, the stronger of the ability that firm creates the cash flow. Net operating cash flow is the total current ability of cash dividend payment when firms make cash dividend decision. The difference between FCFE and NCF is that the latter including the amount of current equity financing.

The sample was cross section data of companies listed on the China (Shanghai and Shenzhen) Stock Exchanges in the end of 2000. 299 listed companies were randomly chosen; Special Treatment (ST) and Particular Transfer (PT) companies were not included. The accounting data was obtained from listed companies' annual reports, which were published on the web site (http://www.csrc.gov.cn) of China's Securities Regulatory Commission (CSRC), others were obtained from the web site: http://www.cninfo.com.cn, and Shenglong software.

4 Results

Our analysis is from three aspects:

1) Ability of cash dividend payment analysis. Sample descriptive statistics is presented in Table 2.

According to the EPSR and FCFER, the 209 firms were divided into 11 groups, the statistical analysis shows that cash dividend payout ratio of the most firms were between 20%~50%, this means cash dividend payment is lower than accounting profit or book value; there are 50 percent of sample firms that cash dividend payment are higher than the FCFE. This situation is revealed as figure follows (Figure 1).

2) Cash dividend payment on relative variables. From the relationship between the cash dividend payment and each variable, the relationship between cash dividend payment and EPS, However, the non-significant relationship between cash dividend payment and FCFE found in Table 3.

We chose various variable of EPS, ROE, ONCF, TA and NPR as independent variable, chose DPS as dependent variable, the results of regress analysis

(observation of 299 firms) that is the positive relationship between cash dividend and EPS, also between cash dividend and total assets; the negative relationship between cash dividend and debt-to-asset ratio; the other variable which has not passed test were eliminated. Sample descriptive statistics is presented in Table 4.

Table 2. Statistics of dividend payment firms

		Non-dividend firms （90，30%）		Dividend firms*（209，70%）		Total	
		Number of firms	Proportion	Number of firms	Percent	Number of firms	Percent
EPS	Positive	86	95%	209	100%	295	98%
	Negative	4	5%	0	0	4	2%
FCFE	Positive	53	59%	117	55%	170	56%
	Negative	37	41%	92	45%	129	44%
ONCF	Positive	68	75%	170	83%	238	79%
	Negative	22	25%	39	17%	61	21%
NCF	Positive	56	62%	144	69%	200	67%
	Negative	34	38%	65	31%	99	33%

* including cash dividend and mix of cash dividend and bonus.

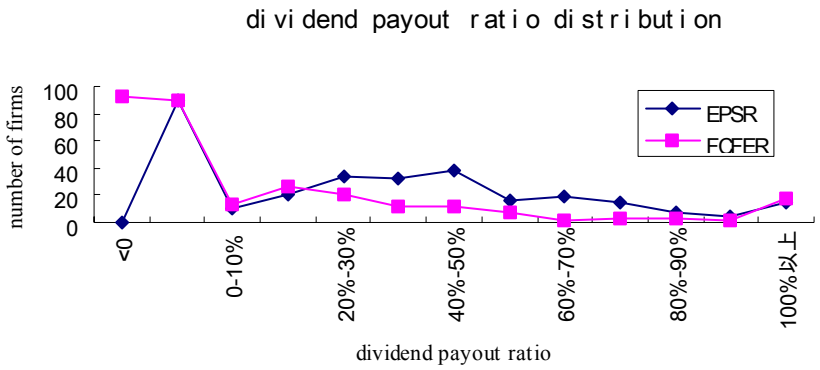

Figure 1. Dividend Payment Ratio

Table 3. Coefficients of variables for payment of cash dividend and test

	r	Sig. (2-tailed)
EPS	0.879	0.000
FCFE	-0.203	0.550
ONCF	0.671	0.024
NCF	0.181	0.594

Remarks: t values is at 5% level

Table 4. Statistic regress analysis

	Unstandardized Coefficients	Standardized Coefficients	t	Sig.	F	R^2
	B	Beta				
(Constant)	-.248		-4.080	.000		
Earnings per share	.155	.358	6.914	.000	29.567	0.231
Total Asset	6.498E-02	.287	5.133	.000		
Debt-to-assets ratio	-9.110E-02	-.168	-3.012	.003		

3) Industry and investment opportunity analysis. In this study, we found that listed companies involve in widespread industries. Different industries differ greatly in the size of assets, the character of operating, and the payment of cash dividend. If the market is regarded as a whole, it is possible to ignore the characters of industries and to affect the result of research. So, we consult the industry classification of listed companies that were reported by the Zixun web site. This paper divided the sample 299 companies into 16 industries according to the index of ROE and ONCF. The industries, such as Energy and Power, Beverages, Metallurgy and Utilities show higher ROE and ONCF; the Healthcare, Financial and Real Estate reveal higher ROE and lower ONCF; the Transportation display lower ROE and higher ONCF; and the Commerce, Tourist and Light Industry show lower ROE and ONCF.

5 Conclusions

Firstly, the payment of cash dividend is usually less than accounting profit in Chinese listed companies, but quite a number of listed companies which had more payment of cash dividend than free cash flow to equity, the gap between cash dividend and FCFE is right issue. By theory, the phenomenon of both cash dividend and right issue is contrary to basic regulation of corporate financial management. This phenomenon of self-contradiction[2] may be related to the rule by China security commission in 2000, which the listed companies must have cash dividend payment last three years while they finance by adding shares or right issue. In contrast, cash dividend payment in some listed companies were less than free cash flow to equity, which is result in forming cash storage in these firms. In China, dividend payment of firm can be described as: the firms have very few cash dividend payment and more stock dividend payment, while some firms have not paid any dividend . This is maybe one of the evidences that Chinese stock market full of speculation and unfair financing from stock market.

Secondly, payment of cash dividend in Chinese listed companies is relevantly positive for current return per share and total assets but negative for debt to asset ratio. For the index of cash flow, it is closely related to the payment of cash dividend and net operating cash flow; the index of free cash flow to equity is irrelevant . This is because listed companies understand the index of free cash flow to equity in significant limit, they seldom use free cash flow. Additionally, the payment of cash dividend is irrelevant to non-outstanding shares.

Lastly, comparatively, the results indicate that firms with a higher ROE, ONCF and higher cash dividend payment belong to traditional industry; the firms with a higher ROE , lower ONCF and lower cash dividend payment belong to high-tech industry. We find there are quite many firms, which cannot make enough residual cash flow, but they still invest big projects. They return back cash dividend to shareholders by financing from stock market. Other firms with little investment opportunity have plenty of cash flow but no cash dividend payment, still finance too. These phenomena should be paid more attention to.

Correspondence to:
Shulian Liu, Yanhong Hu
School of Accounting
Dongbei University of Finance and Economics
Dalian, Liaoning, China
Telephone: 0086-411-8471-2716
Email: msy8895@sohu.com

References

[1] Aswath Damodaran. Applied Corporate Finance, Translate by Zhenlong Zheng, Mechanism and Industry Press. 2000 (in Chinese)

[2] Black Fischer. The dividend puzzle. Journal of Portfolio Management 1976;2:5-8..

[3] Changjiang Lu, Kemin Wang. The empirical analysis of dividend policy in Chinese listed firms. Economic research 1999; (in Chinese).
[4] Chunguang Zhao, Xueli Zhang, Long Ye. Dividend policy, selection incentive: an empirical evidence from Chinese stock market. Financial and Economic Research 2001;2 (in Chinese).
[5] Gang Wei. Dividend policy under asymmetry information. Economic Research 2000;2 (in Chinese).
[6] Hai Lin. An empirical analysis between dividend policy and performance in Chinese listed firms. World Economics 2000;5 (in Chinese)
[7] .Lintner J. Distribution of incomes of corporations among dividends, retained earnings, and taxes. American Economic Review 1956;46:97-113.
[8] Merton H Miller, Franco Modiglian. Dividend policy, growth, and the valuation of shares. Journal of Business, 1961;34:411-33.
[9] Runan Chen, Zhencun Yiao. The empirical study of the effect of dividend policy signaling. Finance Research 2000;10 (in Chinese).
[10] Shue Yang, Yong Wang, Geping Bai. The empirical analysis of the factors of dividend payout policy in China. Accounting Research 2000;2 (in Chinese).
[11] Wei Chen, Xing Liu, Yuanxin Yang. An empirical study on the signaling effect of dividend policy in Shanghai Stock Market. Chinese Journal of Management Science 1999;7(3) (in Chinese).
[12] Yu Qiao, Yin Chen. Dividend policy and fluctuation of stock market in Chinese companies. Economic Research 2001;4 (in Chinese).

[1] The following model describes this process in mathematical terms: $DPS_{t+1}-DPS_t=ADJ[POR(EPS_{t+1})-DPS_t]$, where DPS is the dividend per share, ADJ is the adjustment to dividends, POR is the payout ratio, and EPS is earnings per share.
[2] If cash dividend is really return to shareholders, right issue can be treated as negative cash dividend.

A New Method for Calculating Molecular Genetic Similarity

Huijiang Gao[1], Runqing Yang[2], Wenzhong Zhao[1], Yuchun Pan[2]

1 School of Animal Science, Northeast Agriculture University, Harbin, Heilongjiang 150030, China
2 School of Agriculture and Biology, Shanghai Jiaotong University, Shanghai 201101, China

Abstract: Nei's genetic similarity is a similar coefficient for describing the difference of two binary variables, and it hasn't a connection with the relationship between individuals. According to the definition of the relationship coefficient, a new formula of genetic similarity is put forward as $r_{A(x,y)} = \frac{2N_{xy}^2}{N_x N_y \sqrt{(1+F_x)(1+F_y)}}$ or $r_{A(x,y)} = \frac{N_{xy}^2}{N_x N_y}$. An example confirms that this calculating formula of genetic similarity is significantly better than Nei's on judging relationship between individuals. [Nature and Science. 2005;3(1):71-74].

Key Words: genetic similarity; relationship coefficient; verification

Introduction

The method for estimating genetic distance according to the polymorphism of genetic productions, as isozyme， blood type and leukocyte antigens, is increasingly replaced by DNA polymorphism. The most common methods for testing the DNA polymorphism include restrictive fragment length polymorphism (RFLP), variable number of tandem repeats (VNTR) and random amplified polymorphic DNA (RAPD), etc[1]. It has been verified in many experience that the genetic purity in breed and genetic diversity between breeds can be determined effectively by proper statistical method according to the fingerprinting atlas of individual DNA. At present, the genetic similarity between individuals is scaled by Nei's formula, and the individuals' relationship is estimated from it. But this index is a kind of distance or similarity coefficient for describing the difference of two binary variables, and it has no certain connections with the relationship between individuals. So a new calculating formula of genetic similarity is preserved, according to the definition of relationship coefficient. An example proved that it is significantly better than Nei's on judging relationship between individuals.

1 Genetic Similarity

One can get an electrophoretic atlas by using present molecular mark, and comparing them binately. Using 1-1 denotes having no polymorphism, namely, monomorphism, if both two parallel samples with the same molecular weight have all bands, and 1-0 denotes having polymorphism if only one sample. For estimating the genetic purity in a breed and comparing the difference between breeds, Nei defined the genetic similarity of any two individuals in 1979 as:

$$S = \frac{2N_{xy}}{N_x + N_y} \quad (1)$$

Here, N_{xy} is the sharing bands of two individuals, x and y; N_x and N_y represent the individual bands of x and y, respectively. The mean S in a breed reflects the similarity or different degree of DNA fingerprinting atlas accusing in this breed. When the mean genetic similarity matrix of multi-breeds is calculated, the tree derivation of relationship can be made through cluster analysis.

In fact, formula (1) is a kind of distance coefficient for describing the difference or similarity degree of two binary variables. As an index of relationship between individuals, the relationship coefficient is the frequency that two individuals are of the same genes from a common ancestor. According to the mark results, the common genes in both x and y has N_{xy}, genes in x has N_x, in y has N_y, so the frequency that x has common gene is N_{xy}/N_x, that y has common gene is

N_{xy}/N_y , then the inbreeding coefficient of the progenies of two individuals, namely, the frequency that the progenies are of same gene from patents can be calculated by [5]:

$$F_{xy} = \frac{N_{xy}}{N_x} \times \frac{N_{xy}}{N_y} = \frac{N_{xy}^2}{N_x N_y} \quad (2)$$

Supposing an inbreeding coefficient of x and y is F_x and F_y respectively, then the relationship coefficient between x and y is:

$$r_{A(x,y)} = \frac{2F_{xy}}{\sqrt{(1+F_x)(1+F_y)}} \quad (3)$$

If x and y are not inbreeding individuals, that is $F_x = F_y = 0$, then formula (3) may be as follow:

$$r_{A(x,y)} = 2F_{xy} = \frac{2N_{xy}^2}{N_x N_y} \quad (4)$$

If x and y are inbreeding individuals, formula (2) and (3) show that F_{xy} may be bigger when F_x and F_y are bigger. If F_x and F_y are ignored, the relationship coefficient estimated by formula (4) may be over 1. So for assuring $0 \leqslant r_{A(x,y)} \leqslant 1$ and allowing for comparability of the genetic similarity between individuals when F_x and F_y are still unknown, formula (4) can be simplified as:

$$r_{A(x,y)} = \frac{N_{xy}^2}{N_x N_y} \quad (5)$$

Since $N_x + N_y \geqslant 2\sqrt{N_x N_y}$, so $\frac{2N_{xy}}{N_x + N_y} \leqslant \frac{N_{xy}}{\sqrt{N_x N_y}} = \sqrt{r_{A(x,y)}}$, and $S \leqslant \sqrt{r_{A(x,y)}}$.

When $N_x = N_y = N_{xy}$, namely, the bands of both individual are all the same, then $S = \sqrt{r_{A(x,y)}}$.

2 Example and Verification

Analyze the nucleus DNA genetics and variation of 9 Min pigs with a known relationship RAPD and ISSR respectively. After selecting 12 primers with polymorphism and separating amplification productions by electrophoresis, the fingerprinting atlas of RAPD including 97 amplification segments can be obtained. And 64 amplification segments can be tested by 8 ISSR primers and can obtain accordingly fingerprinting atlas of ISSR. To calculate the genetic similarities of any two individuals by formula (1) and (5), take them as the estimation of relationship coefficients between accordingly individuals and put the results in Tables 1 and 2.

Table 1. Genetic similarities between 9 individuals of Min pigs by RAPD

Pigs	1	2	3	4	5	6	7	8	9
1		0.6642	0.9321	0.7426	0.8726	0.6970	0.6321	0.7901	0.8875
2	0.5868		0.6254	0.8058	0.8546	0.7315	0.6532	0.9568	0.8198
3	0.8867	0.6831		0.6825	0.9458	0.8846	0.9114	0.8974	0.6142
4	0.6717	0.6501	0.4744		0.8456	0.7745	0.9271	0.6452	0.8954
5	0.8232	0.7825	0.9015	0.8032		06983	0.9019	0.7249	0.9358
6	0.6228	0.7674	0.8484	0.7376	0.7712		0.9238	0.9010	0.6888
7	0.6185	0.5532	0.8470	0.8603	0.8233	0.8714		0.6247	0.7542
8	0.6285	0.9352	0.8245	0.5716	0.5511	0.8501	0.4542		0.9215
9	0.7888	0.6821	0.8521	0.7488	0.8965	0.5488	0.7232	0.8683	

Table 2. Genetic similarities between 9 individuals of Min pigs by ISSR

Pigs	1	2	3	4	5	6	7	8	9
1		0.7412	0.9218	0.8125	0.8612	0.7158	0.8412	0.9123	0.5486
2	0.6369		0.9123	0.5486	0.5649	0.7315	0.7456	0.9546	0.9218
3	0.8642	0.8443		0.8821	0.7864	0.7489	0.8787	0.9215	0.9141
4	0.7835	0.8321	0.5512		0.8541	0.8742	0.7154	0.5478	0.9147
5	0.7982	0.8343	0.6972	0.7777		0.9412	0.9123	0.8326	0.8519
6	0.8625	0.7446	0.8446	0.7974	0.9124		0.9356	0.9159	0.8745
7	0.6064	0.6733	0.7878	0.5512	0.8344	0.8882		0.6415	0.7542
8	0.7332	0.9357	0.8623	0.5488	0.7232	0.8611	0.6484		0.7058
9	0.8514	0.8505	0.8483	0.8476	0.7505	0.8500	0.6676	0.8634	

To evaluate the relationship and difference between the genetic similarities different formulas in Tables 1 and 2 and the relationship coefficient between accordingly individuals in Table 3 by rank correlation and mean absolute error. It can be obtained by calculating the rank correlation between the S in Table 1 and the relationship coefficient between accordingly individuals in Table 3 is 0.1907 ($P>0.05$), their mean absolute error is 0.4113; the rank correlation between the $r_{A(x,y)}$ in Table 1 and the relationship coefficient between according individuals in Table 3 is 0.4821 ($P<0.01$), the mean absolute error is 0.3486; the rank correlation between the S in Table 2 and the relationship coefficient between according individuals in Table 3 is 0.3411 ($0.01<P<0.05$), the mean absolute error is 0.4290; the rank correlation between the $r_{A(x,y)}$ in Table 2 and the relationship coefficient between according individuals in Table 3 is 0.6093 ($P<0.01$), the mean absolute error is 0.3486. It shows that $r_{A(x,y)}$ by RAPD and ISSR are both significantly better than Nei's on judging relationship between individuals.

Table 3. The relationship and inbreeding coefficients of 9 individuals

Pigs	1	2	3	4	5	6	7	8	9
1	0.0557	0.3586	0.3462	0.4143	0.2415	0.5432	0.3259	0.1598	0.4158
2		0.0625	0.5872	0.2548	0.4872	0.7214	0.3541	0.6841	0.2147
3			0.0901	0.0320	0.1478	0.3214	0.4325	0.6741	0.5874
4				0.1462	0.4857	0.4754	0.0576	0.2174	0.3214
5					0.0876	0.5417	0.3541	0.0147	0.4874
6						0.0434	0.6487	0.6547	0.2514
7							0.1066	0.1147	0.3258
8								0.0543	0.6841
9									0.0885

Limited by outlay it only allows for a few animals and primers in verifying the validity of the new formula, but doesn't study the effect of the number of animals and primers on the validity of the new formula. It needs further research on this point.

Correspondence to:
Runqing Yang
School of Agriculture and Biology
Shanghai Jiaotong University
Shanghai 201101, China
E-mail: runqingyang@sjtu.edu.cn

References

[1] Chao Yongxin, et al. The protection of animal variety [M] Beijing: Agricultural Science Press of China. 1995:111-24.
[2] Lynch M. The similarity index and DNA fingerprintinging[J]. Mol Bio Evol 1990;7:478-80.
[3] Zhang Raoting, Fang Kaitiai. Introduction of multivariate statistical analysis [M] Beijing: Science Press. 1999:393-401.
[4] Bai Liping. The fingerprinting analysis of random amplification polymorphic DNA of pigs [Master thesis]. Haerbin: The Animal Science Department of Northeast Agriculture University. 1996.
[5] Sheng Zhilian, Wu Changxin. Quantitative genetics [M] Beijing: Agriculture Press of China. 1995:28-4

Chirp Parameter Estimation in Colored Noise Using Cross-Spectral ESPRIT Method

Xiaohui Yu, Yaowu Shi, Xiaodong Sun, Jishi Guan

College of Communication Engineering, Jilin University, Changchun, Jilin 130025, China
xiaohuiyurita@hotmail.com, rita@email.jlu.edu.cn

Abstract: In this paper a new method for estimating the parameters of chirp signals (LFM signals) is provided. It is based on an especial quadratic form transform and cross-spectral ESPRIT method. Compared with general approaches, the method here has many prominent virtues such as low complexity, low computational cost and working in relatively low SNR almost without any prior information about coloured noise. The correctness and the validity of the new approach are verified by computer emulations. [Nature and Science. 2005;3(1):75-80].

Key words: chirp signals; ESPRIT method; Colored noise; Cross-spectral estimation

1 Introduction

Chirp parameter estimation is a well-known problem in signal processing community. Chirp signals occur in many applications, e.g., radar, sonar, bioengineering, gravity waves and seismography. Various spectral analysis techniques have been used to perform chirp signals estimation and detection. Most are based on the maximum likelihood (ML) principle [1]. However, the accuracy of ML strongly depends on the grid resolution in the search procedure. The computational burden may be too high to obtain reasonable accuracy. There are other procedures to this problem. Such as phase unwrapping [2, 3], which is simple but only suitable for estimation of mono-chirp signal under higher signal-to-noise-ratio (SNR) environment; Wigner-Ville distribution (WVD)[4], which is poor in estimation of multi-chirp signals because of Cross-term interferences; Radon transform applied to the Wigner-Ville distribution of the signals (RWD) was suggested in [5], which can be directly extended to the analysis of multi-component chirp signals, but it also has the disadvantage of high complexity.

In this paper a cross-spectral ESPRIT method based on quadratic form transform for detecting and estimating chirp signals is presented. First, using quadratic form transform [6] we can convert nonstationary chirp signals into stationary state. Then the cross-spectral method [7] idea is introduced in ESPRIT [8] to produce a cross-spectral ESPRIT method. Last, the cross-spectral ESPRIT method is applied to process the stationary signal after the quadratic form transform. Replacing the two-dimensional search with mathematical operation, the method in this paper is considerably simpler to implement than ML or RWD. Because of the appliance of the cross-spectral ESPRIT method, it has another advantage that it can restrain independent colored noise and work in relatively low SNR environment.

2 Estimation of Frequency Change Rate

2.1 Quadratic Form Transform of Chirp Signals

Suppose that the mono-component chirp signal model is:

$$s(t) = A\exp\left\{ j2\pi(f_0 t + \frac{1}{2}mt^2)\right\} \qquad (1)$$

Where A denotes the amplitude of chirp signal; f_0 denotes initial frequency; m denotes frequency change rate.

Let

$$Z(t) = s(t+\frac{\tau}{2})s^*(t-\frac{\tau}{2}) = A^2\exp\left\{ j2\pi\left(f_0 + mt\right)\tau\right\} \quad (2)$$

It is easy to show that the correlation of Z(t) is:

$$R_z(t,\tau') = E\left[Z(t)Z^*(t-\tau')\right] = A^4\exp\left\{ j2\pi m\tau\tau'\right\} \qquad (3)$$

This function is independent of time t. In another word, Z(t) is a stationary random signal. Hence, via quadratic form transform above, the nonstationary chirp

signal is converted into stationary state. So methods for stationary signal processing can be used to do the following treatment. But the transform above is based on mono-chirp signal with no additive noise. In this paper we want to talk about multi-chirp signals and the additive noise is colored. Obviously using the simple transform combined with common stationary signal processing methods (the MUSIC method [9], the ESPRIT method [8] etc.) cannot reach the estimation target. So this paper provides the following cross-spectral ESPRIT method based on an especial quadratic form transform:

Generally in practice, we can acquire only one observed sequence.

$$x(n) = \sum_{i=1}^{q} A_i \exp\left\{ j2\pi (f_i n + \frac{1}{2} m_i n^2) \right\} + \omega_x(n) = s_x(n) + \omega_x(n) \quad (4)$$

With $x(n)$, time delay method [10] is introduced to produce the other three sequences as follows:

$$y(n) = \sum_{i=1}^{q} A_i \exp\left\{ j2\pi [f_i (n+\tau_1) + \frac{1}{2} m_i (n+\tau_1)^2] \right\} + \omega_x(n+\tau_1) = s_y(n) + \omega_y(n) \quad (5)$$

$$z(n) = \sum_{i=1}^{q} A_i \exp\left\{ j2\pi [f_i (n+2\tau_1) + \frac{1}{2} m_i (n+2\tau_1)^2] \right\} + \omega_x(n+2\tau_1) = s_z(n) + \omega_z(n) \quad (6)$$

$$g(n) = \sum_{i=1}^{q} A_i \exp\left\{ j2\pi [f_i (n+3\tau_1) + \frac{1}{2} m_i (n+3\tau_1)^2] \right\} + \omega_x(n+3\tau_1) = s_g(n) + \omega_g(n) \quad (7)$$

Where $A_i (i = 1, \cdots, q)$ are amplitudes of chirp signals; $f_i (i = 1, \cdots, q)$, $m_i (i = 1, \cdots, q)$ are initial frequencies and frequency change rates of chirp signals respectively; τ_1 is a constant, which value is bigger than correlated time of colored noise; $\omega_x(n)$, $\omega_y(n)$, $\omega_z(n)$ and $\omega_g(n)$ are zero-mean independent colored noises with unknown spectral density.

ombining (4)~(7), we use the following especial quadratic form transform:

$$\begin{aligned} x_1(n) &= x(n+\frac{\tau}{2}) y^*(n-\frac{\tau}{2}) \\ &= s_x(n+\frac{\tau}{2}) s_y^*(n-\frac{\tau}{2}) + s_x(n+\frac{\tau}{2}) \omega_y^*(n-\frac{\tau}{2}) \\ &\quad + \omega_x(n+\frac{\tau}{2}) s_y^*(n-\frac{\tau}{2}) + \omega_x(n+\frac{\tau}{2}) \omega_y^*(n-\frac{\tau}{2}) \end{aligned} \quad (8)$$

$$\begin{aligned} y_1(n) &= z(n+\frac{\tau}{2}) g^*(n-\frac{\tau}{2}) \\ &= s_z(n+\frac{\tau}{2}) s_g^*(n-\frac{\tau}{2}) + s_z(n+\frac{\tau}{2}) \omega_g^*(n-\frac{\tau}{2}) \\ &\quad + \omega_z(n+\frac{\tau}{2}) s_g^*(n-\frac{\tau}{2}) + \omega_z(n+\frac{\tau}{2}) \omega_g^*(n-\frac{\tau}{2}) \end{aligned} \quad (9)$$

Then the correlation of $x_1(n), y_1(n)$ is:

$$\begin{aligned} r_{x_1 y_1}(k) &= E[x_1^*(n) y_1(n+k)] \\ &= \sum_{i=1}^{q} A_i^4 e^{j4\pi m_i \tau_1 (\tau - \tau_1)} e^{j2\pi m_i (\tau - \tau_1) k} \end{aligned} \quad (10)$$

For the convenience of notation, let

$\phi_i = 4\pi m_i \tau_1 (\tau - \tau_1)$ and $\tau_2 = 2\pi(\tau - \tau_1)$

Inserting them in (10), we obtain:

$$r_{x_1 y_1}(k) = \sum_{i=1}^{q} A_i^4 e^{j\phi_i} e^{j m_i \tau_2 k} \quad (11)$$

2.2 Cross-spectral ESPRIT Method

By inserting $r_{x_1 y_1}(k)$ in $p \times p$ cross-correlation matrix, we get

$$R_{x_1 y_1} = \begin{bmatrix} r_{x_1 y_1}(0) & r_{x_1 y_1}(-1) & \cdots & r_{x_1 y_1}(-p+1) \\ r_{x_1 y_1}(1) & r_{x_1 y_1}(0) & \cdots & r_{x_1 y_1}(-p+2) \\ \vdots & \vdots & \ddots & \vdots \\ r_{x_1 y_1}(p-1) & r_{x_1 y_1}(p-2) & \cdots & r_{x_1 y_1}(0) \end{bmatrix} \quad (12)$$

Then the matrix can be expressed as:

$$R_{x_1 y_1} = F E^{j\phi} P F^* \quad (13)$$

Where $F = [F_1, F_2, \cdots, F_q]$ is a $p \times q$ complex matrix, and $F_i = [1, e^{j m_i \tau_2}, e^{j 2 m_i \tau_2}, \cdots, e^{j(p-1) m_i \tau_2}]^T$ is a complex column vector; $E^{j\phi} = diag[e^{j\phi_1}, e^{j\phi_2}, \cdots, e^{j\phi_q}]$ is a complex diagonal matrix; $P = diag[A_1^4, A_2^4, \cdots, A_q^4]$ is a real diagonal matrix.

Let: $r_{x_1y_1}^{'}(k) = r_{x_1y_1}(k-1) = \sum_{i=1}^{q} A_i^4 e^{j\phi_i} e^{j2\pi m_i(k-1)}$ (14)

Insert $r_{x_1y_1}^{'}$ in $p \times p$ cross-correlation matrix:

$$R_{x_1y_1}^{'} = \begin{bmatrix} r_{x_1y_1}^{'}(0) & r_{x_1y_1}^{'}(-1) & \cdots & r_{x_1y_1}^{'}(-p+1) \\ r_{x_1y_1}^{'}(1) & r_{x_1y_1}^{'}(0) & \cdots & r_{x_1y_1}^{'}(-p+2) \\ \vdots & \vdots & \ddots & \vdots \\ r_{x_1y_1}^{'}(p-1) & r_{x_1y_1}^{'}(p-2) & \cdots & r_{x_1y_1}^{'}(0) \end{bmatrix}$$

$$= \begin{bmatrix} r_{x_1y_1}(-1) & r_{x_1y_1}(-2) & \cdots & r_{x_1y_1}(-p) \\ r_{x_1y_1}(0) & r_{x_1y_1}(-1) & \cdots & r_{x_1y_1}(-p+1) \\ \vdots & \vdots & \ddots & \vdots \\ r_{x_1y_1}(p-2) & r_{x_1y_1}(p-3) & \cdots & r_{x_1y_1}(-1) \end{bmatrix} \quad (15)$$

Then we get:

$$R_{x_1y_1}^{'} = FE^{j\phi}P\Phi^*F^* \quad (16)$$

Where $\Phi = diag[e^{j2\pi m_1}, e^{j2\pi m_2}, \cdots, e^{j2\pi m_q}]$ is a unitary matrix. In the complex field, it is a simple scaling operator.

Theorem: Define Γ as the generalized eigenvalue matrix associated with the matrix pencil $\{R_{x_1y_1}, R_{x_1y_1}^{'}\}$. Then the matrices Φ and Γ are related by

$$\Gamma = \begin{bmatrix} \Phi & 0 \\ 0 & 0 \end{bmatrix} \quad (17)$$

to within a permutation of the elements of Φ

Proof: Consider the matrix pencil

$$R_{x_1y_1} - \gamma R_{x_1y_1}^{'} = FE^{j\phi}P(1-\gamma\Phi^*)F^* \quad (18)$$

When frequency change rates m_i are different, the matrices F and $E^{j\phi}P$ are non-singular evidently. So we get the following equation:

$$rank(R_{x_1y_1} - \gamma R_{x_1y_1}^{'}) = rank(I - \gamma\Phi^*) \quad (19)$$

Φ is a $q \times q$ diagonal matrix. So in general

$$rank(R_{x_1y_1} - \gamma R_{x_1y_1}^{'}) = q \quad (20)$$

However, if

$$\gamma = e^{j2\pi m_i} \quad (21)$$

the i^{th} row of $(I - e^{j2\pi m_i}\Phi^*)$ will become zero. Thus,

$$rank(R_{x_1y_1} - e^{j2\pi m_i}R_{x_1y_1}^{'}) = rank(I - e^{j2\pi m_i}\Phi^*) = q-1 \quad (22)$$

Consequently, the pencil $\{R_{x_1y_1} - \gamma R_{x_1y_1}^{'}\}$ will also decrease in rank to q-1 whenever γ assumes values given by (21). However, by definition these are exactly the generalized eigenvalues (GE's) of the matrix pair $\{R_{x_1y_1}, R_{x_1y_1}^{'}\}$. Also, since both matrices in the pair span the same subspace, the GE's corresponding to the common null space of the two matrices will be zero, i.e., GE's lie on the unit circle and are equal to the diagonal elements of the rotation matrix Φ, and the remaining $p-q$ GE's are at the origin.

This completes the proof of the theorem.

Once Φ is known, the estimation of frequency change rates m_i can be obtained. But using the basic cross-spectral ESPRIT method above, the final results are not satisfied because of errors in estimating $R_{x_1y_1}$ and $R_{x_1y_1}^{'}$ from finite data as well as the morbidity question hiding in the algorithm itself. Herein the TLS-ESPRIT idea [11] is introduced to solve this problem:

The singular value decomposition (SVD) of $R_{x_1y_1}$ is showed as:

$$R_{x_1y_1} = U\begin{bmatrix} \Sigma_1 & 0 \\ 0 & 0 \end{bmatrix}V^* \quad (23)$$

Where the columns of U and V are the left and right singular vectors. $\Sigma_1 = diag[\sigma_1, \sigma_2, \cdots, \sigma_q]$; Where $\sigma_i (i = 1, \cdots, q)$ is non-zero singular value of $R_{x_1y_1}$, and $\sigma_i \geq \sigma_{i+1} (i = 1, 2, \cdots, q-1)$.

Separate the right singular vector V as $V = [V_1, V_2]$, where V_1 is composed of the previous section of V and its rank is q; V_2 is composed of the follow section which rank is p-q. In the same way, the left singular vector U is divided into $U = [U_1, U_2]$. From which, we obtain:

$$R_{x_1y_1} = [U_1, U_2]\begin{bmatrix} \Sigma_1 & 0 \\ 0 & 0 \end{bmatrix}\begin{bmatrix} V_1^* \\ V_2^* \end{bmatrix} \quad (24)$$

Thus $R_{x_1y_1} = U_1\Sigma_1V_1^*$

Left multiplied by U_1^* and right multiplied by V_1, the expression $R_{x_1y_1} - \gamma R_{x_1y_1}^{'}$ is equal to $\Sigma_1 - \gamma U_1^* R_{x_1y_1}^{'} V_1$. So the $p \times p$ generalized eigenvalue problem of the

matrix pencil $\{R_{x_1y_1}, R_{x_1'y_1'}\}$ turn to be the $q \times q$ generalized eigenvalue problem of the matrix pencil $\{\Sigma_1, U_1^* R_{x_1'y_1'} V_1\}$.

Once the generalized eigenvalues z_i of the matrix pencil $\{\Sigma_1, U_1^* R_{x_1'y_1'} V_1\}$ are calculated, m_i can be gained from:

$$m_i = \arctan[\mathrm{Im}(z_i) / \mathrm{Re}(z_i)] \tag{25}$$

It is the cross-spectral ESPRIT estimation of frequency change rates.

3 Estimation of Initial Frequencies

Supposing the estimates of $\hat{m}_i (i = 1, \cdots, q)$ are accurate enough, we can consider approximatively $\hat{m}_i \approx m_i$.

$$\text{Let } r(n) = \sum_{i=1}^{q} e^{-j(2\pi \times \frac{1}{2}\hat{m}_i n^2)}. \tag{26}$$

Multiplying it by (4), we get:

$$x_2(n) = x(n) r(n) \approx \sum_{i=1}^{q} A_i \exp\{j2\pi f_i n\} + \omega_x(n) \sum_{i=1}^{q} e^{-j(\pi \hat{m}_i n^2)} \tag{27}$$

Applying time delay method also, a sequence $y_2(n)$ that is independent of $x_2(n)$ is produced:

$$y_2(n) = x_2(n+\tau_3) = \sum_{i=1}^{q} A_i \exp\{j2\pi f_i (n+\tau_3)\} + \omega_x(n+\tau_3) \sum_{i=1}^{q} e^{-j\{\pi \hat{m}_i (n+\tau_3)^2\}} \tag{28}$$

The correlation of $x_2(n)$, $y_2(n)$ is:

$$r_{x_2 y_2}(k) = E[x_2^*(n) y_2(n+k)] = \sum_{i=1}^{q} A_i^2 e^{j2\pi f_i \tau_3} e^{j2\pi f_i k} \tag{29}$$

Using the cross-spectral ESPRIT method depicted in section 2.2, the initial frequency estimates are easily obtained. Herein we do not explain it in detail.

4 Simulation

In this section the estimated results of frequency change rates and initial frequencies of chirp signals will be brought forth and we will compare them with outcomes of RWD method.

The model of multicomponent chirp signals in colored noise is taken into account as:

$$x(n) = A_1 \exp\left\{j2\pi(f_1 n + \frac{1}{2} m_1 n^2)\right\} + A_2 \exp\left\{j2\pi(f_2 n + \frac{1}{2} m_2 n^2)\right\} + \omega_x(n) \tag{30}$$

Where $m_1 = 0.17$, $m_2 = 0.19$, $f_1 = 0.1$, $f_2 = 0.12$; $\omega_x(n)$ is zero-mean, stationary colored noise with unknown spectral density. It is derived by a white noise with zero mean and variance 1 passing through a band-pass filter, which has the follow expression:

$$H(z) = \frac{k(1 - 2z^{-2} + z^{-4})}{1 - 1.637z^{-1} + 2.237z^{-2} - 1.307z^{-3} + 0.641z^{-4}} \tag{31}$$

Curve of power spectral density is showed in Figure 1.

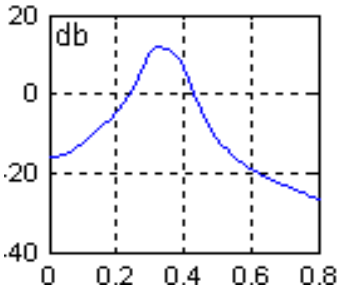

Figure 1. Unitary Power Spectral of Colored Noise

It is easy to obtain the correlation time of colored noise $\omega_x(n)$ be $\tau_0 = 25$. We assume delay time $\tau = 30$.

Let

$y(n) = x(n+30)$, $z(n) = x(n+60)$, $g(n) = x(n+90)$.

As we see, the colored noise in $x(n), y(n), z(n), g(n)$ is independent of each other. Let every data lengths of the four sequences be 512. Both SNRs of two chirp components are –5dB.

After 30 Monte-Carlo simulations under the same test conditions, the statistics of chirp parameter estimates using cross-spectral ESPRIT method are shown in Table 1.

For the convenience of compare, keep the emulational model and conditions of previous test

invariable, but $\omega_x(n)$ in model is changed into white Gaussian noise. Applying the well-known Radon-Wigner distribution method, the estimated curve is shown in Figure 2 and the statistics of estimation results are shown in Table 2.

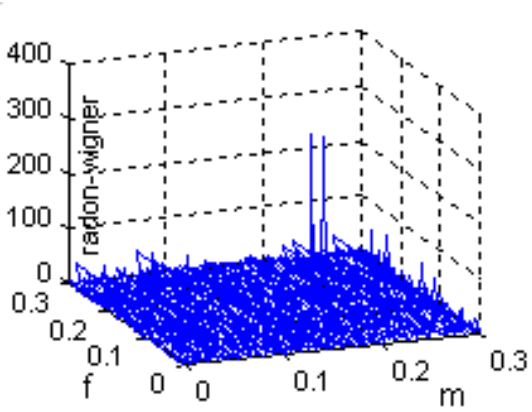

Figure2 RWD of chirp signals

We can get from the simulation results that when both SNRs are –5dB, for frequency change rates, the estimated accuracy of cross-spectral ESPRIT method is close to the accuracy of RWD method, but the computational burden of the first method is lower than the second method to heavens; for initial frequency *f*, the accuracy of method in this paper is bad comparing with RWD because of the assumption that $\hat{m}_i \approx m_i$. However, in practice it is often the case that the frequency change rates are the only parameters for interest, so the method in this paper is applicable in engineering. If the high estimated accuracy of parameter *f* is requested by all means, the method in literature [12] can be used.

Table 1. Statistic of estimates by cross-spectral ESPRIT method (SNR=-5dB)

Parameter	m_1	m_2	f_1	f_2
Real value	0.17	0.19	0.1	0.12
Estimated mean	0.1700	0.1900	0.1026	0.1213
Estimated variance	3.6667E-09	8.3000E-09	1.3998E-04	1.5405E-04

Table 2. Statistic of estimates by RWD (SNR=-5dB)

Parameter	m_1	m_2	f_1	f_2
Real value	0.17	0.19	0.1	0.12
Estimated mean	0.1701	0.1901	0.1001	0.12
Estimated variance	9.2689E-09	7.6695E-09	2.5673E-08	3.3686E-08

5 Conclusion

In this paper a new approach for detecting and estimating chirp signals is presented. Both theoretical evaluations and simulations prove that cross-spectral ESPRIT method decreases a good number of computational complexities because it avoids the two-dimensional search, which RWD method and so forth must confront. Even working in colored noise and relatively low SNR phenomena, the method here is very accurate, highly reliable, and can operate efficiently.

Correspondence to:

Xiaohui Yu, Yaowu Shi, Xiaodong Sun, Jishi Guan
College of Communication Engineering
Jilin University
Changchun, Jilin 130025, China
Email:xiaohuiyurita@hotmail.com

References

[1] Abatzoglou TJ. Fast maximum likelihood joint estimation of frequency and frequency rate. IEEE Trans on AES 1986;22(6):708-15.

[2] Alex B Gershman and Marius Pesavento. Estimating parameters of multiple wideband polynomial-phase sources in sensor arrays. IEEE Trans. on signal processing. 2001;49(12):2924~34.

[3] Djurie PM, Kay SM. Parameter estimation of chirp signals. IEEE Trans on Acoustics, Speech and Signal Proc 1990;38:2118-6.

[4] Lang SW, Musicus BR. Frequency estimation from phase differences. In IEEE Int Conf on Acous, Speech and signal Proc 1989;4:2140-3.

[5] Kay S Boudreaux-Bartels GF. On the optimality of the Wigner distribution for detection. In Proc ICASSP'85. 1985:27.2.1-4.

[6] Paulraj A, Roy R, Kailath T. Estimation of signal parameters via Rotational Invariance techniques – ESPRIT, Circuits, Systems and Computers, Nineteeth Asilomar Conference. 1985:83-9

[7] Roy R, Kailath T. Total least squares ESPRIT, Proc. 21st Asilomar Conf Signals, Syst, Computer. 1987:297-31.

[8] Shi Y, Dai Y. Estimation of Sinusoidal Parameters in Measurement Noise by Cross-Spectral Method J of Electronics 1994;22:1-8.

[9] Schmidt RO, Multiple emitter location and signal parameter estimation, IEEE Trans Antennas Propagat 1986;34:276-80

[10] Shi Y, Dai Y, Gong W. Cross-spectral Moment and SVD Methods Estimating the Parameters of Close Sinusoids in Colored Noise, J of Electronics 1995;4:14250

[11] Wood JC, Barry DT. Radon transformation of time-frequency distributions for analysis of multicomponent signals. IEEE Int Conf Acoust, Speech, Signal Processing, 1992;4:257-61.

[12] Zhang X, Zheng B. Analysis and processing of nonstationary signals, National Defence Engineering Publishing Company, Beijing, China. 53-4

Comparison Analysis of Foreign Capital Used in China's Northeast Three Provinces

Juan Xiong[1], Jiancheng Guan[2]

1 School of Management, Beijing University of Aeronautics and Astronautics, Beijing, China; Heilongjiang University, Harbin, Heilongjiang, China; xiongjhlju@hotmail.com
2 Research Unit for R&D/Innovation Management at the School of Management, Beijing University of Aeronautics and Astronautics, Beijing, China

Abstract: After China Government implemented a strategy to develop China's western region, it decided to implement a strategy to revitalize the old industrial bases in China's northeast. But how about is the situation of China's northeast? This article analyses the situation and characteristic of foreign capital used in China's northeast three provinces—Heilongjiang province, Jilin province and Liaoning province to find the difference among the eastern parts. At the same time, we put forward the way to utilize foreign capital in China's northeast to participate in the reform of the old industrial bases, to improve economic development of three provinces in China's northeast. [Nature and Science. 2005;3(1):81-87].

Key words: foreign capital used; three provinces in China's northeast; old industrial bases

1 Introduction

According to UNTDO statistics, from 1980 to 2002, the whole world FDI increased constantly. Up to 2002, the accumulative total volume of global FDI was USD 7.1 trillion, and the country of absorbing FDI most was America, its total volume was USD 1351 billion. UK and Germany were in the second and the third places, the total volumes were USD 639 billion and USD 452 billion. As the country developed most rapidly in the developing countries, China was in the forth place in 2002 from the 17th place in 1990, the total volume of FDI was 448 billion. In 2003, the amount of foreign capital actually used was USD 53.505 billion in China. (Appendix I). Foreign capital gets an increasingly important role of China economic development. At the same time Chinese economy improved rapidly to create favorable conditions for utilization of foreign capital.

— Increasing employment opportunity;

— Increasing financial revenue;

— Improving foreign trade and foreign economic cooperation development.

But the regional distribution differs greatly from the utilization of foreign capital in China. Up to 2003, the east part of the country was 86.27%, the central region was 8.93% and western region was 4.8% in Chin total amount of foreign capital actually used. (Table 1, Table 2). So we will analyze the situation and characteristic of foreign capital used in three provinces —Heilongjiang province, Jilin province and Liaoning province of China central region to find the difference between them and east part.

Table 1. Up to 2003, China east, central and western region utilization of foreign capital

(USD 100 million)

Region	Number of projects Ratio(%)	Amount of foreign capital specified in contracts Ratio(%)	Amount of foreign capital actually used Ratio(%)

Total	100	100	100
East region	82.00	86.86	86.27
Central region	11.27	7.55	8.93
Western region	6.73	5.59	4.80

According to：<China Foreign Capital Utilization Report > 2004

Table 2. 2003 China east, central and western region utilization of foreign direct investment (USD 100 million)

Region	Number of projects	Ratio(%)	Amount of foreign capital specified in contracts	Ratio(%)	Amount of foreign capital actually used	Ratio(%)
Total	41081	100	1150．70	100	535．05	100
East region	36159	88．02	1005．30	87．36	459．51	85．88
Central regio	3177	7．73	95．52	8．30	58．31	10．90
Western regio	1745	4．25	49．88	4．33	17．23	3．22

According to：<China Foreign Capital Utilization Report > 2004

2 The general situation of the foreign capital utilized in China northeast three provinces

Heilongjiang Province: Up to the end of 2003, the accumulative number of foreign capital projects approved 6876, the amount of foreign capital specified in contracts was USD 7.102 billion, total amount of foreign capital actually used was USD 4.682 billion, and foreign funded enterprisers were 2980. And in 2003, the new foreign capital projects increased 239, the amount of foreign capital specified in contracts was USD 0.488 billion, the amount of foreign direct investment actually used was USD 0.322 billion.

Jilin Province: Up to the end of 2003, the accumulative number of foreign capital projects were 6986, accumulative total amount of foreign capital actually used was USD 3.659 billion, and in 2003, the new foreign capital projects increased 340, the amount of foreign direct investment actually used was USD 0.191 billion.

Liaoning Province: Up to the end of 2003, the accumulative number of foreign capital projects were 12437, the amount of foreign capital specified in contracts was USD 32.928 billion, accumulative total amount of foreign capital actually used was USD 16.253 billion, and in 2003, the new foreign capital projects increased 2231, the amount of foreign direct investment actually used was USD 2.824 billion.

For the circumstances of foreign capital used in northeast three provinces, Liaoning Province was in the first place, which led Heilongjiang Province and Jinlin Province on matter what the number of foreign enterprisers, the amount of foreign capital actually used, or the increasing rate of foreign capital used. The main reasons of these were the favorable geographical position and good foundation of an open economy policy in Liaoning Province.

Although the number and amount of foreign capital used in Northeast are increasing continuously, especially Liaoning Province, whose number of foreign enterprisers was near the coastal provinces and city, they fell behind comparing eastern coastal provinces and city (Table 3).

Table 3. Up to the end of 2003, the utilization of foreign direct investment in some east part in China -- five provinces and one city (USD 100 million)

Province or city	Numbers of foreign enterprises	Accumulative total amount of foreign capital specified in contracts (USD 100 million)	Total amount of foreign capital actually used (USD 100 million)
Shandong Province	19737	399.67	248.97
Jiangsu Province	25061	990.15	522.38
Zhejiang Province	14722	315.23	159.35
Fujian Province	12974	320.59	262.20
Guangdong Province	34507	737.77	777.58
Shanghai City	16510	487.81	278.56

According to: <China Foreign Capital Utilization Report > 2004

3 Analyzing the main Characteristics of foreign capital used in China Northeast three provinces

We know that attracting foreign capital actively is essential condition to speed economic development. The contributing effect and big or small has closed relations for coordinating level of local region factor and the government policy. China's middle region has a vast land where the situations of industrial development have differed greatly with eastern part.

Northeast three provinces were the base camp of China industrial economy in the period of planned economy. It was the most abundant region of industrial resources that almost concentrated all China heavy and chemical industry, such as Daqing oil field in Heilongjiang province, the chemical and automobile industry in Jilin province, iron and steel industry in Liaoning province, and some large mines. So we can say that China's northeast almost represent China industry. In the industrial basis field, it is the first for not only heavy and chemical industry, but also communication and transportation in China. In the human resources field, it is in the lead for the rate of technical staff in China. In the agriculture field, it is rich in natural resources – Heilongjiang and Jilin is the agricultural – produced base. But the people are only 100 million, just near Shandong province. So in the early days of China reform, northeast had more strength to compare with eastern coastal part.

But with the deepening of China reform, the development of northeast fell behind eastern coastal part. The main reasons were that it is didn't do its best at its economic transform. It has differed greatly with eastern part in the ownership structure. Up to the end of 2001, the rates of state-owned enterprises in northeast three provinces were 78.2%of Liaoning, 86.2% of Jilin, and 87.2% of Heilongjiang. These rates were higher than eastern coastal part, and also higher than all county's average level – 64.9% (Huang, 2003). And the more scales of state-owned enterprise, the more difficult it adjusted. On the other hand, northeast three provinces have some problems in the market opening, the government ideas and the whole investment environment fields. So it has characteristics of foreign capital used.

3.1 The function of government

In the course of utilization foreign capital, the government of northeast three provinces attaches great importance to organizing function of the government, combine government affairs with economy and trade closely. They help enterprises to build the platform to find the cooperating partner. On the other hand, the government which attracted investment can solved the contradictions of the high costs and low successful rate for enterprises that temper themselves in the market. For example, Heilongjiang government held the fourteenth economy and trade fairs, twentieth Harbin ice and snow festivals; Liaoning government held Dalian international fashion festival, Shenyang – China

international equipment manufacture fair, APEC Dalian conference. Through these activities, they extend China's northeast well-know measures and effects at home and abroad, promote foreign investors' understanding for prospect of economy and social development, improve foreign investors' confidence.

But in China's northeast three provinces, the whole investment environment is not perfect. For example, some laws and regulations didn't amplify; they stressed management environment to the neglect of law environment; there are more examination and approval systems; and sometimes happened charging and checking decision. All of these obstruct the reform of northeast three provinces.

3.2 The fields and region of absorbing foreign capital

The beginning of the reform, the fields for utilization of foreign capital centralized the processing industry of the second industry and real estate of the third industry. After over ten years developing, the field for utilization of foreign capital has changed greatly in northeast three provinces. In the field of the first industry, foreign capital is entering the projects of green food and deep process of agriculture products; in the second industry, it got actual effect for utilization of foreign capital to transform state-owned big and middle enterprises, now the step is speeding for foreign capital to enter the high technology industry field; in the third industry, the field of foreign capital is extending, such as the fields of finance, insurance and tourist. And the scale for utilization of foreign capital is extending in the field of basis facilities construction and education.

In the northeast, the regions for utilization of foreign capital were disequilibrium. In Liaoning province, the foreign capital centralized in Shenyang and Dalian city; in Jilin province, it centralized in Changchun and Jilin cities; and in Heilongjiang province, it centralized in Harbin. Except them, other area had a little amount of foreign capital. For example, during "the ninth –five years plan", the amount of foreign capital used was USD 2.2 billion annual, and USD 1.2 billion was invested in Dalian, other cities were invested a little in Liaoning province (Jiang, 2003).

3.3 The scale and quality for utilization of foreign capital

Now the large project is increasing evidently. In Liaoning province, in 2001, the number of projects which invested above USD 5 million was 310, the amount of foreign capital utilized through the signed contracts was USD 4.18billion, increased by 54.2% and 66.5% over the preceding year. In Heilongjiang province, the number of the new projects approved 17 in 2001, which invested over USD 10 million each, the total amount was USD 0.37 billion. Every project was USD 15 million equally.

At the same time, northeast provinces attach importance to absorb the investments of the world top 500 company. Now there are many world-famous companies to invest here, such as Volkswagen, Wal-Mart, Samsung, and there were 15companies of the top 500 companies to invest in Jilin province, 16 companies invested in Heilongjiang province. And the invested scale and technology content are increasing continuously, the amount of investment are added obviously. For example, the amount of added investment was USD 0.86 billion, 28.6% of the total foreign investment in 2001 in Liaoning province.

But comparing with east part, northeast three provinces have not changed the comparative advantage to competitive advantage. The big projects which can improve the local economic development are not more. So there is a long way to compare with the east part, not only in the scale but project of foreign capital used. In 2001, the total amount of foreign capital used was USD 5.262 billion in northeast three provinces, just was 33.4% of Guangdong province(which total amount was USD 15.755 billion in 2001.), 71.6% of Jiangsu province (which total amount was USD 7.35 billion).

On the other hand, the successful rate of foreign projects is low. In Liaoning province from 1979 to 2001, accumulative amount for foreign capital specified in contracts was USD 53.81 billion, the amount of foreign capital actually used was USD 28.66 billion, just 52.5% of the one of foreign capital specified in contracts. Heilongjiang province was 73% at the same time. The main reason was that the project didn't have appeal. And the governments pay attention to formulate preferential policies to the neglect of the project demonstration. Others owing to the northeast three provinces in remote districts, they didn't have quick access to information, which led not to understand the detailed credit standing for foreign investors. So sometimes the enterprisers were deceived.

3.4 The ways for utilization of foreign capital

There are many ways for utilization of foreign capital in northeast provinces, such as, foreign direct investment, foreign government loans, international finance corp. loans, enterpriser stock in the abroad financial market. For example, Heilongjiang province, there were 27 projects of international finance corp. loan and foreign government loan in 2001, the amount was USD 0.29 billion, increased by 6.2% over the preceding year. Jilin province, the foreign loan was USD 0.18 billion in 2001, increased by 17.7% over the preceding year, such as Jilin Hada bay electric power factory (Japanese loan), the project of chemical fertilizer (Span loan). All of these improved the economic development of Jilin province.

4 Developing course for utilization of foreign capital in northeast three provinces

Now the central government stress to reform the old industrial bases in China's northeast. It is the most important strategy after the strategies of opening China's coastal region and developing China's western region. Under these circumstances, the northeast three provinces should utilize foreign capital effectively to adjust their industrial structure, improve economic development according to their industrial condition and distribution condition.

4.1 Improve the whole investment environment

The whole investment environment is the sign of economy and culture level in one area, which is the main factor to effect foreign investment. The reforming and adjusting the old industrial bases in China's northeast will improve the investment environment of northeast three provinces. The government of northeast three provinces should take positive measures to promote foreign investment other than the national favorable policies.

Firstly, the local government should analyze and research distribution conditions of every region carefully, define industrial and styles of foreign investment clearly, and put forward implementation plan to avoid the competition blindly for foreign projects among enterprises. While government guides investment work, they should avoid more interventions, stress on long-term plan to invest foreign capital and the substance of foreign capital, guide the enterprises to stress on digest and absorb what they invest the technology, and help them to form their own R&D ability. At the end, it will get common development between foreign and local enterprises which help each other to increase the local industrial level.

Secondly, they should strengthen the building of basis facilities. Now the central government is putting into effect for 100 projects to adjust and reform the old industrial bases in China's northeast. These projects will improve the northeast three provinces' basis facilities and revitalize the old industrial bases. At the same time, they also be perfecting some law and regulations, improving work efficiency of government, simplify the examination and approval system of foreign investment, and increase transparency of examination and approval.

4.2 Utilization of foreign capital according to the concrete industrial condition and distribution condition of northeast three provinces, and bring along the development of related industry

Northeast region is the bases of heavy and chemical industry. The industry is their economic mainstay which affects the social and economic development. But others estate didn't develop enough. As the case of Harbin, the ratio between the estates of agriculture, animal husbandry, fishery and processing as these raw material was 1: 0.38. If this ratio gets 1: 0.85 that is the average level of the whole nation, even if the scale estate of agriculture, animal husbandry and fishery doesn't enlarge, the output value will increase RMB 15 billion annually. The developing potentials are very huge, and the region of northeast three province is rich in natural resources. So the foreign capital should bring along the development of related industry. For example, absorbing foreign capital and using modern productive and processing technology to develop characteristic production of agriculture and animal husbandry, and actively expend follow-up processing to add to the additional value of products, accomplish the industry management of agriculture and animal husbandry.

Firstly, we should absorb the foreign capital to distinctive and superior resources' development and deep-processing. For example, we can choose some projects, such as the dairy products, green agriculture products and feed, which are high technology applicable. These products can replace import- products, and have large export- market. These projects don't need large money, so it is relatively easy to absorb foreign investment and will be high technology applicable. They can combine speedily with the local superior

conditions to improve the productive ability, adapt the demand of home and abroad markets, and improve the product's sales volume.

Secondly, we should absorb foreign capital to the superior industry to reduce its cost of production, improve its competitive power. So these industries should absorb foreign investments which have abundant funds and technology, such as transnational corporation, which has higher technology than domestic enterprises, and has large R&D capacity to make technology renewal and progress, also bring along the local middle and small enterprises development.

4.3 Encourage the foreign capital to invest the high and new technology industry

Three Northeast provinces had better science and technology capacity. Shenyang, Changchun, Harbin and Dalian have many universities and institutes and abundant human resources. They have formed some technology-intensive industries, such as oil and chemical, automobile, equipment manufacturing and biological industries. So we should give full play to the science and technology of three northeast provinces to combine with foreign capital and advanced R&D institutes, develop high and new technology industry to bring along local technology progressed in order to reduce the distinction between home and world advanced technology. On the other hand, because there is big risk to invest in high and new technology industry, we should absorb not only FDI, but also indirect investment, such as the capital of international capital market. It is an effective way to invest in high and new technology industry which can adjust the industrial structure of old industry bases in China's northeast.

Correspondence to:
Juan Xiong
School of Management
Beijing University of Aeronautics and Astronautics, Beijing 100086, China
Email: xiongjhlju@hotmail.com

Acknowledgement:

This paper was a part of the program of science and technology by the Science and Technology Government Office, Heilongjiang Province of China.

References:

[1] Heilongjiang Statistical Yearbook.
[2] Jilin Statistical Yearbook.
[3] Liaoning Statistical Yearbook.
[4] Chin Statistical Yearbook.
[5] Sibao Ding. "The way of China's Northeast Appearance". CHINA OPENING HERALD, No.9, 2003.
[6] Sibao Ding. "The Problem and Outlet of China's Northeast". CHINA OPENING HERALD, No.9, 2003.
[7] Xiaoling Huang. "Geographic Advantage of Central/Western China and FDI Promotion". JOURNAL OF INTERNATIONAL TRADE, No.1, 2003.
[8] Jinping Zhao: Utilization of Foreign Capital and China Economic Development P36, People Publishing House June, 2001.
[9] Shuhe Huang, Economic Daily, Dec.28, 2003.
[10] Rong Jiang, China Management Daily, Aug.4, 2003.
[11] <China Foreign Capital Utilization Report > 2004,12.

Appendix 1. Total Amount of Foreign Capital Actually Used (USD 100 million)

Year	Total		Foreign Loan		Direct Foreign Investments		Other Foreign Investments
	Number of projects	Value	Number of projects	Value	Number of projects	Value	
1993	83595	389.60	158	111.89	83437	275.15	2.56
1994	47646	432.13	97	92.67	47549	337.67	1.79
1995	37184	481.33	173	103.27	37011	375.21	2.85
1996	24673	548.04	117	126.69	24556	417.25	4.10
1997	21138	644.08	137	120.21	21001	452.57	71.30
1998	19850	585.57	51	110.00	19799	454.63	20.94
1999	17022	526.59	104	102.12	16918	403.19	21.28
2000	22347	593.56		100.00	22347	407.15	86.41
2001	26140	496.72			26140	468.78	27.94
2002	34171	550.11			34171	527.43	22.68
2003	41081	561.40			41081	535.05	26.35

According to 2004China Statistical Yearbook

Appendix 2. Actually Used Foreign Direct and Other Investment by Region (USD 10000)

Region and Sector	2002		2003	
	Foreign Direct Investment	Foreign Other Investment	Foreign Direct Investment	Foreign Other Investment
Liaoning	431168		282410	
Jilin	24468		19059	
Heilongjiang	35511		32180	
Shandong	473404	6606	601617	
Jiangsu	1018960		1056365	
Shanghai	427229		546849	
Zhejiang	307610		498055	
Fujian	383837		259903	
Guangdong	1133400	197732	782294	227041

According to 2004China Statistical Yearbook

Water-saving and Anti-drought Combined Technological Measures' Influences on Maize Yield Formation Factors and Water Utilization Efficiency in Semi-arid Region

Limin Wang, Yongxia Wei, Tianfang Fang

Northeast Agricultural University, Harbin, Heilongjiang 150030, China, wanglm0318@163.com

Abstract: Adopting the split sections design method, the influences of water-saving and anti-drought combined technological measures (bed-irrigating sowing, seedling stage mending irrigation, and ridge plotted field water conservation) on maize yield formation factors and water utilization efficiency (WUE) in semi-arid region in china was studied. Through the intensive studies on the dry matter accumulation status, on changes to leaf area, to LAD, to net assimilation rate, to yields and to WUE under different technological measures, the relations between maize yield and the amount of limited water supply and ridge plotted field were obtained, and through the optimization analysis, the regress equations of maize yields under the conditions with and without ridge plotted field were established respectively, and the extent of the water amount for bed-irrigating and mending irrigation were proposed in the paper. [Nature and Science. 2005;3(1):88-94].

Key words: semi-arid region, maize, yield, technology integration, water-saving, anti-drought, water utilization efficiency (WUE)

1 Preface

The scarcity of water resources has been always the restrictive factor on agriculture sustainable intensive development in northeast semi-arid area of china. Utilizing water resources sufficiently, increasing water utilization ratio, developing water-saving irrigation agriculture are efficient measures for the agriculture sustainable development of the region. The influences of water-saving and anti-drought combined technological measure (mechanized implicit bed-irrigating sowing, mechanized seeding stage implicit mending irrigation, and ridge plotted field water conservation) on maize yield formation factors and water utilization efficiency (WUE) have been studied.

Bed-irrigating sowing is a kind of local irrigation method of injecting some fixed quality water into local soil, so that the minimal amount of water for seeds budding can be met. The method has lower cost and easy operation, and it is suitable for the conditions of lower soil water content when sowing in northeast semi-arid regions. Seeding stage mending irrigation is a method of fulfilling cropland crops' water demand by field mending irrigation when cultivation, and it has good effects on anti-drought. Ridge plotted field is a method of dealing with sloping cultivated land. Earth blocks are built in ridges of sloping arable land, Continuous water storage shallow holes are formed, which have effects of holding back rainfall, deferring path flows, preventing from soil erosion, and increasing crop yield.

2 Experimentation conditions and study methods

2.1 Basic conditions of experimentation region

The experimentation locus was selected in the demonstration area of national "863" project named "experimentation and demonstration of Water-saving agriculture integration technology system in anti-drought irrigation area in northeast semi-arid region in china". The concrete experimental locus was in Dongxing village, Gannan County, Heilongjiang province, China. In this region, spring drought was the main restraining factor on agriculture production. The main reasons for spring drought were the shortage of spring rainfall, heavy evaporation quantum; strong spring wind; thin soil layer, coarse texture, no soil-water conservation and large acreage of wind erosion soil.

2.2 Experimentation design

Adopting split sections experimentation design, taking the disposals with and without ridge plotted field as two main disposals, taking the disposals with different amount of water supply (including bed-irrigating and mending irrigation) as subsidiary disposals, we made the experimentation plan. That is, among these sections, the sections with and without ridge plotted field are called main sections (complete sections), the sections divided by the amount of limited water supply are called subsidiary sections (split sections), split sections distributed in main sections. For the two factors including bed-irrigating and mending irrigation in the subsidiary disposals an experimentation plan called two factors twice satiation D-optimization design was adopted. There were 6 experimental disposals, 3 iterations, and all together 36 experimental sections. Each section had a length of 12 m, width of 2.6 m, acreage of 31.2 m^2, and the arrangement was random. The amount of water supply for bed-irrigating and mending irrigation can been seen Table 1.

2.3 Collection and mensuration of samples

Sampling periods included emergence stage, jointing stage, teaselling stage, silking stage, grain filling stage, milk ripe stage, and harvest stage. After analyses and computings, we got physiological parameters such as leaf area, LAD, net assimilation ratio, dry matter weight, economic coefficient, water utilization efficiency and etc, and gained spike length, kilo-grain weight, single grain weigh etc.

Table 1. The amount of water supply for bed-irrigating and mending irrigation

Disposals	Bed-irrigating quantum（m^3/ hm^2）	Mending irrigation quantum（m^3/ hm^2）
1	0	0
2	120	0
3	0	120
4	52.05	52.05
5	120	83.70
6	83.70	120

Crop variety for experimentation was maize (Haiyu 4).

3 Results and analyses

3.1 Dry matter accumulation status under different technological measures

The results indicate that the dry matter for single plant above ground measured continuously fits the "S" type of plant growth in the whole procreation process. At the same time, under different water supply conditions, dry matter accumulation of different procreation stage represents distinctive diversity. From the view of water supply gross, the more supplied water, the more dry matter accumulation of disposals (Figure 1, 2). Contrasting the effects between bed-irrigating and mending irrigation, we can draw the conclusion that mending irrigation has more distinct help for the increase of dry matter accumulation than bed-irrigating under the same condition of water supply gross. From the view of effects of ridge plotted field, disposals with ridge plotted field increase 5.6% to disposals without ridge plotted field in average.

3.2 Changes to leaf area under different technological measures

The main photosynthesis organ of maize is leaf, namely the more leaf area, the more absorption of solar energy, the more yields [3]. So study on leaves changes of different disposals is necessary for the study on yields under different technological measures.

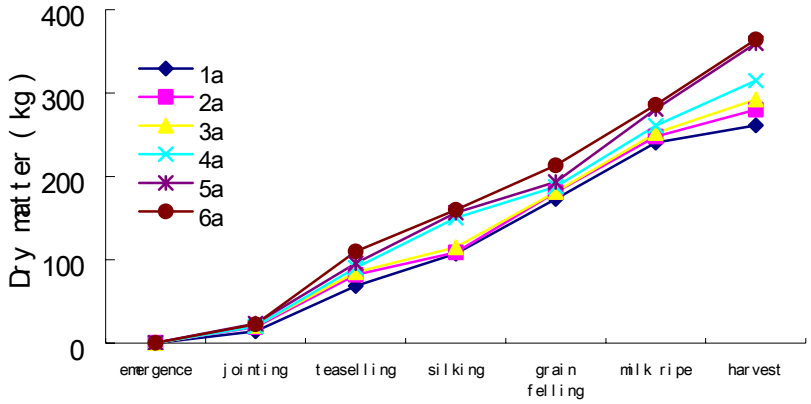

Figure 1. Contrasts on maize dry matter accumulation without ridge plotted field

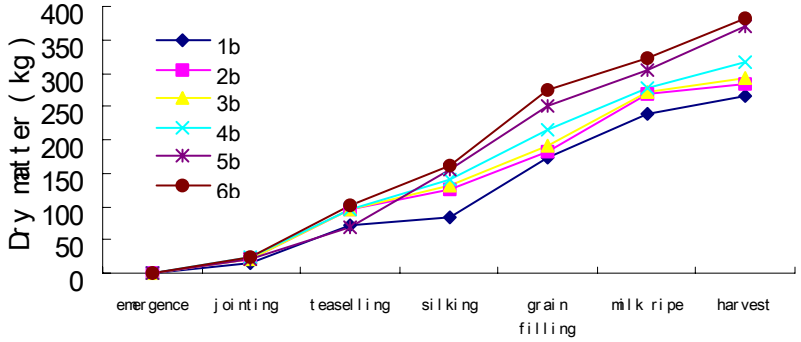

Figure 2. Contrasts on maize dry matter accumulation with ridge plotted field

Since an infrequent drought occurred in Gannan county in 2003 and 2004, maize leaves fell off ahead of schedule, maize plants had no enough leaves for photosynthesis in milk ripe stage, but from figure 3 and 4 mentioned above, we can find that leaf area in more water supplied dispose is bigger regardless with ridge plotted field or not, leaf area with more bed-irrigating is smaller than those with more mending irrigation when water supply grosses are same. This shows that mending irrigation's effects are more marked than bed-irrigating at the two experimentation years. From the effects of ridge plotted field, single plant leaf area of disposals with ridge plotted field increase 173.9cm^2 to those without ridge plotted field, that is ridge plotted field have relative good effects.

3.3 Changes to LAD under different technological measures

The longer plant photosynthetic production accumulation time, the higher plant LAD, and the higher yield correspondingly. From the figure 5, it is obviously that the LAD of the disposals with ridge plotted field are higher than those without ridge plotted field under same amount of water supply; disposals' LAD increase along with the increase of water supply basically under same ridge plotted field conditions.

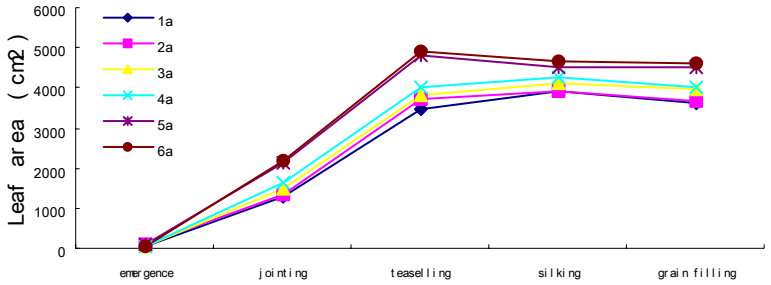

Figure 3. Maize leaf area contrasts of different disposals without ridge plotted field

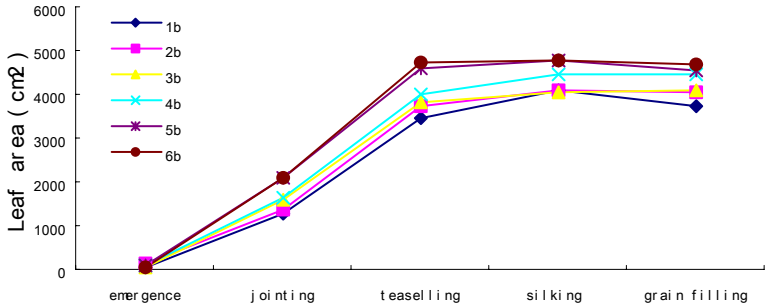

Figure 4. Maize leaf area contrasts of different disposals with ridge plotted field

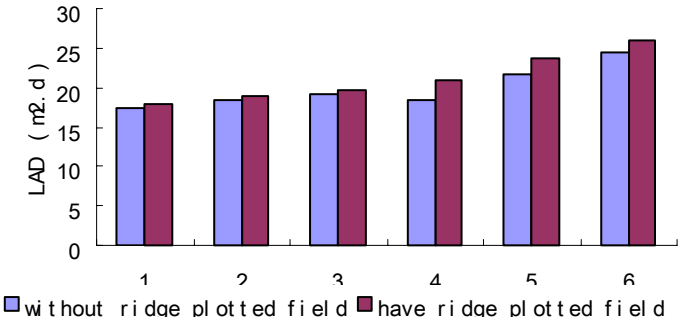

Figure 5. Maize single plant LAD contrasts of difference disposals

3.4 Changes to net assimilation rate under different technological measures

From the whole tendency, changes to net assimilation rate in maize growing period can be divided into 3 stages: rise stage, decline stage and rise again stage.

From the effects of ridge plotted field, the net assimilation rates in the disposals with ridge plotted field increase 6.74% to those without ridge plotted field in average (Figure 6, 7). From the effects of water supply, disposals with more water supply gross have higher net assimilation ratio in each stage basically, and it is obviously that the effects of bed-irritating are rather distinct, prophase net assimilation rates of disposal 2 are relative high regardless with ridge plotted field or not. On the whole, mending irrigation's effects represent more evident.

3.5 Changes to economic coefficient under different technological measures

Economic coefficient is the ratio of economic yield and biological yield, and it reflects the efficiency of biological yield convert into economic yield. From

Figure 8, we can conclude that under same water supply conditions, disposals' economic coefficients with ridge plotted field are higher than those without ridge plotted field, and increase 8.4% in average; under same ridge plotted field conditions, disposals' economic coefficients increase along with the increase of water supply basically.

3.6 Changes to yields under difference technological measures

The disposals' yields can be seen in Table 2. The statistic software—SAS was used in maize yields analyzing, and the regress equations are as follows:

a. Regress equation of maize yields under the condition without ridge plotted field:

$$\hat{y} = 4006.00 + 13.939x_1 + 14.871x_2 + 0.834x_1x_2 - 0.090x_1^2 - 0.073x_2^2$$

b. Regress equation of maize yields under the condition with ridge plotted field:

$$\hat{y} = 4169.33 + 18.389x_1 + 8.055x_2 + 0.081x_1x_2 - 0.119x_1^2 + 0.001x_2^2$$

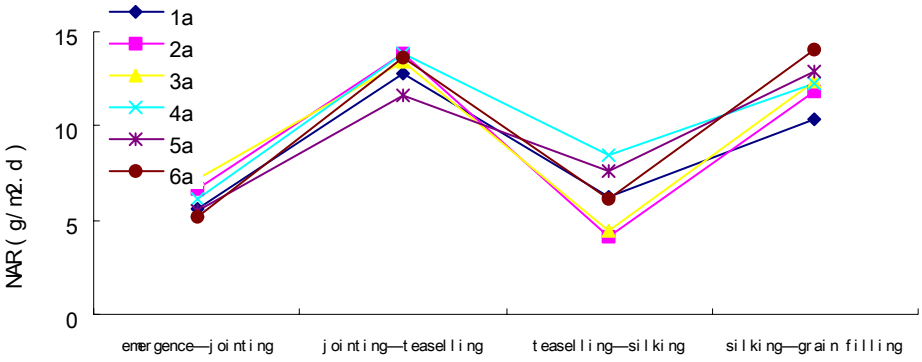

Figure 6. Maize single plant NAR contrasts of different disposals with ridge plotted field

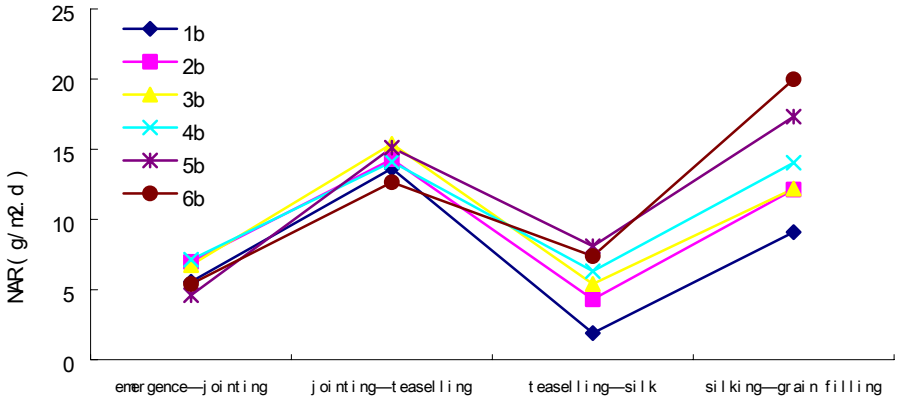

Figure 7. Maize single plant NAR contrasts of different disposals without ridge plotted field

We can conclude that under same water supply conditions, disposals' yields with ridge plotted field are always higher than those without ridge plotted field, and increase 5.8% in average. For getting the optimal amount of water supply for bed-irrigating and mending irrigation respectively, we optimize the equations above, and gain: when we fix a kind of water supply factor to some level, maize yield increase along with the increment of another water supply factor basically regardless with ridge plotted field or not, and the

maximal theoretical quantum occurs when bed-irrigating quantum is 120m^3/hm^2 and mending irrigation quantum is 120m^3/hm^2.

3.7 Changes to WUE under different technological measures

According to the soil moisture differences in 1m depth under the ground surface between the stages of sowing and harvesting, and the amount of irrigation water and rainfall in the whole growing period, the amount of water consumption in all disposals' in the whole growing period were obtained, and the farmland WUE (kg/m^3) was calculated.

From Table 2 we can conclude: ①the WUE increase along with the increment of limited water supply basically regardless with ridge plotted field or not; ②Under same water supply conditions, WUE of disposals with ridge plotted field are always higher than those without ridge plotted field, the WUE increase range from 16.35% to 39.47%, and 5.8% in average; ③Under same water supply quantum conditions, disposal 3 behaves higher WUE than disposal 2, disposal 6 behaves higher WUE than disposal 5, these show that effects of seedling stage mending irrigation toward maize WUE are better than those of bed-irrigating.

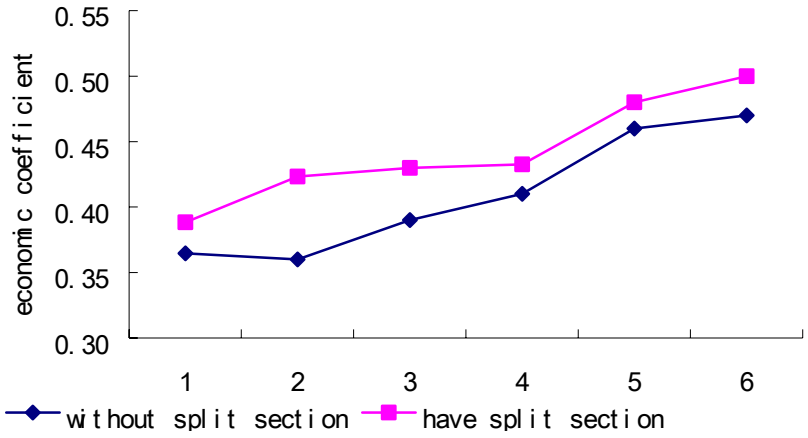

Figure 8. Maize economic coefficient contrasts of different disposals

Table 2. Maize yields and WUE under different disposals conditions

Disposals	Farmland with ridge plotted field.		Farmland without ridge plotted field.		Yields increment (kg/hm^2)	WUE increment (%)
	Yields (kg/hm^2)	WUE (kg/ m^3)	Yields (kg/hm^2)	WUE (kg/ m^3)		
1	4169	1.32	4006	0.95	163	39.47
2	4660	1.39	4385	1.19	275	16.35
3	5151	1.75	4733	1.27	418	37.72
4	5456	1.67	5298	1.35	158	23.89
5	6163	1.92	5957	1.58	206	21.74
6	6674	1.97	6110	1.59	564	23.65

4 Conclusions

a) The dry matter production of maize for single plant is influenced by the factors of procreation period, leaf area, LAD, and NAR and so on. The analyses of

the influences of water-saving and anti-drought combined technological measures on these factors make clear that they have the same tendency with dry matter accumulation: under the same water supply quantum conditions, effects of mending irrigation are better than those of bed-irrigating; from the effects of ridge plotted field, effects of disposals with ridge plotted field are higher than those without ridge plotted field.

b) 4.2 Through statistic analyses, the relations between maize yield and limited water supply and ridge plotted field were obtained, and the optimization analysis were made, from which theoretical extent of the water amount for bed-irrigating and mending irrigation were deduced, and drawing the conclusion that ridge plotted field can increase yield.

c) 4.3 From the analyses of WUE under different technological measures, we can see that ridge plotted field can increase the WUE efficiently under the experimental conditions, and that effects of seedling stage mending irrigation toward maize WUE are better than those of bed-irrigating.

Correspondence to:

Wei Yongxia

School of Water Conservancy and Civil Engineering

Northeast Agricultural University

Harbin, Heilongjiang 150030, China,

Email: wyx0915@163.com

Acknowledgement:

This study is imbursed by national Chinese “863” plan program (No. 2002AA2Z4251).

References

[1] Agricultural Science Institute of Shandong province. Chinese maize planting. Shanghai Science and Technology Press. 1986;117-27

[2] Chen Guo-ping. Maize’s dry matter production and distribution. Journal of Maize Sciences 1994(3):48-53.

[3] Cui Jun-ming, et al. Maize forepart and spinning stage defoliation’s influences on growth. Journal of Maize Sciences 2004;12(2):52-5.

[4] Li Zhen-hua, et al. A Study on The High-Yielding Physiological Indices in Corn. Journal of Northeast Agricultural University 1995;3:34-43.

[5] Plant physiological laboratory, Agricultural Science Institute of Shandong province. Physiological base of maize yield formation (study bulletin 3). 1977;35-46 .

[6] Song Bi, et al. Different individual plant type maize high yield colony’s quality indexes. Journal of Mountain Agriculture and Biology 2001;20(1):1-8.

[7] Tang Yong-jin, et al. Growth Characteristics of Different Ecotypes of Maize Dabin. Journal of Maize Sciences 1999;7(3):62-7.

[8] Xie Feng. Summer maize procreation status’ analysis contrast under different water conditions. Journal of Yangling Profession Technology College 2002;9:39-41.

Nature and Science

Call for Papers

The new international academic journal, "**Nature and Science"** (ISSN: 1545-0740)**,** is registered in the United States, and invites you to publish your papers.

Any valuable papers that describe natural phenomena and existence or any reports that convey scientific research and pursuit are welcome, including both natural and social sciences. Papers submitted could be reviews, objective descriptions, research reports, opinions/debates, news, letters, and other types of writings that are nature and science related.

This journal will be supported by manuscript contributors. To cover the printing cost, this journal will only charge authors the actual printing fee (about US$30 per printed page). At least one hard copy of the printed journal will be given to each author free of charge. Here is a new avenue to publish your outstanding reports and ideas. Please also help spread this to your colleagues and friends and invite them to contribute papers to the journal. Let's work together to disseminate our research results and our opinions.

Papers in all fields are welcome, including articles of natural science and social science.

Please send your manuscript to editor@sciencepub.net.

For more information, please visit http://www.sciencepub.org.

Marsland Company
P.O. Box 21126
East Lansing, Michigan 48909
The United States
Telephone: (517) 980-4106
E-mail: editor@sciencepub.net
Website: http://www.sciencepub.org

Marsland Company

P.O. Box 753

East Lansing,Michigan 48826

The United States

Tel:(517)862 - 6881

http://www.sciencepub.org

E-mail:editor@sciencepub.net